DOCTOR OF SCIENCES

Short-period effects in the rotation of Mercury

Dufey, Julien

Award date:
2010

Awarding institution:
University of Namur

FACULTES UNIVERSITAIRES NOTRE-DAME DE LA PAIX NAMUR

FACULTE DES SCIENCES

DEPARTEMENT DE MATHEMATIQUE

Short-period effects in the rotation of Mercury

Dissertation présentée par
Julien Dufey
pour l'obtention du grade
de Docteur en Sciences

Composition du Jury:

Timoteo CARLETTI
Véronique DEHANT
Anne LEMAÎTRE (Promoteur)
Andrea MILANI
Guy TERWAGNE

2010

Rempart de la Vierge, 13
B-5000 Namur (Belgique)

Imprimé en Belgique

ISBN-13 : 978-2-87037-681-2
Dépôt légal: D / 2010 / 1881 / 27

Facultés Universitaires Notre-Dame de la Paix
Faculté des Sciences
rue de Bruxelles, 61, B-5000 Namur, Belgium

Les effets à courtes périodes dans la rotation de Mercure

par Julien Dufey

Résumé: Dans le cadre de la mission spatiale BepiColombo, un modèle très précis de la rotation de Mercure est requis. Dans cette thèse, nous étudions les différentes causes affectant la rotation de la planète sur une période allant de quelques jours à plusieurs dizaines d'années. Dans la première partie de ce travail, nous décrivons le modèle d'une planète constituée d'un manteau ellipsoïdal et d'un noyau liquide sphérique (sans interaction), et sans perturbation planétaire. Nous déduisons la valeur des librations en longitude et en latitude ainsi que le mouvement du pôle de Mercure. Dans la deuxième partie, nous étudions les effets des perturbations planétaires indirectes sur la rotation. Nous mettons en évidence plusieurs résonances potentielles susceptibles de faire exploser les librations en longitude et en latitude. Dans la troisième partie, nous analysons les interactions entre noyau et manteau en prenant comme hypothèse que le noyau est une cavité ellipsoïdale. Nous montrons qu'une résonance additionnelle joue un rôle majeur dans ce cas et que les observations de la rotation du manteau peuvent nous donner des informations sur la taille du noyau, mais pas sur sa forme. Enfin, nous étudions de manière plus théorique une résonance entre une période fondamentale du système et la période orbitale de Jupiter, augmentant l'influence de Jupiter sur la rotation. Tous les résultats ont été obtenus de manière analytique en utilisant une étude hamiltonienne du problème et une méthode de perturbations par transformée de Lie, et ont ensuite été vérifiés par intégration numérique et analyse en fréquence.

Short-period effects in the rotation of Mercury

by Julien Dufey

Abstract: In the framework of the space mission BepiColombo, a very accurate model of rotation of Mercury is required. In this thesis, we study various causes affecting the rotation of the planet on a time span going from a few days to several decades. In the first part of this work, we describe the model of a planet constituted of an ellipsoidal mantle and a spherical liquid core (no interaction), and without planetary perturbations. We compute the libration in longitude and in latitude as well as the polar motion of Mercury. In the second part, we study the effects of the indirect planetatery perturbations in the rotation. We emphasize several potential resonances capable of enhancing the longitudinal and latitudinal librations. In the third part, we analyse the core-mantle interactions assuming that the core is an ellipsoidal cavity. We show that an additional resonance plays a major role in this case and that the observations of the rotation of the mantle can yield information on the size of the core but not its shape. Finally, we study more theoretically a resonance between a free period of the system and the orbital period of Jupiter, raising the influence of Jupiter in the rotation. All the results were obtained analytically using a Hamiltonian approach of the problem and a perturbation method based on canonical Lie transforms, and were then verified using numerical integrations and frequency analysis.

Dissertation doctorale en Sciences mathématiques (Ph.D. thesis in Mathematics)
Date: 21-06-2010
Département de Mathématique
Promoteur (Advisor): Prof. Anne LEMAÎTRE

Remerciements

Un voyage de cinq années se termine et il y a un bon nombre de personnes que je tiens à remercier dans ces quelques lignes pour m'avoir aidé ou tout simplement accompagné lors de la réalisation de cette thèse.

La première personne est évidemment Anne sans qui rien de tout ça n'aurait été possible, littéralement. De la 1ère candi à la 2ème licence, tu m'as enthousiasmé avec tes cours de méca, enthousiasme qui s'est ensuite transformé en véritable passion durant mon mémoire. Lors de mon périple au pays des maths théoriques à Louvain, tu as continué à m'encourager et m'as finalement permis de retourner à Namur pour travailler sur cette thèse. Et pendant toutes ces années, tu as toujours fait preuve d'un dynamisme, d'une disponibilité et d'une motivation dont je ne connais pas d'égal. Sincèrement Anne, merci!

J'ai également une pensée envers Jacques, qui m'a éclairé plus d'une fois au début de ma thèse et dont le génie nous manque tous.

Ensuite, je voudrais remercier les membres de mon jury d'avoir accepté d'en faire partie et d'avoir lu et rendu des remarques très pertinentes sur mon manuscrit de thèse.

Mes prochains remerciements sont pour Benoît et Nicolas. Je suis très heureux et fier d'avoir pu accomplir les travaux que nous avons réalisés et j'ai appris énormément grâce à vous, toujours dans une ambiance décontractée mais productive. Merci d'avoir eu la patience de répondre à toutes mes questions!

Merci à Marie pour ton intérêt et tes corrections (quel oeil!), ainsi que pour nos discussions.

Merci à nos deux secrétaires Pascale et Martine pour leur efficacité et disponibilité constante!

Merci à tous les membres de ce département bien chaleureux!

Le côté professionnel n'est pas tout, je tiens aussi à remercier de nombreuses personnes qui ont rendu ces cinq années très agréables.

Tout d'abord, mes deux collègues de bureau Stéphane et Nico, dont la complicité, les fous rires, les discussions au quotidien ont débouché sur de belles amitiés. Vous m'avez aussi ap-

pris de nombreuses choses dans plus d'un domaine et je tiens à vous remercier pour toutes ces raisons. Nico, merci aussi pour tes corrections et discussions boulot ces derniers mois, ça va me manquer!

Merci à mes trois compagnons d'études, Anne-So, Cha et Seba pour votre amitié durant toutes ces années passées avec vous (10 ans!), agrémentées d'excellentes soirées, et de grands moments!

Merci à Sandrine, en premier lieu d'avoir commencé le boulot, de m'avoir épaulé et aidé au début de cette thèse puis pour ces discussions et rires, que ce soit en colloque, ou lors de passages dans nos bureaux respectifs.

Je veux aussi remercier Jehan, Pat, Joffray, Jojo, Audrey, Melissa, Ben, Vincent, Martine, Fabien, Laeti, André, Charlotte, Emilie, Charles, Jérémy pour (les gens se reconnaitront) les guindailles (passées et futures), soutiens mutuels, colloques, cours partagés, soupers,...

Merci à mes amis, qu'ils soient tout près ou loin et qui ont rendu ces années grandioses. Lie, Nyouf, notre trio et petite famille a encore de belles années à venir! Merci à toi Edith pour tous ces Chapitres et cette grande amitié! Merci à Céline, Benja, Max, Carole pour ces soirées, discussions et projets futurs. Merci aux potes du basket, spécialement Ludo, Georges, Pierre et Oli pour tous les délires et divertissements en tous genres! Merci à Claire et Malo pour ce voyage fantastique aux Philippines et pour toutes les soirées qui ont suivi. Merci à Eniac, Phil, Tof pour tous ces bons moments et cette longue amitié. Enfin, merci à Ariane, merci à Jipi pour nos fabuleuses amitiés qui perdurent malgré la distance!

Je tiens aussi à remercier tous les gens d'Amnesty et de l'Autre Pack qui ont donné une dimension en plus à ces années passées aux facs.

Merci Maman, merci Papa pour votre soutien constant depuis toujours. Merci de m'avoir donné les moyens de réaliser ce travail, d'avoir toujours cru en moi. J'espère qu'un jour mes enfants seront aussi heureux d'avoir leur papa que je le suis de vous avoir.
Merci Line, merci Ri, mes p'tites grande et moyenne soeurs pour votre soutien depuis tout petits, pour notre complicité et pour tout ce que je ne peux même pas exprimer ici.
Merci Katty, merci Gilbert de nous rendre heureux!
Merci à Marc, Denis, Myriam et Francis pour me faire sentir comme chez moi à chaque fois!

Enfin, merci à toi Cécile. Comme il est d'usage d'introduire des références de mécanique céleste, je ne vais pas m'en priver. Par une (très) belle coïncidence, cette planète Mercure et toi êtes entrées dans ma vie presque simultanément. Vous m'avez toutes les deux bien fait tourner la tête et j'avoue ne pas avoir tout compris à plusieurs moments... Alors que ma route avec Mercure s'achève, la nôtre continue, avec j'en suis sûr, les plus beaux moments à venir. Merci d'être toi, de me soutenir, d'apporter ce fun, ce désordre et cette géniale fantaisie dans ma vie! Du moment qu'on est heureux, que demander de plus!

Contents

Introduction

The rotation of Mercury has been studied thoroughly since 1965, when Pettengill and Dyce, using radar observations, computed that the planet was rotating in approximately 59 days. Until then, Mercury was often compared to the Moon and it was thought that the planet was in a synchronous rotation (same orbital and rotational periods). Colombo (1965) proposed the first simplified model of the rotation of Mercury and noticed that the rotational period found by Pettengill and Dyce (1965) might be exactly two-thirds of the orbital period (87.97 days). He conjectured that this particular rotational motion called a 3:2 spin-orbit resonance (3 rotations on its spin axis during 2 orbits around the Sun) might be stable. The rotation of Mercury could then be described by a periodic stable solution such that the smallest axis of inertia would be almost aligned with the vector Sun-Mercury each time it passes at the perihelion.

In the following decade, many authors studied different aspects of Mercury's rotation. Goldreich & Peale (1966) analysed the spin-orbit coupling phenomena in the Solar System and tested their hypotheses on Mercury and the Moon. They concluded that tidal effects probably slowed down the planet, making it cross several resonance zones and that the capture in this particular resonant state was due to the eccentricity of the orbit and the triaxiality of the body.

In 1969, Peale, using a Hamiltonian constituted of a rotational kinetic energy, a gravity potential and a precession of the orbital node, showed that Mercury blocked in a 3:2 spin-orbit resonance verifies the generalised Cassini's laws (Beletsky (2000), see Chapter 3).

Peale again, in 1974, using a similar Hamiltonian model and introducing for the first time a resonant angle and tidal forces, was able to deduce the most probable equilibrium state of Mercury referred to as the Cassini state.

At the same time, Beletskii (1972) studying a 3-degree of freedom model of Mercury and computing the equilibria came to similar conclusions: the 3:2 spin-orbit resonance is indeed an equilibrium state verifying the generalised Cassini's laws.

In 1976, Peale examined how to get information on the interior structure of Mercury. He came up with the so-called "Peale's experiment" (Peale, 1976, 2005):

$$\left(\frac{C_m}{B-A}\right)\left(\frac{B-A}{mR_e^2}\right)\left(\frac{mR_e^2}{C}\right)=\frac{C_m}{C},$$

showing that if we can determine precisely the amplitude of the librations in longitude (related to the first factor), the value of the second-order gravitational coefficient C_{22} (second factor) and the obliquity of Mercury (related to the third factor, together with the second-order spherical harmonics coefficients), we would have a very good estimation of the size of Mercury's core. In

this equation, $A < B < C$ are the principal moments of inertia of Mercury, C_m is the moment of inertia of the mantle, m is the mass of the planet and R_e its equatorial radius.

More recently, this experiment has known a renewed interest with the two space missions to Mercury of the 21st century: MESSENGER from the NASA and BepiColombo from the ESA-JAXA. These missions should be able to determine the three factors of Peale's experiment with a high accuracy and constrain the size of the core. As a matter of fact, Margot et al. (2007), using radar speckle patterns tied to the rotation of Mercury, were able to determine a value for the obliquity and rather large libration in longitude, indicating that the mantle of Mercury should be decoupled from a partially molten core. The first data from MESSENGER should provide definite values for these parameters.

Correia and Laskar (2004 and 2009), taking into account tidal effects, planetary perturbations and core-mantle frictions, showed how a capture in the 3:2 spin-orbit resonance is possible and is in fact the most probable outcome (from 26 to 73% of the cases studied, depending whether Mercury had an extremely low value of the eccentricity in the past or not).

In 2004, Rambaux and Bois were able to characterize the orbital motion of a rigid Mercury by two proper frequencies and give the value of its mean obliquity. They used a numerical theory integrating the motions of the planets and spin-orbit motion of Mercury simultaneously. They suggested that the obliquity of the planet was subject to large variations on thousand-year timescales due to planetary perturbations, potentially ruining the implementation of Peale's experiment.

In the same year, D'Hoedt & Lemaitre (2004) used an analytical method with a 2-degree of freedom Hamiltonian and computed the equilibria of the rigid model as well as the fundamental periods, obtaining an excellent agreement with those found by Rambaux and Bois (2004). They described their model as a kernel for the study of Mercury's rotation and the Hamiltonian of the present work is indeed based on this kernel.

Yseboodt & Margot (2006) also used this kernel, adding the planetary perturbations in order to evaluate as precisely as possible the value of the obliquity. They were able to reproduce an obliquity evolution similar to that of Rambaux and Bois (2004), but with a set of initial conditions differing from the Cassini state. However, they showed that these variations disappear with initial conditions at the Cassini state, indicating that planetary perturbations should not yield large variations in the obliquity.

D'Hoedt & Lemaître (2005) and Lemaitre et al. (2006) continued the in-depth analytical study by adding another degree of freedom (the wobble) to the rotational motion of a rigid Mercury, and showing that the equilibria associated with their model verify the generalised Cassini's laws.

Indirect planetary perturbations were introduced in a paper by Peale et al. (2007). They used JPL ephemeris and numerical integrations on a one-degree of freedom model of a non-rigid Mercury and found several significant planetary contributions on the libration in longitude. In a following paper Peale et al. (2009) used a similar model but with a different value of the moment ration $(B - A)/C_m$ and corrected a mistake from their previous paper. They emphasized a resonant forcing between one of the free periods of the model and the orbital period of Jupiter, resulting in a large amplitude of the 11.86-year libration.

To complete this non-exhaustive review of the theories of rotation of Mercury, we mention

the work of Rambaux et al. (2007b). They studied a core-mantle coupling in the rotation of Mercury considered as a solid body including either a solid or a liquid core. They found that the amplitude of the 88-day libration essentially depends on the radius of the core and that it should be possible to discriminate between models of internal structure with accurate libration measurements.

In this work, we deal with the short-period effects on the rotation, over 100 years at most. Starting from the kernel model first described in D'Hoedt & Lemaitre (2004), we gradually refine it. From a model allowing a mantle decoupled from a spherical liquid core in a one-degree of freedom Hamiltonian, we complexify it to finally get to a four-degree of freedom Hamiltonian with a non-spherical core, including planetary perturbations.

Chapter 1 sets the context of this study. With two space missions about to visit Mercury in the close future, a very accurate model of rotation of Mercury taking into account the short-period effects was needed. After depicting several features of Mercury and a brief description of the space missions, we explain where this work stands in this framework.

Chapter 2 aims at explaining in a practical and educational way the perturbation theory based on canonical Lie transforms used throughout our work. Even though the well-informed reader may choose to skip this part, we think it is valuable to explain this rather difficult theory and show a few of its subtleties.

Chapter 3 finally gets to the thick of things. After setting our general model for the rotation as a planet constituted of a mantle and a spherical liquid core, we develop and use our perturbation theory on the 3 degrees of freedom of the rotation: the longitude, the latitude and the wobble motion, and show how to obtain the time evolution of any variable of the system.

In Chapter 4, we include *indirect* planetary perturbations on the rotation of Mercury. In other words, the perturbations affect the orbit of Mercury and this change of the orbit will affect the rotation. We perform several comparisons to ensure the validity of our method and are able to emphasize a couple of secondary resonances that may affect greatly the rotation.

Chapter 5 considers core-mantle interactions in the rotation. We study the observable consequences of an ellipsoidal core on the rotational motion of the planet.

Finally, in Chapter 6 we study one of the secondary resonances found in Chapter 4 in a more extended way and deal with the *direct* planetary perturbations on the rotation, expected to be insignificant.

In order to understand this work thoroughly, the reader should have a basic knowledge of celestial mechanics and Hamiltonian theory.

1 Context and motivations

Mercury has always been the “forgotten” telluric planet. The Earth is of course very well known and there have been many missions to Mars (Mariner 4, the Phobos program, Mars Exploration Rovers, Mars Express, ...) and Venus (Venera program, Mariner 2 and 5, Venus Express, ...).

Until a few years ago Mariner 10, launched in November 1973, was the only mission sent to explore Mercury. Its main scientific objectives were the study of a potential atmosphere, of the surface, and of other features of the planet. This mission was able to discover the existence of a very thin atmosphere called the exosphere and the existence of an unexpected magnetosphere, generated by the planet itself and not by solar wind (see Dunne and Burgess (1978) and references therein). It also allowed to have an idea of the first gravity field coefficients, representing the flattening of the pole and the ellipticity of the equator. About 45% of the planet was mapped during the mission, revealing a surface similar to the Moon. This mission was the first to use the gravity assist of a planet (Venus) using an idea of Giuseppe (Bepi) Colombo.

Nowadays, two other missions are following the steps of Mariner 10. MESSENGER (Solomon et al., 2006), a NASA mission launched in August 2004 has its orbit insertion planned for March 2011 and the ESA-JAXA BepiColombo mission (Anselmi and Scoon (2001), Milani et al. (2001)) will be launched in 2014 with an orbit insertion planned for 2020.

In this first chapter we start by describing Mercury and its different features that make it so particular and fascinating. Then we present a very brief overview of the MESSENGER mission and its scientific objectives. Finally we explain the features of the BepiColombo mission and more precisely, where this work stands in the mission framework, through the ROMEO team involvement in the MORE radio-science experiment of BepiColombo.

1.1 Mercury’s ID

In our Solar System, Mercury is the closest planet to the Sun (its semi-major axis is 0.397 AU) and also the smallest, with an equatorial radius of 2439.7 km. It is almost 3 times smaller than the Earth, smaller than Jupiter’s satellite Ganymede and Saturn’s Titan, and barely larger than the Moon. Several features make it very interesting:

- the proximity to the Sun,
- the high density,

- the high eccentricity,

- the unique 3:2 spin-orbit resonance in the solar system.

The proximity of the Sun

Because Mercury is the innermost planet of the Solar System it can only be observed in early morning or early evening, its orbit being close to the Sun and its radius about one third of that of the Earth.

This proximity also makes it difficult to reach with a spacecraft. The gravitational potential well of the Sun and the large orbital speed of Mercury require either large Δv's or a very long trip for a probe to reach a stable orbit around Mercury. Without planetary flybys, going to Mercury would cost even more fuel than a journey to Pluto!

Another effect of this closeness is also very well known. In 1859, Urbain Le Verrier computed that the perihelion of Mercury precessed with an excess rate of 38 arcsec (later recalculated as 43) per century. This could not be explained by Newtonian mechanics. We had to wait until the beginning of last century and the general theory of relativity of Albert Einstein to have a satisfying explanation. He showed that his theory predicts exactly the shift of precession inexplicable until then. The curvature of space-time in the vicinity of the Sun forces to add a relativistic correction term in the equations. This is one of the strongest reasons for adopting the general relativity.

In this particular environment, a relativity experiment will be carried out by the Bepi-Colombo mission and will be able to constrain the main post-Newtonian parameters (Milani et al., 2002).

The high density

Another particularity of Mercury is its very high density of about 5.427 g/cm^3. This is the second highest density in the Solar System, only trailing our planet whose density is 5.515 g/cm^3. However, given the small size of the planet (small self-compression by gravity), this is very surprising. Figure 1.1 shows the density of the telluric planets and the Moon in function of the radius. The probable reason for this high density is that its core should be rich in iron and significantly larger than any other planet of the Solar System (at least twice as large as that of the Earth).

Mercury's interior structure is one of the most puzzling questions that the space missions will have to answer to.

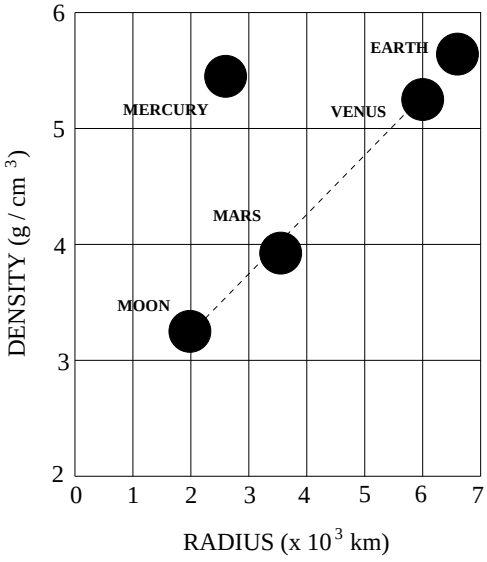

Figure 1.1: Plot showing the density (in g/cm^3) of the telluric planets and the Moon as a function of their radius.

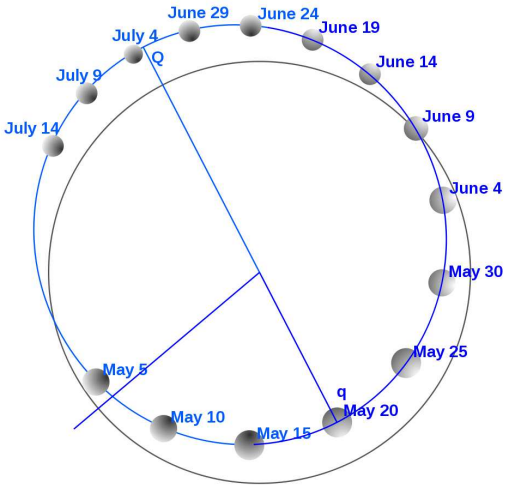

Figure 1.2: This figure represents the difference between the orbit of Mercury and a circular one with the same semi-major axis. The spheres shown at different longitudes represent the size of the Sun as seen from Mercury at that particular place.

The high eccentricity

The eccentricity of Mercury is the highest of the planets. With $e = 0.206$, it is more than 10 times larger than the Earth eccentricity and twice as large as the second highest eccentricity (Mars). Figure 1.2 shows the difference between a circular orbit and that of Mercury around the Sun. Correia and Laskar (2004) showed that the eccentricity varies chaotically over billions of years. It can go from a nearly circular motion to over 0.45. Recently Laskar and Gastineau (2009) computed integrations of the Solar System over 5 billions of years, using non-averaged equations and including the relativistic effects. One percent of these simulations led to a large increase in Mercury's eccentricity (pumped by a proximity of a resonance with Jupiter), large enough to allow Mercury to collide with Venus or the Sun.

The 3:2 spin-orbit resonance

Probably the most peculiar aspect of Mercury is the 3:2 spin-orbit resonance. While performing 2 orbits around the Sun, Mercury rotates exactly 3 times around its spin axis. This is the unique case of 3:2 spin-orbit resonance known. Figure 1.3 illustrates this particularity of Mercury. This resonance induces particular effects on the dynamics of the rotation, as we will see during this work. It was first discovered by Pettengill and Dyce (1965), using radar observations. At that time, it was commonly admitted that Mercury was synchronously tidally locked, rotating only once for each orbit, thus presenting always the same face to the Sun (the same way that we always see the same face of the Moon). This belief was

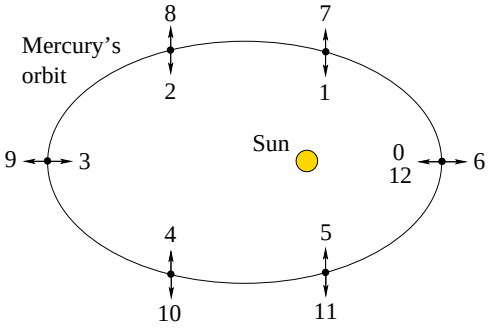

Figure 1.3: Illustration of the 3:2 spin-orbit resonance: Mercury rotates exactly 3 times around its spin axis in 2 orbital periods. The arrows with the numbers from 0 to 6 represent a person standing on Mercury at a fixed longitude during the first orbit around the Sun, numbers from 6 to 12 during the second.

ended by Pettengill and Dyce who measured that the period of rotation of the planet was around 59 days, and Colombo (1965) conjectured that this value might be exactly 2/3 of the 87.969-day orbital period of Mercury, locking the planet in this 3:2 spin-orbit commensurability.

Other interesting aspects of Mercury

We should also mention other particular aspects of Mercury:

- Even though Mercury is too small to retain any significant atmosphere, a very tenuous and unstable **exosphere** was detected by Mariner 10, ground-based telescopic observations and lately, MESSENGER.
- A very weak **magnetic field** was detected by Mariner 10 during its 1st and 3rd close approaches with Mercury. It came as a surprise since no one expected such a slow rotating planet to be able to generate a significant dynamo effect. The shape and the characteristics of the magnetosphere encountered by Mariner 10 are similar to that of the Earth, only 100 times weaker.
- The **obliquity** of Mercury or the angle between its spin axis and the normal to its orbital plane is the smallest of all the planets, it should be around 2 arcmin, depending on the interior of Mercury.
- Without significant atmosphere and so close to the Sun, Mercury suffers **extreme temperatures**: from -173° to 427°.

1.2 MESSENGER

Thirty years after Mariner 10 gathered information on Mercury, a new spacecraft is on its way to orbit the planet. MESSENGER (MErcury Surface, Space ENvironment, GEochemistry and Ranging), a NASA space mission launched in 2004 already performed three flybys around the planet. The scientific questions addressed by MESSENGER are:

- What planetary formation processes led to the high metal/silicate ratio in Mercury?
- What is the geological history of Mercury?
- What are the nature and origin of Mercury's magnetic field?
- What are the structure and state of Mercury's core?
- What are the radar-reflective materials at Mercury's poles?
- What are the important volatile species and their sources and sinks on and near Mercury?

Its orbit insertion is planned for March 18, 2011. We should then get valuable information on the gravity coefficients of the planet (up to order 16), on the magnetosphere and the exosphere. It will also provide the first images of unmapped areas and high resolution data of about 25% of the surface.

1.3 The BepiColombo space mission

To quote Dr. Johannes Benkhoff, BepiColombo Project Scientist at the ESA: “After the ’appetizer’ mission MESSENGER, BepiColombo will be the ’main course’ ”.

1.3.1 The mission profile

BepiColombo is the planetary Cornerstone of the ESA’s Cosmic Vision Programme. With its state-of-the-art equipment, it is devoted to a thorough exploration of Mercury and its environment.

This mission is a partnership between the ESA and the Japan Aerospace Exploration Agency (JAXA). This is the first time both agencies cooperate. It is also the first dual spacecraft mission to Mercury composed of an orbiter studying the magnetic field (MMO, Mercury Magnetospheric Orbiter) and an other one studying the planet (MPO, Mercury Planetary Orbiter). In addition to the orbiters, the two other components of the spacecraft are the Mercury Transfer Module (MTM) providing the acceleration and brakes during the cruise to reach a stable orbit around Mercury and the MMO sunshield and interface structure, providing a protection to the Sun for the MMO and interface structure between the orbiters until their separation. Figure 1.4 illustrates how the composite spacecraft looks like during the launch and the cruise.

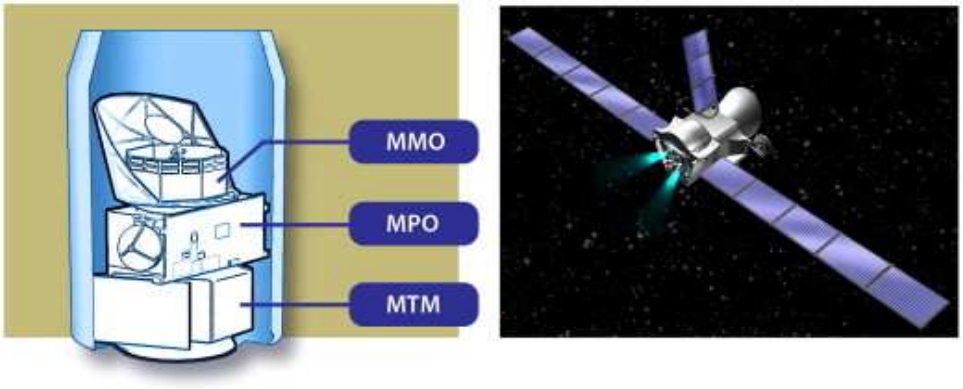

Figure 1.4: On the left panel, a drawing of the dual spacecraft with the MMO and its sunshield, the MPO and the Transfer Module during the launch. On the right panel, the same elements in cruise configuration.

At the early stages of the mission, a lander was also planned but had to be cancelled for budgetary reasons.

Table 1.1 contains the event calendar of the mission (Benkhoff et al., 2010).

The scientific objectives

The main scientific goals of BepiColombo are

- the origin and evolution of a planet close to its parent star;

Date	Mission Event
19 July 2014	Launch
25 July 2015	Earth flyby
17 January 2016	First Venus flyby
29 August 2016	Second Venus flyby
4 September 2017	First Mercury flyby
27 May 2018	Second Mercury flyby
17 August 2019	Third Mercury flyby
25 September 2019	Fourth Mercury flyby
21 May 2020–13 November 2020*	Arrival at Mercury
20 August 2021–10 February 2022*	End of nominal mission
20 August 2022–10 February 2023*	End of extended mission

Table 1.1: Calendar of the mission. The last three elements with * actually depend on the performance of the solar electric propulsion.

- Mercury's figure, interior structure and composition;
- the interior dynamics and origin of its magnetic field;
- exogenic and endogenic surface modifications, cratering, tectonics, volcanism;
- the composition, origin and dynamics of Mercury's exosphere and polar deposits;
- the structure and dynamics of Mercury's magnetosphere;
- test of Einstein's theory of general relativity.

The MPO and MMO

The 2 spacecrafts are called the Mercury Planetary Orbiter (MPO), designed by the ESA and the Mercury Magnetospheric Orbiter (MMO), built under JAXA responsibility. At their arrival at Mercury, the two orbiters will be separated. The MPO will have an orbit close to Mercury, with a periherm at 400 km of altitude and an apoherm at 1500 km. For the MMO, the periherm altitude will also be at 400 km, but the apoherm will reach an altitude of 11800 km.

The main scientific themes of the MPO are:

- the surface: topography, morphology, composition;
- the interior: study of the core, composition of the planet, magnetic field;
- the gravity field;
- the exosphere: composition, dynamics, surface release;
- the magnetosphere: structure dynamics and compositions;

while the ones of the MMO are:

- the internal magnetic field: structure and origin;
- the magnetosphere: structure, kinetics and processes;
- the atmosphere: structure, variations, production from surface, loss to solar wind;
- the surface crust: present structure, status, evolution;
- the interplanetary plasma and dust.

1.3.2 The MORE project

MORE is the acronym for Mercury Orbiter Radio-science Experiment. It consists of a device of approximately 4 kg included in the MPO, addressing scientific goals in geodesy, geophysics and fundamental physics.

It should help determine the gravity field of Mercury up to degree and order 25. The 2nd degree coefficients should be determined with a 10^{-9} accuracy (signal/noise ratio (SNR) of about 10^4), the degree 10 coefficient with a SNR of about 300 and degree 20 coefficients with a SNR around 10. It will provide constrains to determine the size and physical state of the core. With other scientific devices on board, it will also give the obliquity of the planet and the amplitude of physical librations in longitude with an accuracy of a few arcsec. All this information will indicate whether or not Mercury has a molten core and give its size.

1.3.3 The ROMEO team

ROMEO is the acronym for Rotation of Mercury and Equations of an Orbiter.
In order to process the data obtained by MORE, the software ORBIT14 will be used. The working group of this project is led by Andrea Milani from Pisa. The goal of this work is not to describe this software, and we will not go into it. However, we must mention that a very accurate model of the rotation of Mercury is required for ORBIT14. That is where the ROMEO team comes in.

The role of this team of Namur is to provide a model of rotation for Mercury, as accurate as possible, including the planetary perturbations and the non-spherical shape of the planet. The purpose of the project is double: evaluate the direct influence of Mercury's rotation on the motion of an orbiter and build a reference for the measurements of the non-rigidity of the planet.

This work originates in the second objective. We introduce the short-periodic terms in a complete and accurate model of rotation of Mercury. The Ph.D. thesis of Sandrine D'Hoedt (2007) built the foundation of this model, with long-period terms and this thesis is the continuation and expansion of her work.

2

Canonical Lie transforms for dummies

The aim of this work is to study the rotation of the planet including its short-period variations. In other words we want to compute the evolution of particular angles of the rotation such as the libration angles. We choose to use a Hamiltonian formalism, very convenient to express the equations of motion. The perturbation method chosen in this Hamiltonian framework is that of the canonical Lie transforms using the Deprit-Henrard method. It is described in several papers, in particular in Deprit (1969) and Henrard (1970), and has been used successfully in the celestial mechanics team of Namur for decades now: the libration of the Moon by M. Moons 1982, the rotation of Galilean satellites by J. Henrard (2005a, 2005b, 2005c, 2008, Henrard & Schwanen (2004)) and more recently the Ph.D. theses of B. De Saedeleer (2006) and A.-S. Libert (2007). However, even though this perturbation theory was described succinctly in each of these works, there has never been a practical reference on how to implement and use this perturbation method by canonical Lie transforms. This is the goal of the next pages.

We must mention that the Deprit-Henrard method of using canonical Lie transforms is not the only one. Hori (1966) first developed its own procedure which was adopted in many papers later on. However, as mentioned in Henrard (1970): “It should be noted that Deprit’s technique has a marked advantage over Hori’s method in that it produces a recursive algorithm generating directly the coefficients [of the transformation] up to any order”.

Giorgilli & Locatelli (1997) also used Lie series and expansions in the small parameter and, with a tree representation of their algorithm, they managed to prove the formal convergence of the method with a nonresonance condition of the frequencies of the problem.

In this chapter we explain in a practical way how to apply this perturbation method. We do not develop the theoretical results, but rather use them on a classical example to capture a few of the subtleties of this extremely rich theory. In other words, this chapter should be viewed as a manual explaining how to use this perturbation method and not how it was developed.

This chapter is displayed in three parts. First we state some theoretical results and different formulas necessary to implement the method. After this brief introduction, we develop our example to obtain an extremely simple Hamiltonian. Finally, with this Hamiltonian, we apply the Lie triangle algorithm. The theoretical references and formulas are written in boxes and we develop the direct application of the formulas on our example right after each box.

2.1 A brief overview of canonical Lie transforms

Let us consider a transformation of coordinates $x \to y$, expanded in powers of a "small" parameter ϵ and close to the identity:

$$x = \mathcal{X}(y, \epsilon) = y + \epsilon \mathcal{X}_1(y) + \epsilon^2 \mathcal{X}_2(y) + \dots . \tag{2.1}$$

For ϵ small enough, this transformation is invertible

$$y = \mathcal{Y}(x, \epsilon) = x + \epsilon \mathcal{Y}_1(x) + \epsilon^2 \mathcal{Y}_2(x), \tag{2.2}$$

and (2.1) can be defined as the solution of a system of differential equations

$$\frac{dx}{d\epsilon} = \mathcal{W}(x, \epsilon) \tag{2.3}$$

for the initial conditions $x(\epsilon = 0) = y$. This transformation (depending on the parameter ϵ) is then considered as a flow generated by a non-autonomous system of differential equations. Let us note that, for ϵ small enough and given the transformation $x = \mathcal{X}(y, \epsilon)$, it is always possible to take as generating vector field:

$$\mathcal{W}(x, \epsilon) = \left[\frac{\partial \mathcal{X}(y, \epsilon)}{\partial \epsilon} \right]_{y = \mathcal{Y}(x, \epsilon)} . \tag{2.4}$$

Let us consider the Hamiltonian systems, characterised by

$$\dot{x} = \mathcal{I} H_x^T , \tag{2.5}$$

where $\mathcal{I}$ is the symplectic matrix, $x = (q, p)$ the vector of generalized coordinates and associated moments, and the notation H_x is the gradient of H with respect to x: $H_X = \nabla_x H$. In order to keep on using the simple formalism of Hamilton's equations, we want to keep a canonical set of variables. For that, we must restrict the group of Lie transforms to the subgroup of symplectic Lie transforms for which it is necessary and sufficient to impose that the generator vector field $\mathcal{W}$ is a Hamiltonian field, i.e.

$$\mathcal{W} = \mathcal{I} W_x^T , \tag{2.6}$$

for some function W. Putting together the equations (2.3) and (2.6), we define the canonical Lie transforms as the transformations $x = \mathcal{X}(y, \epsilon) = y + \epsilon \mathcal{X}_1(y) + \epsilon^2 \mathcal{X}_2(y) + \dots$, solutions of the auxiliary Hamiltonian system

$$\frac{dx}{d\epsilon} = \mathcal{I} W_x^T . \tag{2.7}$$

Expanding any analytical function $f(\mathcal{X}(y, \epsilon), \epsilon)$ in Taylor series around $\epsilon = 0$, the expression of the transform $g(y, \epsilon)$ of this function $f(x, \epsilon)$ by the transformation (2.1) induced by the generating vector field (2.7) is

$$g(y, \epsilon) = f(\mathcal{X}(y, \epsilon), \epsilon) = \sum_{i \leq 0} \frac{\epsilon^i}{i!} \left[D^i f(x, \epsilon) \right]_{x = y; \epsilon = 0} , \tag{2.8}$$

where the operator D is defined by

$$Df(x,\epsilon) = \frac{\partial f}{\partial \epsilon} + \frac{\partial f}{\partial x}\mathcal{I}W_x^T = \frac{\partial f}{\partial \epsilon} + (f;W), \tag{2.9}$$

with $(f;W)$ standing for the Poisson bracket of the two functions:

$$(f;W) \equiv f_x \mathcal{I} W_x^T = \sum_i \left(\frac{\partial f}{\partial q_i}\frac{\partial W}{\partial p_i} - \frac{\partial f}{\partial q_i}\frac{\partial W}{\partial p_i} \right). \tag{2.10}$$

These formulas allow to write a simple and systematic procedure for the computation of a Lie transform of an analytic function. Let f be that analytic function

$$f(x,\epsilon) = \sum_{i=0} \frac{\epsilon^i}{i!} f_i^0(x) \tag{2.11}$$

and the generators W

$$W = \sum_{i=0} \frac{\epsilon^i}{i!} W_{i+1}(x). \tag{2.12}$$

From the expansion of the derivatives

$$\frac{d^j}{d\epsilon^j} f(\mathcal{X}(y,\epsilon),\epsilon) = \sum_{i=0} \frac{\epsilon^i}{i!} f_i^j(x), \tag{2.13}$$

the intermediate functions f_i^j are built successively with the recurrence formula

$$f_i^j = f_{i+1}^{j-1} + \sum_{k=0}^{i} C_i^k \left(f_{i-k}^{j-1}; W_{k+1} \right), \tag{2.14}$$

where $C_i^k = \begin{pmatrix} i \\ k \end{pmatrix} = \frac{i!}{k!(i-k)!}$ is the binomial coefficient. The recurrence formula is easy to picture if we consider the functions f_i^j placed in the so-called Lie triangle such as in Figure 2.1. The transform $g(y,\epsilon)$ of the function $f(x,\epsilon)$ is then given by

$$g(y,\epsilon) = \sum_{i=0} \frac{\epsilon^i}{i!} \left[f_0^i(x) \right]_{x=y}. \tag{2.15}$$

In our theory, we use these canonical Lie transforms on Hamiltonians. Namely, we have a quasi-integrable Hamiltonian in the form

$$H(q,p) = H_0(-,p) + \epsilon H_1(q,p), \tag{2.16}$$

where the dash emphasizes the non-dependency on the angles in the integrable part. We use the Lie transforms theory to average the Hamiltonian. The purpose is twofold: to use a perturbation

$$
\begin{array}{ccccc}
f_0^0 & & & & \\
f_1^0 & f_0^1 & & & \\
f_2^0 & f_1^1 & f_0^2 & & \\
f_3^0 & f_2^1 & f_1^2 & f_0^3 & \\
\vdots & \vdots & \vdots & \vdots & \ddots
\end{array}
$$

Figure 2.1: Lie triangle, useful to picture the intermediate function f_i^j of the Lie transforms

theory in order to average a Hamiltonian until a given order and to use the generators of the transformation to re-introduce short-period terms in variables that we want to study.

Another thing worth mentioning is that we do not choose the transformation itself (from the coordinates x to y), but we choose the transform $\bar{H}(-, \bar{p})$ of the Hamiltonian and we deduce the generators of the transformation, without computing it explicitly. Indeed the transformation does not give information while the generators contain all the short-period terms of an averaging transformation.

Finally let us add that we will use the Lie triangle procedure described above in two different ways:

1. taking the function $f(x, \epsilon)$ as the Hamiltonian, as we already mentioned,

2. computing any function $f(x, \epsilon)$ of the variables of the problem, using the generators to re-introduce short-period terms and compute the evolution .

Figure 2.2 depicts our use of this very rich theory

2.2 A simple example: dynamics of a satellite around a planet with J_2 and C_{22}.

In this section, the aim is to develop a case with a very simple 1-degree of freedom Hamiltonian on which we will apply the procedure described above. The reader must however not be misled: it is not necessary (or recommended) to use such a complicated theory to compute the motion of a body in a 1-degree of freedom case. Usually, a simple change of variables to action-angle coordinates is enough. This 1-degree of freedom Hamiltonian considered here is nevertheless a very good example to introduce some of the features of a perturbation theory by canonical Lie transforms without obscuring the theory by a large number of variables and even more complicated formulas which must be used.

The case studied is that of a satellite (of unit mass) orbiting in the equatorial plane of a planet considered as an ellipsoid (with J_2 representing the flattening at the poles and C_{22} the ellipticity of the equator). We consider the orbit of the satellite as circular and we choose an inertial reference frame centred at the centre of mass of the planet. The Hamiltonian of such a problem consists of two parts: the kinetic energy of the satellite and the gravity potential of the planet. Expanding the gravity potential up to the 2nd order in spherical harmonics (see e.g.

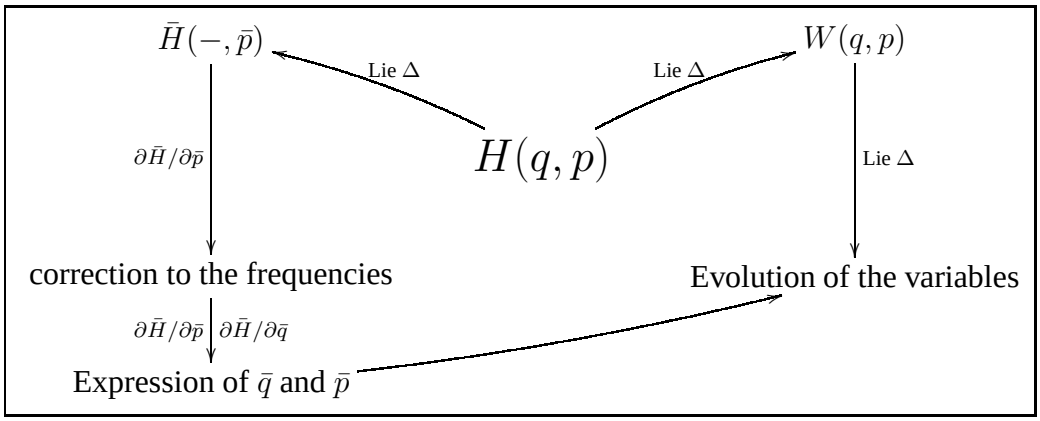

Figure 2.2: Schematic view of our use of the canonical Lie transforms theory. From the quasi-integrable Hamiltonian $H(q,p) = H_0(-,p) + \epsilon H_1(q,p)$, we use the Lie triangle procedure a first time (up to a given order, large enough for the remainder to be under the accuracy level) to transform the Hamiltonian to an averaged, integrable one, and to get the generators of this transformation (diagonal arrows). With Hamilton's equations (vertical left arrow), we compute how the frequencies are modified from $H_0(-,p)$ to $\bar{H}(-,\bar{p})$ and the expressions of the transformed variables $\bar{q}$ and $\bar{p}$. Using the Lie triangle procedure a second time (vertical right arrow), not with the Hamiltonian function but with any analytical function of the variables, together with the generators of the transformation and the expressions of $\bar{q}$ and $\bar{p}$ already computed, it is possible to re-introduce the short-period terms into any function of the variables.

Kaula (1966)) yields

$$V = -\frac{GM}{r} - \frac{GMR_e^2}{r^3}\left(-\frac{J_2}{2}(2-3(x^2+y^2)) + 3C_{22}(x^2-y^2)\right), \tag{2.17}$$

with G the gravitational constant, M the mass of the planet, R_e its equatorial radius, r the distance between the centre of mass of the planet and the satellite, and x and y the components of the unit vector pointing to the satellite. Since the satellite moves in the equatorial plane of the planet, we have $x = \cos l$ and $y = \sin l$, with l the (true or mean since $e = 0$) anomaly of the satellite. The potential then becomes

$$V = -\frac{GM}{r} - \frac{GMR_e^2}{r^3}\left(\frac{J_2}{2} + 3C_{22}\cos 2l\right). \tag{2.18}$$

Using the canonical variables of Delaunay (l, L), with $L = \sqrt{\mu a}$ where $\mu = GM$ and a is the semi-major axis (equivalent to the radius of the orbit since we assumed a null eccentricity), we have

$$V = -\frac{\mu^2}{L^2} - \frac{\mu^4 R_e^2}{L^6}\left(\frac{J_2}{2} + 3C_{22}\cos 2l\right). \tag{2.19}$$

Adding the kinetic energy to the first term of the potential gives the well-known Hamiltonian of the 2-body problem and the Hamiltonian of this problem is simply written:

$$H = \underbrace{-\frac{\mu^2}{2L^2}}_{H_{2B}} \underbrace{-\frac{\mu^4 R_e^2}{L^6}\left(\frac{J_2}{2} + 3C_{22}\cos 2l\right)}_{V_G}, \tag{2.20}$$

with H_{2B} being the Keplerian contribution and V_G the 2nd order gravitational potential. With higher-degree of freedom Hamiltonians, we will always try to get to a similar form: an integrable part (here corresponding to H_{2B}) and a small perturbation (because of J_2 and C_{22}). H_{2B} is the Hamiltonian of a perfectly spherical or point mass planet:

$$H_{2B} = -\frac{\mu^2}{2L^{\star 2}} \tag{2.21}$$

with $L^\star$ now constant[1] and its value being $L^\star = \sqrt{\mu a^\star}$, with $a^\star$ the semi-major axis of the Keplerian case. We now expand the Hamiltonian (2.20) around this value: $L = L^\star + X$. We stop the expansion at the 1st order in order to have the simplest possible Hamiltonian. The results are not altered qualitatively. The Hamiltonian then reads

$$H = -\frac{\mu^2}{2L^{\star 2}}\left(1 - 2\frac{X}{L^\star} + O(X^2)\right) - \frac{\mu^4 R_e^2}{L^{\star 6}}\left(1 - 6\frac{X}{L^\star} + O(X^2)\right)\left(\frac{J_2}{2} + 3C_{22}\cos 2l\right), \tag{2.22}$$

with the canonical variable l and moment X. Forgetting the constant terms, we have

$$H = \left(\frac{\mu^2}{L^{\star 3}} + 3\frac{\mu^4 R_e^2 J_2}{L^{\star 7}}\right)X + 18\frac{\mu^4 R_e^2 C_{22}}{L^{\star 7}}X\cos 2l - 3\frac{\mu^4 R_e^2 C_{22}}{L^{\star 6}}\cos 2l + O(X^2). \tag{2.23}$$

In the first term of the Hamiltonian, the first coefficient is $\mu^2/L^{\star 3} = \sqrt{\mu/a^{\star 3}} = n$, corresponding to the mean motion of the satellite in an unperturbed 2-body problem, while the other coefficient is only a small correction to this frequency. Renaming the constants, the Hamiltonian is actually very simple:

$$H = \underbrace{n'X}_{H_0} + \underbrace{bX\cos 2l + c\cos 2l}_{\epsilon H_1}, \tag{2.24}$$

with $n' = n + 3\frac{\mu^4 R_e^2 J_2}{L^{\star 7}}$. The integrable part is now $H_0(-, X)$ and the perturbation $\epsilon H_1(l, X)$ with ϵ implicitly included in the coefficients b and c.

Using this Hamiltonian, we would like to know how a variable of this problem, the semi-major axis for example, is affected by the perturbation $bX\cos 2l + c\cos 2l$ and what are the other changes related to this perturbation.

2.3 The implementation and the use of the Lie triangle procedure

2.3.1 The generators of the transformation and the transformed Hamiltonian

CHOOSING THE TRANSFORM AND THE PARTS OF THE HAMILTONIAN

Choose the transform $\bar{H}$ that you want to obtain. This choice actually induces a transfor-

[1] because H_{2B} is independent of its associated variable l and Hamilton's equation gives $\dot{L} = -\frac{\partial H}{\partial l} = 0$, implying that L is constant.

mation of coordinates close to the identity (assuming a small perturbing part). Typically in Hamiltonian cases, this is an averaging transformation over one or several fast angular variables included in the perturbation.
We use the so-called Lie triangle to apply the perturbation theory. The triangle is viewed as follows:

$$\begin{array}{cccc} H_0^0 & & & \\ H_1^0 & H_0^1 & & \\ H_2^0 & H_1^1 & H_0^2 & \\ H_3^0 & H_2^1 & H_1^2 & H_0^3 \\ \dots & & & \end{array} \tag{2.25}$$

The non-transformed Hamiltonian (the input) is present in the first row, its different parts (H_i^0) are chosen as proportional to the powers of a small parameter ϵ (implicitly or explicitly given):

$$H = \sum_{i=0}^{n} H_i^0 \, \frac{\epsilon^i}{i!}.$$

The transformed (averaged) Hamiltonian $\bar{H}$ that we wish to obtain lies in the diagonal:

$$\bar{H} = \sum_{i=0}^{n} H_0^i \, \frac{\epsilon^i}{i!}.$$

The transformation that we use is of course an averaging transformation over the angular variable l. This transformation is close to the identity because the parameters J_2 and C_{22} (included in the coefficients b and c) are supposed to be small compared to the corrected mean motion n'.

Now that the transformation is decided, we must choose how to share the Hamiltonian $H = \sum_0^n \frac{\epsilon^i}{i!} H_i^0$ between the different H_i^0. These early stages of the procedure (choices of the transformation (which angles) and of the H_i^0) are critical since they may lead to a non-convergent process or other problems.

In our example H_0^0 is obviously the unperturbed (averaged) Hamiltonian: $H_0^0 = n'X$. Since the two other terms of H are of the same order, we put all the perturbation in H_1^0:

$$H_1^0 = bX\cos 2l + c\cos 2l, \tag{2.26}$$

and $H_i^0 = 0 \ \ \forall i > 1$.

BUILDING THE TRANSFORMED HAMILTONIAN AND THE GENERATORS

The formulas to build the averaged Hamiltonian are

$$H_0^n = H_1^{n-1} + \left(H_0^{n-1}; W_1\right) \tag{2.27}$$

with the intermediate H_j^n computed as follows:

$$H_j^n = H_{j+1}^{n-1} + \sum_{i=0}^{j} C_j^i \big(H_{j-i}^{n-1}; W_{1+i}\big). \tag{2.28}$$

where W_i is the generator of the ith floor of the Lie triangle, $(\ ;\ )$ designates the Poisson bracket and C_j^i is the binomial coefficient.

Equations (2.27) and (2.28) should answer the question "How to compute the transformed Hamiltonian?". However we do not know the generators W_i yet and it is not possible to compute the transformed Hamiltonian or the generators of the transform without prior explanation.
Equation (2.27) with $n = 1$ is called the first-order homological equation:

$$H_0^1 = H_1^0 + \big(H_0^0; W_1\big) \tag{2.29}$$
$$= bX\cos 2l + c\cos 2l + (n'X; W_1)\,. \tag{2.30}$$

In this equation, since we are looking for periodic generators W_i, we **choose** H_0^1 to be the average of H_1^0 with respect to the angles of the averaging transformations (here l):

$$H_0^1 = \frac{1}{2\pi}\int_0^{2\pi} H_1^0 dl = \frac{1}{2\pi}\int_0^{2\pi} (bX\cos 2l + c\cos 2l)dl = 0 \tag{2.31}$$

As a consequence, the first-order homological equation gives

$$0 = bX\cos 2l + c\cos 2l + (n'X; W_1) \tag{2.32}$$
$$= bX\cos 2l + c\cos 2l + \frac{\partial(n'X)}{\partial l}\frac{\partial W_1}{\partial X} - \frac{\partial(n'X)}{\partial X}\frac{\partial W_1}{\partial l} \tag{2.33}$$
$$= bX\cos 2l + c\cos 2l - n'\frac{\partial W_1}{\partial l}, \tag{2.34}$$

and we find the first-order generator

$$W_1 = \frac{1}{n'}\int H_1^0 dl = \frac{b}{2n'}X\sin 2l + \frac{c}{2n'}\sin 2l. \tag{2.35}$$

At first order the transformed Hamiltonian is then

$$\bar{H}(\bar{X}) = H_0^0 + H_0^1 = n'\bar{X}, \tag{2.36}$$

where the variables are "barred" to notify that they are the variables after the transformation. Let us note that this Hamiltonian is the same as the unperturbed Hamiltonian.

We now push the transformation one order further. To compute H_0^2, we need H_1^1, computed as follows:

$$H_1^1 = H_2^0 + C_1^0(H_1^0; W_1) + C_1^1(H_0^0; W_2). \tag{2.37}$$

However, we have two unknowns in this equation: H_1^1 and W_2. The solution is to introduce the expression of H_1^1 into H_0^2:

$$H_0^2 = H_1^1 + (H_0^1; W_1)$$
$$= \underbrace{H_2^0 + C_1^0(H_1^0; W_1) + (H_0^1; W_1)}_{\tilde{H}_2^0} + C_1^1(H_0^0; W_2). \tag{2.38}$$

What we called $\tilde{H}_2^0$ can be calculated since all the components are known. This equation, very similar to the first-order homological equation (2.29), is called the second-order homological equation. H_0^2 is computed in the same way as H_0^1: $H_0^2 = \langle \tilde{H}_2^0 \rangle$, where $\langle \quad \rangle$ representing the average with respect to l. We have

$$\begin{aligned}
\tilde{H}_2^0 &= H_2^0 + C_1^0(H_1^0; W_1) + (H_0^1; W_1) && (2.39)\\
&= 0 + (H_1^0; W_1) + 0 && (2.40)\\
&= \frac{\partial}{\partial l}(bX\cos 2l + c\cos 2l)\frac{\partial}{\partial X}\left(\frac{b}{2n'}X\sin 2l + \frac{c}{2n'}\sin 2l\right) && (2.41)\\
&\quad -\frac{\partial}{\partial X}(bX\cos 2l + c\cos 2l)\frac{\partial}{\partial l}\left(\frac{b}{2n'}X\sin 2l + \frac{c}{2n'}\sin 2l\right) && (2.42)\\
&= (-2bX\sin 2l - 2c\sin 2l)\frac{b}{2n'}\sin 2l - b\cos 2l\left(\frac{b}{n'}X\cos 2l + \frac{c}{n'}\cos 2l\right) && (2.43)\\
&= \frac{-b^2}{n'}X - \frac{bc}{n'}. && (2.44)
\end{aligned}$$

We see no angle dependency for H_1^1, as a consequence, we have $H_0^2 = \langle \tilde{H}_2^0 \rangle = \tilde{H}_2^0$. It is now easy to deduce the generator W_2 from equation (2.38):

$$\begin{aligned}
& H_0^2 = \tilde{H}_2^0 + (H_0^0; W_2) = H_0^2 - \frac{1}{n'}\frac{\partial W_2}{\partial l} && (2.45)\\
\Leftrightarrow \quad & \frac{\partial W_2}{\partial l} = 0, && (2.46)
\end{aligned}$$

and, looking for periodic generators by definition, W_2 is a constant that we choose equal to 0 since the generators will be used with derivatives only.
The reader should not be misled here, this is a particular result caused by the extreme simplicity of the Hamiltonian. Had we expanded it to the second order in X, we would have a second order generator different than 0.
With this second-order generator, it is now possible to compute H_1^1 (necessary for higher orders).

The transformed Hamiltonian at second order is then:

$$\bar{H}(\bar{X}) = n'\bar{X} + \frac{1}{2}\left(\frac{-b^2}{n'}X - \frac{bc}{a}\right). \tag{2.47}$$

We note that if one of the frequencies of the system (here n') is small, we may have convergence issues, especially in the cases of slow varying angles and resonances.

THE ALGORITHM OF THE LIE TRIANGLE

1. Compute $\tilde{H}_i^0$, only depending on components of the Lie triangle and generators already computed in previous orders,

2. Choose the value of H_0^i as the average of $\tilde{H}_i^0$,
3. Compute the i-th order generator using the equation i-th order homological equation:

$$H_0^i - \tilde{H}_0^i = \left(H_0^0; W_i\right) = -\sum_{j=1}^{n} \omega_i \frac{\partial W_i}{\partial q_j}, \tag{2.48}$$

   with n being the number of degrees of freedom of the problem and ω_j the frequency of the j-th degree of freedom of the unperturbed problem.
4. Compute the term H_{i-1}^1 for which we needed the generator W_i,
5. Go on to the next row and start over at 1.

2.3.2 The correction to the frequency and expressions of the transformed variables

CORRECTION TO THE FREQUENCY

Let us suppose that the transformation to be applied on the Hamiltonian $H(q,p)$ is an averaging over some angular variables q_i. After applying the Lie triangle algorithm, the transformed Hamiltonian (truncated at an order n) is now

$$\bar{H}(-,\bar{p}) = \sum_{i=0}^{n} \frac{\epsilon^i}{i!} H_0^n, \tag{2.49}$$

independent of any angular variable. As a consequence, the new frequency associated with each angular variable $\bar{q}_i$ (or each degree of freedom) is then, using Hamilton's equations:

$$\dot{\bar{q}}_i = \frac{\partial \bar{H}}{\partial \bar{p}_i} \tag{2.50}$$

and may be different than the frequencies of the unperturbed problem (integrable Hamiltonian).
If the expression of $\dot{\bar{q}}_i$ is a constant ($\bar{H}$ linear in $\bar{p}_i$), we immediately have the frequency of this degree of freedom. However, when $\bar{H}$ has higher order terms in $\bar{p}_i$, these frequencies depend on initial conditions of the problem.

In our example the small parameter ϵ is included in the coefficients b and c. The transformed Hamiltonian (at order 2) is

$$\bar{H}(\bar{X}) = \sum_{i=0}^{2} \frac{H_0^i}{i!} = n'\bar{X} + 0 + \frac{1}{2}\left(\frac{-b^2}{n'}\bar{X} - \frac{bc}{a}\right) \tag{2.51}$$

showing that the frequency of the unperturbed problem can vary. The frequency associated with

the variable $\bar{l}$ is now

$$\dot{\bar{l}} = \frac{\partial \bar{H}}{\partial \bar{X}} = n' - \frac{b^2}{2n'} = n'' \tag{2.52}$$

To give an idea of the correction, let us take the case of a satellite performing a full orbit in a day around a planet with the mass of the Earth and $J_2 = C_{22} = 10^{-3}$. With these values we have:

$$T = \frac{2\pi}{n} = 1 \text{ day} \qquad T' = \frac{2\pi}{n'} = 0.9999316226 \text{ day} \qquad T'' = \frac{2\pi}{n''} = 0.9999317067 \text{ day} \tag{2.53}$$

The period of the unperturbed problem (associated with n) is obviously 1 day. The correction due to J_2 (transition from n to n') is about 5 seconds while the correction due to the transformation itself (in H_0^2, from n' to n'') is about 10^{-2} seconds.
In this example the correction to the frequency is extremely small but in other cases, especially when a resonance is involved, the frequency may change drastically. In the chapter on core-mantle interactions (Chapter 5) we see that one of the fundamental frequencies of the perturbed problem can be several times smaller than in the model without interactions.
In that case, it is required to use the Lie triangle procedure up to a large order for the frequencies to converge[2].

Milani and Knezevic (1990) used another method for the convergence of the frequencies for proper elements of asteroids. With Hori's technique up to the second-order in the small parameter, they developed and used a fixed point iteration algorithm until the convergence of their frequencies.
In this work, we never use such an iterative method and compensate it by using the Lie triangle procedure up to a large order, which allows for a good convergence of the series far enough from resonances, but takes a very large amount of CPU time.

EXPRESSION OF THE TRANSFORMED VARIABLES

Two scenarios are possible:

- The system is at the exact equilibrium
  In that case, going to cartesian coordinates ($\bar{x}_i = \sqrt{\bar{p}_i}\sin\bar{q}_i, \bar{y}_i = \sqrt{\bar{p}_i}\cos\bar{q}_i$) and equaling Hamilton's equations to 0, we have $\bar{x}_i = \bar{y}_i = 0$, implying $\bar{p}_i = 0$. It is then easy to see that the frequencies of the variables $\bar{q}_i$ are simply the coefficient ($\bar{\omega}_i$) of the linear term of $\bar{H}$ and we have $\bar{q}_i = \bar{\omega}_i t + \bar{q}_{i,0}$.

- The system is not at the equilibrium
  Hamilton's equation $\bar{p}_i = \frac{\partial \bar{H}}{\partial \bar{q}_i} = 0$ still implies that $\bar{p}_i$ is constant, but not 0 necessarily. To compute this value, the inverse Lie triangle algorithm must be used (Henrard (1973), and Libert (2007) for an application of the algorithm) in order to express the transformed variables in function of the non-transformed ones and include initial conditions of the problem.

  Since we will not meet this case in this work, we only mention that it actually gives rise

[2] in the sense that going to further orders does not bring any significant change to the frequencies

to free amplitudes in the evolution of the variables.

Since the transformed Hamiltonian only has linear terms in $\bar{X}$, we find

$$\bar{l} = n''t + \bar{l}_0 \tag{2.54}$$

with $\bar{l}_0$ the initial condition of the (averaged) anomaly.

We suppose that our system is at the equilibrium and get the expression for $\bar{X}$:

$$\bar{X} = 0. \tag{2.55}$$

2.3.3 Time evolution of the variables including the short-period terms

RE-INTRODUCTION OF THE SHORT-PERIOD TERMS IN THE VARIABLES

With the generators of the transformation, it is possible to compute the evolution of any analytic function of the variable. It is simply the canonical Lie transform of this function and its expression is given by applying the Lie triangle procedure.

We consider the following triangle:

$$\begin{array}{cccc} f_0^0 & & & \\ f_1^0 & f_0^1 & & \\ f_2^0 & f_1^1 & f_0^2 & \\ f_3^0 & f_2^1 & f_1^2 & f_0^3 \\ \dots & & & \end{array} \tag{2.56}$$

We put the expression $f(q,p)$ in f_0^0, $f_i^0 = 0\ \forall i \geq 0$, and we use the Lie triangle as before. The recurrence formula is the same as previously (2.14), and the generators were already computed during the averaging process.

The expression of the function $f(q,p)$, including short-period terms, will be found in the diagonal: $f(\bar{q},\bar{p}) = \sum_{i=0}^{n} \left[\frac{f_0^i}{i!}\right]_{q=\bar{q},p=\bar{p}}$, with the variables and moments q and p evaluated at their transformed values (computed previously).

In our example the Hamiltonian depends on l and X while the transformed (averaged) Hamiltonian depends on $\bar{X}$. Let us assume that we want to compute how the perturbation that we included (J_2 and C_{22}) affects the semi-major axis. The relation between the semi-major axis and the variables is $L = \sqrt{\mu a} = L^\star + X$, or

$$a = \frac{(L^\star + X)^2}{\mu}. \tag{2.57}$$

The equilibrium value of X is zero since it corresponds to the 2-body problem, our H_0^0. Applying the Lie triangle described above, with $f_0^0 = X$ and $f_i^0 = 0\ \forall i$, we have for f_0^1 (we recall that $W_1 = \frac{b}{2n'} X \sin 2l + \frac{c}{2n'} \sin 2l$):

$$f_0^1 = f_1^0 + (f_0^0; W_1) = 0 - \frac{\partial W_1}{\partial l} = -\frac{b}{n'} X \cos 2l - \frac{c}{n'} \cos 2l, \tag{2.58}$$

and for f_0^2

$$f_0^2 = f_1^1 + (f_0^1; W_1) = \underbrace{f_2^0}_{0} + C_1^0(\underbrace{f_1^0}_{0}; W_1) + C_1^1(f_0^0; \underbrace{W_2}_{0}) + (f_0^1; W_1) \tag{2.59}$$

$$= \left(\frac{2b}{n'} X \sin 2l + \frac{2c}{n'} \sin 2l\right) \frac{b}{2n'} \sin 2l + \frac{b}{n} \cos 2l \left(\frac{b}{n'} X \cos 2l + \frac{c}{n'} \cos 2l\right) \tag{2.60}$$

$$= \frac{b^2}{n'} X + \frac{bc}{n'} \tag{2.61}$$

At the second order, after evaluating X and l at their transformed values $\bar{X} = 0$ and $\bar{l} = n''t + \bar{l}_0$, we find the expression of X (up to the second order) containing short-period terms

$$X = \sum_{i=0}^{2} \left[\frac{1}{i!} f_0^i\right]_{X=\bar{X}, l=\bar{l}} = 0 + \frac{c}{2n'} \cos 2\bar{l} + \frac{1}{2} \frac{bc}{n'}, \tag{2.62}$$

where we note a second-order variation in the equilibrium, eventually yielding a correction in the mean value of the semi-major axis.

Using equation (2.57), we find the variation of the semi-major axis induced by the perturbation. Note that here, we computed the value of X and then replaced it in equation (2.57). As the theory predicts, it is also possible to use the Lie triangle algorithm on the function itself as long as it is analytical. The results are the same regardless of the method.

With the same values for the coefficients as earlier ($J_2 = C_{22} = 10^{-3}$), we find a 0.5-day oscillation with an amplitude of 5 km with respect to the 42164 km of the unperturbed (geostationary) semi-major axis while the 0.25-day oscillation (second-order)is much smaller with around 10 cm of amplitude.

With a pretty high value of the perturbing parameter (10^{-3} for J_2 and C_{22}), the second-order is already extremely small, and we do not go to further orders.

2.3.4 Summary of the method

To sum up, here are the different steps to perform in order to use this perturbation method by canonical Lie transforms successfully:

① Choice of the transformation and of the parts H_i^0

② Computation of the transformed Hamiltonian and of the generators of the transformation through the algorithm of the Lie triangle

③ Correction to the frequencies

④ Expression of the transformed variables $\bar{q}$ and $\bar{p}$

⑤ Use of the generators and the expression of $\bar{q}$ and $\bar{p}$ to compute the evolution of the variables

We write the numbers of these different steps in the diagram (Figure 2.3) representing this method.

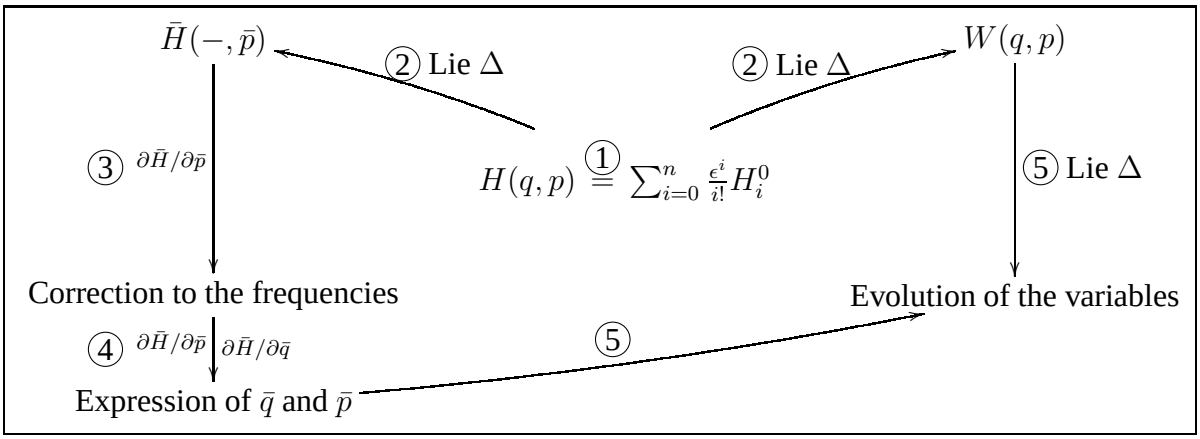

Figure 2.3: Diagram representing our use of the perturbation theory by canonical Lie transforms. The numbers inside circles point where each of the five steps described earlier take place.

2.4 The Poisson series manipulator MSNam

As we saw in the previous sections, the theory of rotation studied in this work will deal with expansions, Poisson brackets, products of periodic and polynomial functions, but also with reference frames in rotation, planetary theories, substitutions of variables by series,... The natural object for the implementaion of this type of studies is obviously Poisson series. Poisson series are Fourier series (linear trigonometric series) with polynomial coefficients:

$$\sum_{\substack{i_1 \dots i_{nvp} \\ j_1 \dots j_{nvt}}} A_{\substack{i_1 \dots i_{nvp} \\ j_1 \dots j_{nvt}}} x_1^{i_1} \dots x_{nvp}^{i_{nvp}} \left\{ \begin{array}{c} \sin \\ \cos \end{array} \right\} (j_1\phi_1 \dots j_{nvt}\phi_{nvt}), \tag{2.63}$$

with *nvp* the number of polynomial variables and *nvt* the number of trigonometric variables. The exponents $i_1 \dots i_{nvt}$ and the arguments $j_1 \dots j_{nvt}$ are integers and the coefficients $A_{\substack{i_1 \dots i_{nvp} \\ j_1 \dots j_{nvt}}}$ are real numbers.

The algebraic computations of this work are realised using the MSNam, standing for "Manipulateur de Séries de Namur". The MSNam is a software gathering very efficient subroutines in order to manipulate Poisson series. It was first written by H. Claes, J. Henrard, M. Moons and J.M. Zune and the idea of the software is described in Henrard (1986). It was later improved by M. Moons (1993) and the last version in Fortran 90 was made by J. Henrard in 2004.

The MSNam is designed to perform efficiently various operations over large Poisson series. The library contains low level subroutines allowing the user to have one Poisson series represented by an integer variable only, thus simplifying the use of the software. The arguments and exponents of the series and the indication that the trigonometric expression is a cosine or a sine are coded and packed in a large array of integers. The coefficients $A_{\substack{i_1 \dots i_{nvp} \\ j_1 \dots j_{nvt}}}$ are stored in a large array of double precision real numbers.

This software allows to perform basic operations such as the addition and the multiplication of two series, the evaluation of trigonometric or polynomial variables, scaling or cutting series at

a given accuracy. It also performs more complicated operations such as the derivation of series, sorting series by largest coefficients, substituting a polynomial variable by another Poisson series, expanding series in the form $(1+x)^y$ around $x=0\ldots$

Especially for problems with a high number of degrees of freedom such as the ones studied in this work, the series of the Hamiltonian or generators of transformation can be extremely large. We experienced the multiplication of series with several hundreds of thousands of terms by each other and the long waiting hours to get the results... We must also mention the work of B. De Saedeleer who, during is Ph.D. thesis (2006), (re-)coded many subroutines improving the efficiency of the MSNam.

With this very performing tool, we take a particular care of having our Hamiltonians and other objects of this work expressed as Poisson series. This underground work as well as the coding (and debugging...) of many subroutines using the MSNam to get our results is actually what required the most efforts, but was rewarded with a very nice understanding of the theory and especially the triggers of particular effects.

As an example, Figure 2.4 shows how series are printed in a file. In this artificial series, the first element is the indication that the term is of a sine or a cosine, then come the 4 angular variables, th numbers below representing the arguments. After the angular variables are displayed the polynomial variables, the numbers below standing for the exponent of each variable, and at the end of each term is the double precision real coefficient of each term of the Poisson series.

```
          SERIES     hamiltonian          0
            NUMBER OF TERMS :      8


       lo  s1  lv  lj        e La1  sK  cK            COEF
cos(    0   0   0   0 ) (    1   0   0   0)   -0.6262692442699455D-01
cos(    0   0   0   0 ) (    0   2   0   0)    0.2539876054048563D+01
cos(    0   0   0   1 ) (    2   0   0   0)    0.7271514303647053D-11
cos(    0   2   0   0 ) (    0   0   1   1)   -0.1335861699494144D-01
cos(    2   0   0   0 ) (    3   0   0   0)   -0.1322945930336678D-01
sin(    2   0   0   1 ) (    0   0   0   0)   -0.2300822235110895D-10
sin(    2   0   0   2 ) (    0   0   0   0)   -0.1067200626336556D-11
sin(    2   2   0   0 ) (    0   0   0   0)   -0.1828882710882281D-01
cos(    2   2   0   1 ) (    0   0   0   0)   -0.1164014344049682D-11
```

Figure 2.4: Example of Poisson series printed by the MSNam in a file.

This artificial Hamiltonian would then be:

$$\begin{aligned} H = &-0.0626\ e + 2.54\ \Lambda_1^2 + 0.72710^{-11}\ e^2\cos(l_j) - 0.0134\ sK\ cK\cos(2\sigma_1) \\ &- 0.0132\ e^3\cos(2l_o) - 0.2310^{-10}\sin(2l_o + l_J) + \ldots. \end{aligned}$$

3

Rotation without planetary forcing

It is finally time to dive into the heart of this work. In this chapter we present various models of rotation, with 1, 2 and then 3 degrees of freedom, but without including any planetary perturbations yet.
After settling the general model and Hamiltonian used in our theory, we develop our 1-degree of freedom model. It is a planar case with only librations in longitude. We will see that this Hamiltonian is quite similar to the example given in the Chapter 2.
The 2-degree of freedom model includes the inclination and obliquity of the planet together with the precessions of the periherm and the ascending node, resulting in the computation of librations both in longitude and latitude.
Finally we introduce the wobble motion of the planet, i.e. the motion of the spin axis with respect to the axis of largest inertia of Mercury.

The model of rotation used here has first been described in two papers of D'Hoedt and Lemaître (2004 and 2005) in which they computed the equilibria and fundamental periods for a rigid Mercury. This chapter is evidently inspired from their theory but our main focus is in the short periods. We also take care that each part of the Hamiltonian is expressed as Poisson series, allowing the use of our series manipulator MSNam, which required a lot of background work.

3.1 The general model

The general model that we use starts similarly to the example described in Chapter 2: we consider a frame centred on the centre of mass of Mercury, a non-spherical planet. The other body orbiting around Mercury is this time not a satellite but the Sun itself, and Mercury is rotating around its spin axis. We are not interested in the variations of the orbit of Mercury around the Sun due to the non-sphericity of the planet (those would be ridiculously small anyway), but rather in the influence of this non-sphericity on the rotation of Mercury itself.
We take into account the 3:2 spin-orbit resonance, the eccentricity of the planet and the fact that Mercury should have a liquid core, that we consider as spherical in this chapter.
Mercury's gravity field is expanded until the order 2 in spherical harmonics, the C_{nm} spherical harmonics being totally unknown for higher orders. Only $J_2 = -C_{20}$, accounting for the oblateness of the planet, and C_{22}, expressing the ellipticity of the equator, are used. To sum up, here are the general hypotheses of this model:

- Mercury's orbital motion is Keplerian,
- Mercury is a non-spherical body, with principal moments of inertia $A < B < C$,
- the gravity field is expanded until order 2 (J_2 and C_{22}),
- the planet is rotating around its spin axis and around the Sun in a 3-2 spin-orbit resonant motion,
- the planet is composed of a spherical liquid core and a mantle, with no core-mantle interaction.

The spherical liquid core hypothesis deserves some more explanation. Mercury has two separate components: a rigid mantle and the liquid core considered as spherical, and we suppose no magnetic or viscous interaction between them. Thus, the rotation of Mercury actually refers to the rotation of its mantle. As a result, the rotational kinetic energy that we consider is that of the mantle and not of the whole body.
The Hamiltonian of this problem is the sum of three parts:

1. H_{2B}, the Keplerian contribution,
2. T, the rotational kinetic energy of the mantle,
3. V_G, the gravitational potential.

In the next subsections, we explain each of these contributions and the set of canonical variables used for this Hamiltonian.

Finally here are the units that we choose: the **Earth year** as time unit, the **equatorial radius of Mercury** as length unit and the **mass of Mercury** as mass unit.

Physical and orbital parameters

Table 3.1 summarizes the main physical and orbital parameters of the planet (at the epoch J2000) adopted for this work.

3.1.1 The Keplerian contribution

Figure 3.1 introduces the orbital variables of our problem, distinguished from other variables by the subscript o. Let us first note that all our reference frames are centred on Mercury. The frame (X_0, Y_0, Z_0) is our inertial reference frame, the ecliptic one and (X_1, Y_1, Z_1) is the orbital frame with Z_1 orthogonal to the orbital plane and X_1 pointing to the periherm. Our variables are

- Ω_o the longitude of the ascending node, positioning the line of nodes, intersection of the inertial and orbital frames,

Orbital period	87.9693 days	Planetary theory (Fienga & Simon, 2004)
Semi-major axis	0.387098 AU	Planetary theory (Fienga & Simon, 2004)
Eccentricity	0.205632	Planetary theory (Fienga & Simon, 2004)
Inclination (to Ecliptic)	$7.005°$	Planetary theory (Fienga & Simon, 2004)
Longitude of the ascending node	$48.331°$	Planetary theory (Fienga & Simon, 2004)
Precession of the ascending node	-0.2189×10^{-4} rad/year	Planetary theory (Fienga & Simon, 2004)
Argument of the perihelion	$29.125°$	Planetary theory (Fienga & Simon, 2004)
Precession of the perihelion	0.4962×10^{-4} rad/year	Planetary theory (Fienga & Simon, 2004)
Rotational period	58.6462 days	Planetary theory (Fienga & Simon, 2004)
Mean radius	2439.7 ± 1 km	NASA website (2010)
Mass	3.3022×10^{23}kg	NASA website (2010)
J_2 (polar flattening)	$(6 \pm 2) \times 10^{-5}$	Anderson et al. (1987)
C_{22} (ellipticity of equator)	$(1 \pm 0.5) \times 10^{-5}$	Anderson et al. (1987)
C_m (greatest moment of inertia of the mantle)	0.19686 (main value used)	Margot et al. (2007)

Table 3.1: Table gathering the main orbital and physical parameters used in this work (centre values in case of intervals). The error bars for the parameters given by the planetary theory are 3.8710^{-13} for the semi-major axis and 10^{-12} for the others (we wrote less significant digits in the table).

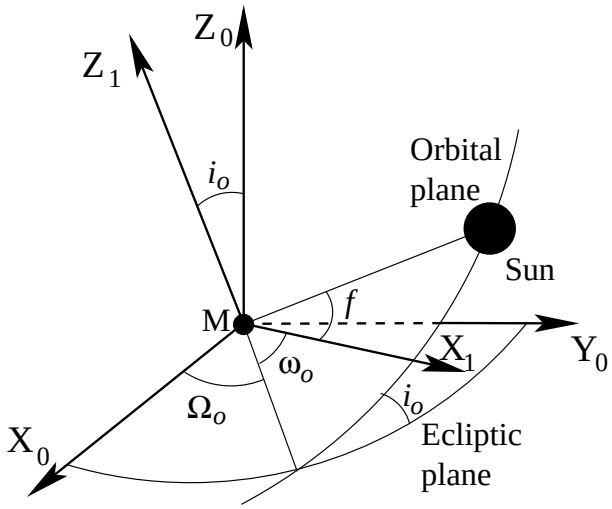

Figure 3.1: The orbital and ecliptic (at J2000) frames, centred on Mercury. The axis X_1 points towards the periherm. The angle i_o is the orbital inclination, Ω_o is the longitude of the ascending node, ω_o is the argument of the periherm and f is the true anomaly.

- i_o the inclination between the ecliptic (inertial) and orbital frames,

- ω_o the argument of the periherm, positioning the orbit with respect to the line of nodes,
- l_o the mean longitude, positioning the Sun on its orbit as if it were moving at a constant angular speed.

The canonical variable associated with the mean anomaly l_o is called L_o and the Hamiltonian of the 2-body problem is simply

$$\boxed{H_{2B} = -\frac{\mu^2}{2L_o^2}} \tag{3.1}$$

with $\mu = G(M + m)$, G the gravitational constant, M the mass of the Sun, and m that of Mercury. In this simple problem, L_o is a constant and its value is $L_o = m\sqrt{\mu a}$, a being the semi-major axis of the orbit.
The variables l_o and L_o are a part of a canonical set of variables called Delaunay's elements and defined as follows:

$$\begin{cases} l_o, & L_o = m\sqrt{\mu a} \\ \omega_o, & G_o = L_o\sqrt{1-e^2} \\ \Omega_o, & H_o = G_o \cos i_o, \end{cases}$$

with e the eccentricity of the orbit.
These orbital variables will be used throughout the work and, due to the 3:2 spin-orbit resonance, they have an important impact on the rotational motion of Mercury, l_o on the longitude and Ω_o on the latitude.

3.1.2 The kinetic energy

The rotational kinetic energy is the Hamiltonian of the free body rotation (Deprit, 1967). The variables that we use are represented in Figure 3.2. As in most theories of rotation, these variables are Andoyer's variables, linked to two sets of Euler angles. The first set is (h, K, g), it locates the position of the angular momentum on our inertial reference frame (the ecliptic). The second set is (g, J, l) and positions the reference frame linked to the shape of the planet (X_3, Y_3, Z_3) (hereafter mentioned as the **figure frame**) in the frame linked to the angular momentum (X_2, Y_2, Z_2) (**spin frame**). The canonical set of Andoyer's variables consists of the three angular variables l, g, h and their conjugated moments L, G, H, defined as follows:

$$\begin{cases} g, & G, \text{ norm of the angular momentum,} \\ h, & H = G\cos K, \\ l, & L = G\cos J. \end{cases}$$

In this formalism, the kinetic energy of a planet whose principal moments of inertia are A, B, C is expressed by (Deprit, 1967):

$$T = \frac{L^2}{2C} + \frac{1}{2}(G^2 - L^2)\left(\frac{\sin^2 l}{A} + \frac{\cos^2 l}{B}\right) \tag{3.2}$$

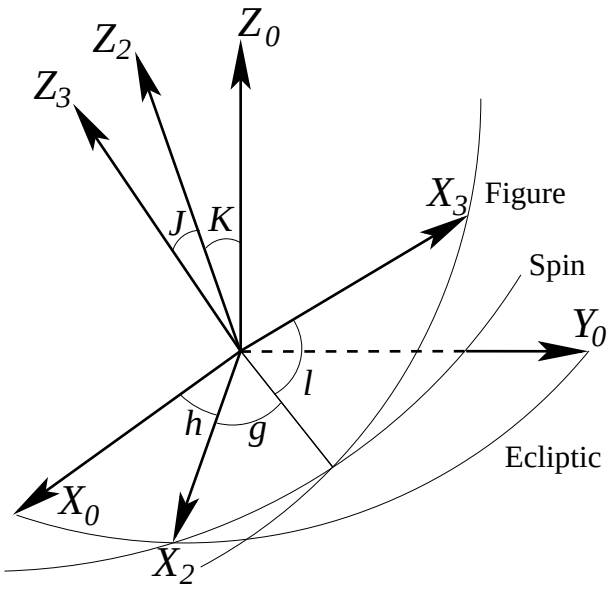

Figure 3.2: The reference frames linked to the rotation (**spin frame**) and the shape of the body (**figure frame**). In the spin frame, X_2 is chosen along the ascending node of the equatorial plane on the ecliptic plane. In the figure frame, X_3 is chosen along the axis of least inertia of the planet. These frames are located with two sets of Euler angles (h, K, g) and (g, J, l) in which K is the ecliptic obliquity and J is the angle between the axis of greatest inertia and the spin axis, that we call the **wobble** angle. Note that (g, h, l) are not well defined whenever J or K is 0.

This set of variables has the major problem that it is singular whenever J or K is zero. Thus we use a set of modified Andoyer's variables defined as follows:

$$\begin{cases} \lambda_1 = l + g + h & \Lambda_1 = G, \\ \lambda_2 = -h & \Lambda_2 = G(1 - \cos K), \\ \lambda_3 = -l & \Lambda_3 = G(1 - \cos J), \end{cases}$$

and the rotational kinetic energy becomes

$$T = \frac{(\Lambda_1 - \Lambda_3)^2}{2C} + \frac{1}{2}(\Lambda_1^2 - (\Lambda_1 - \Lambda_3)^2)\left(\frac{\sin^2\lambda_3}{A} + \frac{\cos^2\lambda_3}{B}\right). \tag{3.3}$$

We chose a model with a spherical liquid core and without core-mantle interactions, implying that only the mantle is rotating. With A_m, B_m, C_m being the principal moments of inertia of the mantle, the rotational kinetic energy is simply that of equation (3.3) where we replace the moments of inertia of the whole body by those of the mantle:

$$\boxed{T = \frac{(\Lambda_1 - \Lambda_3)^2}{2C_m} + \frac{1}{2}(\Lambda_1^2 - (\Lambda_1 - \Lambda_3)^2)\left(\frac{\sin^2\lambda_3}{A_m} + \frac{\cos^2\lambda_3}{B_m}\right)} \tag{3.4}$$

3.1.3 The gravitational potential

The gravitational potential of a body expanded until the second order in spherical harmonics is the following (see e.g. Kaula (1966)):

$$V = \underbrace{-\frac{GMm}{r}}_{V_{2B}} \underbrace{-\frac{GMm}{r}\left(\frac{R_e}{r}\right)^2(-J_2P_2(\sin\eta)+C_{22}P_{22}(\sin\eta)\cos 2\phi)}_{V_G}, \tag{3.5}$$

where V_{2B} is actually included in the Keplerian contribution H_{2B} and V_G is the second order gravitational potential (often referred to as "gravitational potential" only in the text). r is the distance between Mercury and the Sun centres of mass, R_e is the equatorial radius of Mercury, $P_2(x) = \frac{1}{2}(3x^2-1)$ refers to the second order Legendre's polynomial and $P_{22}(x) = 3(1-x^2)$ is its associated polynomial, η is the latitude of the Sun in the figure frame (X_3,Y_3,Z_3), and ϕ its longitude.
Using the usual spherical coordinates, the unit vector pointing towards the Sun in the figure frame (X_3, Y_3, Z_3) is

$$\begin{pmatrix} x \\ y \\ z \end{pmatrix} = \begin{pmatrix} \cos\eta\cos\phi \\ \cos\eta\sin\phi \\ \sin\eta \end{pmatrix}, \tag{3.6}$$

and V_G is now

$$\begin{aligned} V_G &= -\frac{GMm}{r^3}R_e^2\left(\frac{-J_2}{2}(2z^3-x^2-y^2)+3C_{22}(x^2-y^2)\right) && (3.7)\\ &= -\frac{GMm}{r^3}R_e^2\left(\frac{-J_2}{2}(2-3(x^2+y^2))+3C_{22}(x^2-y^2)\right) && (3.8)\\ &= -\frac{GMm}{r^3}R_e^2\left(\frac{-J_2}{2}S+3C_{22}D\right) && (3.9)\end{aligned}$$

where we used the fact that (x, y, z) is a unit vector and we called S the part containing the sum of x^2 and y^2 and D that containing the difference.
Now that we have a rather simple form of the gravitational potential, we try to express it in functions of our canonical set of variables $(l_o, L_o, g_o, G_o, h_o, H_o, \lambda_1, \Lambda_1, \lambda_2, \Lambda_2, \lambda_3, \Lambda_3)$.
Let us first reshape the coefficient of V_G:

$$-\frac{GMm}{r^3}R_e^2 = -\frac{GMmR_e^2}{a^3}\frac{a^3}{r^3} = -\frac{GMm^7\mu^3R_e^2}{L_o^6}\left(\frac{r}{a}\right)^{-3}. \tag{3.10}$$

The next step would be to express the cartesian coordinates (x, y, z) of V_G in function of the true anomaly and of the other variables of our problem. Since the expression of this vector changes if we choose a model with 1, 2 or 3 degrees of freedom, we detail it in each of the following sections. Let us generally consider that we performed that step and that the dependencies of V_G are

$$V_G = V_G(r, f, \omega_o, \Omega_o, L_o\lambda_1, \Lambda_1, \lambda_2, \Lambda_2, \lambda_3, \Lambda_3). \tag{3.11}$$

This set of variables is now almost canonical, only r and f are not canonical variables.
Using Lie transforms (see Appendix A), we express each function of $(r/a, f)$ as functions of the eccentricity e and the mean anomaly l_o. We finally have a gravitational potential depending on canonical variables:

$$V_G = V_G(l_o, L_o, \omega_o, \Omega_o, \lambda_1, \Lambda_1, \lambda_2, \Lambda_2, \lambda_3, \Lambda_3). \tag{3.12}$$

3.1.4 The resonances and the constant precessions in the model

The current Hamiltonian is expressed in a set of canonical variables:

$$H = H_{2B}(L_o) + T(\Lambda_1, \lambda_3, \Lambda_3) + V_G(l_o, L_o, \omega_o, \Omega_o, \lambda_1, \Lambda_1, \lambda_2, \Lambda_2, \lambda_3, \Lambda_3). \tag{3.13}$$

Using the formalism from D'Hoedt & Lemaitre (2004), we now perform a change of variables expressing the 3:2 spin orbit resonance:

$$\sigma_1 = \lambda_1 - \frac{3}{2} l_o - \varpi_o, \tag{3.14}$$

where $\varpi_o = \Omega_o + \omega_o$ is the longitude of the periherm, inducing a change for the moment associated with Ω_o: $H'_o = H_o - G_o$. The variable σ_1 replaces λ_1, and we choose the associated moment to stay Λ_1. However, for this set of variables to remain canonical, the moments associated with l_o (L_o) and ϖ_o (G_o) have to be replaced by $\Lambda_o = L_o + \frac{3}{2}\Lambda_1$ and $G'_o = G_o + \Lambda_1$. Indeed, the following equality must hold:

$$\begin{aligned}
\Lambda_1 d\lambda_1 + L_o dl_o + G_o d\varpi_o &= \Lambda_1 d\sigma_1 + \Lambda_o dl_o + G'_o d\varpi_o & (3.15)\\
&= \Lambda_1 d\left(\lambda_1 - \frac{3l_o}{2} - \varpi_o\right) + \Lambda_o dl_o + G'_o d\varpi_o & (3.16)\\
&= \Lambda_1 d\lambda_1 - \Lambda_1 \frac{3}{2} dl_o - \Lambda_1 d\varpi_o + \Lambda_o dl_o + G'_o d\varpi_o, & (3.17)
\end{aligned}$$

implying that $\Lambda_o = L_o + \frac{3}{2}\Lambda_1$ and $G'_o = G_o + \Lambda_1$.

The second resonant angle describes the 1:1 commensurability between the orbital and rotational nodes, as stated in the third Cassini's law (see Colombo (1966), Peale (1969) or Lemaitre et al. (2006) in the specific case of Mercury):

$$\sigma_2 = \lambda_2 + \Omega_o. \tag{3.18}$$

The moment associated with σ_2 is still Λ_2, but we need to change the one associated with Ω_o to keep a canonical set of variables. With the introduction of ϖ_o, the moment H_o was replaced by $H'_o = H_o - G_o$, and now, H'_o will be replaced by $H''_o = H'_o - \Lambda_2$.

We also add constant precessions of the perihelion and of the ascending node ($\dot{\varpi}_o$ and $\dot{\Omega}_o$, see Table 3.1 for their values). Together with the second resonant angle, they are responsible for the latitudinal motion and the non-zero equilibrium of the obliquity. The Hamiltonian in a more expanded form is then

$$\begin{aligned}
H &= -\frac{\mu^2}{2(\Lambda_o - 3\Lambda_1/2)^2} + T(\Lambda_1, \lambda_3, \Lambda_3) + \dot{\varpi}_o(G'_o - \Lambda_1) + \dot{\Omega}_o(H''_o + \Lambda_2) & (3.19)\\
&\quad -\frac{GMm^7\mu^3 R_e^2}{(\Lambda_o - 3\Lambda_1/2)^6} P(l_o, \varpi_o, \Omega_o, \sigma_1, \Lambda_1, \sigma_2, \Lambda_2, \lambda_3, \Lambda_3), & (3.20)
\end{aligned}$$

P standing for $-\frac{J_2}{2}S + 3C_{22}D$.

3.1.5 Existence of the free librations and Cassini equilibrium

This brief section aims at defining what we call the Cassini equilibrium and explain why we do not consider free librations in our model.

With the constant precessions of the perihelion and ascending node and averaging the Hamiltonian over the mean anomaly, D'Hoedt et al. (2006) computed the equilibria of the Hamiltonian: $(\sigma_1, \sigma_2, \lambda_3) = (0, 0, 0)$ and $(\Lambda_1, \Lambda_2, \Lambda_3) = (\Lambda_1^\star, \Lambda_2^\star, 0)$ with $\Lambda_1^\star$ corresponding to a value computed in the next section and $\Lambda_2^\star$ corresponding to a value of the ecliptic obliquity $K^\star$ slightly different than the inclination i_o (to be computed in later sections). We call it the Cassini equilibrium.

In Lemaitre et al. (2006), the authors show that these equilibria satisfy the generalised Cassini's laws (Beletsky, 2000):

- The body rotates uniformly around a central principal axis of inertia and the angular velocity of this rotation is equal or close to $\frac{3}{2}$ of the mean motion.
- The spin axis of the body (Z_2) and the normal to the orbital plane (Z_1) make a constant angle.
- The spin axis of the body, the normal to the orbital plane and the axis of precession of the orbit (Z_0) lie in one plane.
- Each time the body passes at the pericentre of its orbit, one of the principal axes of inertia and the radius vector of the pericentre lie at equal distances from the line of nodes.

It was also showed by Peale (2005) that Mercury had suffered different non-conservative forces such as tidal forces and core-mantle frictions. Over long periods of times (10^5 years or more), this damping played a major role and reduced the amplitudes of the free motions to very small values, implying that Mercury should be at this Cassini equilibrium.

As a consequence, in this work we consider that Mercury lies at its Cassini equilibrium, with no free motion. Only short-period effects (planetary perturbations) will have an effect on the rotation. This will be useful when computing the transformed expression of the different variables of our problem.

Ideally, this equilibrium should be defined with respect to another inertial reference plane called the Laplace plane, a plane about which the orbital inclination remains constant throughout a precessional cycle. However the motion of the orbital plane is not constant and it is impossible to find a fixed axis which has a constant inclination with respect to the orbital plane. An instantaneous Laplace plane minimizing the variations in inclination over a given period can be defined but is not unique and it is not obvious which is the one to choose. The choice of a suitable Laplace plane for the BepiColombo mission was discussed in D'Hoedt et al. (2009), but this is beyond the scope of this work.

3.1.6 The unperturbed value $\Lambda_1^\star$

We now derive a special value of the angular momentum that we call $\Lambda_1^\star$, corresponding to the norm of the angular momentum in an unperturbed case.
The model is the following: Mercury is a perfect sphere with a spherical liquid core and no core-mantle interaction. The three moments of inertia of the mantle are then equal ($A_m = B_m = C_m$) and $J_2 = C_{22} = 0$. The planet has a proper rotation and orbits around the Sun. The spin axis, the figure axis and the normal to the orbital plane coincide while the orbital inclination is zero ($i_o = K = J = 0$). The Hamiltonian is then simply the sum of the 2-body contribution and of the rotational kinetic energy:

$$H_0 = \frac{-\mu^2}{2L_o^2} + \frac{\Lambda_1^2}{2C_m}, \tag{3.21}$$

Hamilton's equations for the angle λ_1 and l_o give

$$\begin{aligned} \dot{\lambda}_1 &= \frac{\partial H_0}{\partial \Lambda_1} = \frac{\Lambda_1}{C_m} \\ \dot{l}_o &= \frac{\partial H_0}{\partial L_o} = \frac{\mu^2}{L_o^3} = n_o \end{aligned}$$

In our study the orbital motion is always considered as known, either given by a Keplerian orbit or by a planetary theory; our purpose is always to express the motion of the rotation variables. The existence of a $3:2$ spin-orbit resonance, given by the relation:

$$\dot{\lambda}_1 = \frac{3}{2}\,\dot{l}_o$$

corresponds to a specific value, denoted by $\Lambda_1^\star$, of the angular momentum:

$$\Lambda_1^\star = \frac{3}{2}\,n_o\,C_m. \tag{3.22}$$

This special value $\Lambda_1^\star$ will be used later on, as the departure point of series expansion.

3.1.7 Simplifications and expansions

Only one problem remains with this Hamiltonian, but it is this time more of a "technical" issue. As mentioned earlier in Chapter 2.4, our series manipulator MSNam uses Poisson series. As a consequence, it is not possible to implement the denominators of the Keplerian term and of the gravitational potential as they currently are. The obvious solution is performing series expansions around the equilibrium values (understand values of the unperturbed problem) of Λ_o and Λ_1.
We just computed the equilibrium value $\Lambda_1^\star = 3n_oC_m/2$. In the unperturbed problem the value L_o is constant and we have $L_o^\star = m\sqrt{\mu a}$. The relation between L_o, Λ_o and Λ_1 is $L_o = \Lambda_o - 3\Lambda_1/2$, hence we have $\Lambda_o^\star = L_o^\star + 3\Lambda_1^\star/2$.

We now show how to transform H_{2B} and the coefficient of V_G into Poisson series. The Keplerian contribution H_{2B} depends on the variables x and y through $\Lambda_o = \Lambda_o^\star + x$ and $\Lambda_1 =$

$\Lambda_1^\star + y$:

$$H_{2B}(x,y) = \frac{-\mu^2}{2\left(\Lambda_o^\star + x - \frac{3}{2}(\Lambda_1^\star + y)\right)^2} = \frac{-\mu^2}{2\left(L_o^\star + x - \frac{3}{2}y\right)^2}. \tag{3.23}$$

In our units, we have $\Lambda_1^\star \approx 10$ (depending on the value of C_m) and $\Lambda_o^\star \approx L_o^\star \approx 1.5 \times 10^{10}$. Since the parameters J_2 and C_{22} defining the strength of the perturbation are very small (of order 10^{-5}), the variations around the equilibrium values $\Lambda_o^\star$ and $\Lambda_1^\star$ are very small.
Indeed, saying that x is large would mean that the shape of Mercury has a large effect on its orbit around the Sun.
Since $\Lambda_1^\star \approx 10$, we expect y to be small and we expand H_{2B} around $y = 0$. On the opposite $L_o^\star$ is extremely large and expanding H_{2B} around $x = 0$ might seem incorrect. However we see that at each order of the expansion the ratio $\frac{x}{L_o^\star}$ appears, ensuring the convergence of the process.
We thus expand H_{2B} around $x = 0$ and $y = 0$ until the second order.

$$\begin{aligned}
H_{2B}(x,y) &= \frac{-\mu^2}{2L_o^{\star 2}} + \frac{\partial H_{2B}}{\partial x}(0,0)x + 2\frac{\partial H_{2B}}{\partial y}(0,0)y && (3.24)\\
&\quad + \frac{1}{2}\left(\frac{\partial^2 H_{2B}}{\partial x^2}(0,0)x^2 + \frac{\partial^2 H_{2B}}{\partial y^2}(0,0)y^2 + \frac{\partial^2 H_{2B}}{\partial x \partial y}(0,0)xy\right) && (3.25)\\
&= \frac{-\mu^2}{2L_o^{\star 2}} + \frac{\mu^2}{L_o^{\star 3}}x - \frac{3\mu^2}{2L_o^{\star 3}}y && (3.26)\\
&\quad + \frac{1}{2}\left(\frac{-3\mu^2}{L_o^{\star 4}}x^2 - \frac{27}{4}\frac{\mu^2}{L_o^{\star 4}}y^2 + \frac{36}{4}\frac{\mu^2}{L_o^{\star 4}}xy\right). && (3.27)
\end{aligned}$$

The first term is a constant and is dropped. Using $\frac{\mu^2}{L_o^{\star 3}} = n_o$, the mean motion, we have

$$H_{2B}(x,y) = n_o x - \frac{3}{2}n_o y + \frac{1}{2}\frac{n_o}{L_o^\star}(ax^2 + by^2 + cxy). \tag{3.28}$$

With $n_o \approx 26$, the last term is extremely small and we neglect it, showing that an expansion to order 1 only was enough. The Keplerian contribution is then

$$H_{2B}(x,y) = n_o\left(x - \frac{3}{2}y\right) = n_o\left(\Lambda_o - L_o^\star - \frac{3}{2}(\Lambda_1 - \Lambda_1^\star)\right) = n_o\left(\Lambda_o - \frac{3}{2}\Lambda_1\right), \tag{3.29}$$

after coming back to the variables Λ_o and Λ_1 and dropping the constant terms. These expansions were of course checked numerically.

After similar expansions (only linear terms) we have for the coefficient of the gravitational potential

$$\frac{GM\mu^3}{(\Lambda_o - 3\Lambda_1/2)^6} = \frac{GM\mu^3}{L_o^{\star 6}}\left(1 - \frac{6}{L_o^\star}\left(x - \frac{3}{2}y\right)\right), \tag{3.30}$$

and we see that the linear term is 10^{10} (divided by $L_o^\star$) times smaller than the constant term. Bearing in mind that this coefficient is still multiplied by the small parameters J_2 or C_{22}, the linear term in x and y is extremely small and we neglect it.

We can finally write down the general Hamiltonian that will be used in this chapter:

$$H = n_o \left(\Lambda_o - \frac{3}{2}\Lambda_1 \right) + T(\Lambda_1, \lambda_3, \Lambda_3) - \frac{GM\mu^3}{L_o^{\star 6}} P(l_o, \varpi_o, \Omega_o, \sigma_1, \Lambda_1, \lambda_2, \Lambda_2, \lambda_3, \Lambda_3), \quad (3.31)$$

which is now easily implementable as Poisson series.

3.2 Planar case: libration in longitude

3.2.1 Hypotheses

The planar case is a very simplified case of our general model in which:

- the inclination of the orbital plane i_o is 0,
- the (ecliptic) obliquity K of Mercury is 0,
- the wobble angle J between the spin axis and the axis of greatest inertia of the planet is also 0,
- there is no precession of the ascending node or periherm.

With these hypotheses, the Z-axes of all our reference frames (ecliptic, orbital, figure and spin) coincide. The only difference with the case used to compute the special value $\Lambda_1^\star$ is that we consider that the planet is not spherical (J_2 and C_{22}).

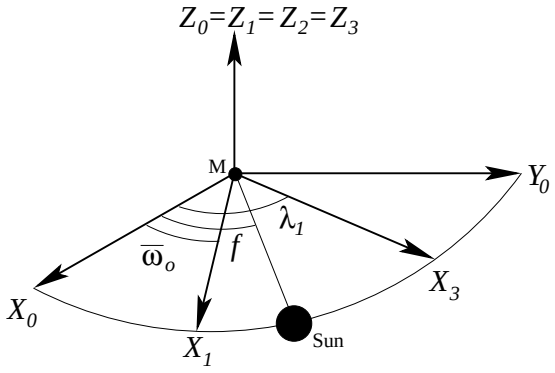

Figure 3.3: Case where $i_o = J = K = 0$. Orbit and rotation occur in the same plane and the axis of greatest inertia coincides with the spin axis.

3.2.2 The Hamiltonian

The first part of the Hamiltonian, the Keplerian H_{2B}, is obviously not affected by the simplifications. The first change comes in the rotational kinetic energy. Since $J = 0$, the kinetic energy is simply

$$T = \frac{\Lambda_1^2}{2C_m}. \quad (3.32)$$

For the gravitational potential, we must first go back to equations (3.8) and (3.10):

$$V_G = -\frac{GM\mu^2}{L_o^{\star 6}} \left(\frac{r}{a} \right)^{-3} \left(\frac{-J_2}{2}(2 - 3(x^2 + y^2)) + 3C_{22}(x^2 - y^2) \right), \quad (3.33)$$

with (x, y, z), the vector pointing towards the Sun that we must express in the figure frame. In the orbital frame we simply have $(x, y, z) = (\cos f, \sin f, 0)$ with f the true anomaly. Then we perform a rotation around the Z-axis of angle $-\varpi$, and another one of angle λ_1. The vector

(x, y, z) in the figure frame is then $(x, y, z) = (\cos(f + \varpi - \lambda_1), \sin(f + \varpi - \lambda_1), 0)$ and the gravitational potential becomes

$$V_G = -\frac{GM\mu^3}{L_o^{\star 6}} \left(\frac{r}{a}\right)^{-3} \left(\frac{J_2}{2} + 3C_{22}\cos(2(f + \varpi - \lambda_1))\right), \tag{3.34}$$

The following step is the expansion of $(r/a)^{-3}$ and of $\cos f$ and $\sin f$ in function of the eccentricity e and the mean anomaly l_o. This step is explained in Appendix A.
Finally a last change of variables from $(l_o, L_o, \lambda_1, \Lambda_1)$ to $(l_o, \Lambda_o, \sigma_1, \Lambda_1)$ to introduce the resonant angle $\sigma_1 = \lambda_1 - 3l_o/2$ and the evaluation of ϖ_o (constant since there is no precession) at its J2000 value (Table 3.1) give the Hamiltonian

$$H(l_o, \Lambda_o, \sigma_1, \Lambda_1) = n_o(\Lambda_o - 3\Lambda_1/2) + \frac{\Lambda_1^2}{2C_m} - \frac{GM\mu^3}{L_o^{\star 6}} \left(\frac{J_2}{2} S(l_o) + 3C_{22} D(l_o, \sigma_1)\right), \tag{3.35}$$

where the functions S and D depend only on the mean anomaly l_o and the resonant angle σ_1:

$$S = \sum_{i=1}^{2*\text{order}} a_i \cos(i l_o) \quad \text{and} \quad D = \sum_{i=-2*\text{order}}^{2*\text{order}} b_i \cos(i l_o + 2\sigma_1) \tag{3.36}$$

with order being the order of the expansion in eccentricity of the functions $\cos f$ and $\sin f$ (we have 2*order in the sum because the square of $\cos f$ and $\sin f$ is computed), and the coefficients a_i, b_i are polynomial functions of the eccentricity.
In this chapter without planetary perturbations, the eccentricity is evaluated at the value of Table 3.1.

3.2.3 Applying the Lie triangle procedure

Now that the Hamiltonian is expanded in Poisson series we want to use it to compute the libration in longitude of Mercury. To do so we use the perturbation method based on canonical Lie transforms developed in Chapter 2. We recall the 5 steps of this method:

① Choice of the transformation and of the parts H_i^0

② Computation of the transformed Hamiltonian and of the generators of the transformation through the algorithm of the Lie triangle

③ correction to the frequencies

④ Expression of the transformed variables $\bar{q}$ and $\bar{p}$

⑤ Use of the generators and the expression of $\bar{q}$ and $\bar{p}$ to compute the evolution of the variables.

In the text, whenever we start a new step it will be indicated by a ⋕.

① The transformation that we use is an averaging transformation. With the generator of this transformation we will be able to compute the libration in longitude, i.e. the evolution of

the resonant angle σ_1.
Before starting the averaging process, from the triangle

$$\begin{array}{lll} H_0^0 & & \\ H_1^0 & H_0^1 & \\ H_2^0 & H_1^1 & H_0^2 \\ \dots & & \end{array} \tag{3.37}$$

in which we find the initial Hamiltonian in the first column and the transformed one in the diagonal, we must choose what to put in H_i^0. This choice and the choice of the transformation itself are critical and can lead to the non-convergence of the process if not well-thought, as we are about to see.

A first choice

The most immediate choice is

$$\begin{aligned} H_0^0(\Lambda_o, \Lambda_1) &= H_{2B} + T \\ H_1^0(l_o, \sigma_1) &= V_G(l_o, \sigma_1) \end{aligned}$$

The transformation we choose to perform is an average over all angular variables.

② In the first-order homological equation

$$H_0^1 = H_1^0 + (H_0^0; W_1), \tag{3.38}$$

we choose the new Hamiltonian H_0^1 to be the average of H_1^0 over all the angular variables:

$$H_0^1 = \left(\frac{1}{2\pi}\right)^2 \int_0^{2\pi}\int_0^{2\pi} H_1^0(l_o, \sigma_1) dl_o d\sigma_1 = 0,$$

since the gravitational potential is composed of periodic terms only. The first-order homological equation is then

$$\begin{aligned} H_0^1 - H_1^0 &= (H_0^0; W_1) \\ -H_1^0 &= -\frac{\partial H_0^0}{\partial \Lambda_0}\frac{\partial W_1}{\partial l_o} - \frac{\partial H_0^0}{\partial \Lambda_1}\frac{\partial W_1}{\partial \lambda_1} \\ -H_1^0 &= -n_o \frac{\partial W_1}{\partial l_o} - \left(\frac{-3}{2} n_o + \frac{\Lambda_1}{C_m}\right)\frac{\partial W_1}{\partial \lambda_1}. \end{aligned}$$

Since we expect Λ_1 to be very close to $\Lambda_1^\star = \frac{3}{2} n_o C_m$, $\frac{\partial H_0^0}{\partial \Lambda_1} = -\frac{3}{2} n_o + \frac{\Lambda_1}{C_m}$ is very small. We call $\nu_1 = \frac{\partial H_0^0}{\partial \Lambda_1}$. The generator is thus

$$W_1 = -Z\left(\frac{J_2}{2}\sum_{i=1}^{6}\frac{a_i \sin(i l_o)}{i n_o} + 3C_{22}\sum_{i=-5}^{5}\frac{b_i \sin(i l_o + 2\sigma_1)}{i n_o + 2\nu_1}\right), \tag{3.39}$$

with $Z = \frac{GM\mu^3}{L_o^{\star 6}}$. Unfortunately, this generator has a small divisor ($\nu_1 \ll n_o$), when $i = 0$ in the second sum, leading to the non-convergence of the Lie triangle procedure. We pushed the computations further (at higher orders of the Lie Triangle) and the obvious non-convergence of the process forced us to review our starting point. The problem of this method was the averaging transformation over angular variables with large and short periods.

The right choice

① We try to introduce the algorithm in another way, with a different choice of the transformation. The transformation chosen is now an average over the fast angular variable only (l_o). We choose H_0^0 to be the pendulum approximation of the problem:

$$H_0^0(-, \Lambda_o, \sigma_1, \Lambda_1) = \langle H \rangle_{l_o} = H_{2B} + T - E\cos(2\sigma_1), \tag{3.40}$$

with $E = 3ZC_{22}b_0 = 3GM\mu^3 C_{22} b_o / L_o^{\star 6}$.
H_1^0 corresponds to all the terms of V_G containing explicitly l_o in the trigonometric terms, i.e. the sum S and the difference D with $i \neq 0$. Therefore $H_0^1 = 0$, after a first order averaging over l_o.

② This time the generator W_1 will not contain any term with small denominators (ν_1). It must however be evaluated carefully. Indeed, if we refer to the first-order homological equation (3.38), we have to evaluate the Poisson bracket $(H_0^0; W_1)$ and at this step of the resolution, it means that 3 partial derivatives of H_0^0 (with respect to Λ_o, to Λ_1 and to σ_1) are different than zero. This gives a three dimensional partial differential equation to solve for W_1 and the derivative with respect to σ_1 is problematic.

The way of avoiding this problematic derivative is well-known: introducing action-angle variables in the pendulum approximation H_0^0 so that it does not depend anymore on any angle. This also allows us to compute the fundamental period of σ_1.
We could perform the complete transformation to action-angle variables, with the elliptic functions expression. However, because Mercury is blocked at the nearly exact resonance corresponding to $\sigma_1 = 0$ (D'Hoedt & Lemaitre, 2004), it is simpler to introduce immediately the action-angle variables of the harmonic oscillator. Here is how we proceed:

Expansions

First we expand functions of σ_1 around $\sigma_1 = 0$ up to the second order: $\cos(2\sigma_1) = 1 - (2\sigma_1)^2/2 = 1 - 2\sigma_1^2$.
Then we expand the 2-body problem Hamiltonian and the kinetic energy around $\Lambda_1^\star$: $\Lambda_1 = \Lambda_1^\star + X$. We have

$$H_{2B} = n_o(\Lambda_o - 3\Lambda_1/2) = n_o(\Lambda_o - 3\Lambda_1^\star/2) - 3n_o X/2. \tag{3.41}$$

The kinetic energy can be described by the same variable X:

$$T(X) = \frac{\Lambda_1^2}{2C_m} = \frac{(\Lambda_1^\star + X)^2}{2C_m} = \frac{\Lambda_1^{\star 2}}{2C_m} + \frac{\Lambda_1^\star}{C_m}\, X + \frac{1}{2C_m}\, X^2. \tag{3.42}$$

The equation (3.22) implies that the linear terms of H_{2B} and T cancel each other.
The Hamiltonian H_0^0 can now be written (the constant terms have been dropped):

$$H_0^0 \simeq n_o\Lambda_o + 2E\sigma_1^2 + KX^2, \tag{3.43}$$

where $K = \frac{1}{2C_m}$.

Changes of variables

The first change of variables is canonical and performed to obtain the same coefficient for σ_1^2 and X^2:

$$\begin{cases} \sigma_1 = \sqrt[4]{\frac{K}{2E}}\, x_s \\ X = \sqrt[4]{\frac{2E}{K}}\, y_s \end{cases} \tag{3.44}$$

The Hamiltonian H_0^0 is now

$$H_0^0 = n_o \Lambda_o + \sqrt{2EK}\left(x_s^2 + y_s^2\right).$$

The second change is the introduction of the action-angle variables.

$$\begin{cases} x_s = \sqrt{2J}\, \sin(\psi) \\ y_s = \sqrt{2J}\, \cos(\psi) \end{cases} \tag{3.45}$$

to have

$$H_0^0 = n_o \Lambda_o + 2\sqrt{2EK}\, J.$$

$H_0^0 = H_0^0(\Lambda_o, J)$ does not depend on any angle anymore. It is now possible to start the averaging Lie process described previously and to compute the first order generator:

$$W_1 = -Z \left(\sum_{i=1}^{\text{order}} \sum_{j=-\text{order}}^{\text{order}} \frac{a_{ij} J'^{|j|} \sin(i l_o + j\psi)}{i n_o + j\dot{\psi}} + \sum_{i=1}^{\text{2*order}} \frac{b_i J'^2 \sin(i l_o)}{i n_o} \right), \tag{3.46}$$

where $J' = \sqrt{2J}$.

Let us remark that the case $i = 0$ does not appear anymore in the sum and the generator does not contain any very small frequency like $\dot{\psi}$ alone in the denominators. This guarantees the numerical convergence of the process.

③ If we stop the procedure at the first order and remind that $H_0^1 = 0$, the averaged Hamiltonian $\bar{H}$ is reduced to H_0^0. Let us denote the transformed variables by $\bar{\psi}$ and $\bar{l}_o$ and the conjugated transformed moments by $\bar{J}$ and $\bar{\Lambda}_1$; the two mean frequencies are given by:

$$\begin{aligned} \dot{\bar{l}}_o &= \frac{\partial \bar{H}}{\partial \bar{\Lambda}_o} = n_o \\ \dot{\bar{\psi}} &= \frac{\partial \bar{H}}{\partial \bar{J}} = 2\sqrt{2EK} = \omega_{\bar{\psi}}. \end{aligned}$$

In our computations, with the values $C_{22} = 10^{-5}$, $J_2 = 6\ 10^{-5}$ (Anderson et al., 1987), $C = 0.34$, $C_m = 0.19686$, the period of l_o is 87.97 days and the period of $\bar{\psi}$ is $T_{\bar{\psi}} = \pi/\sqrt{2EK} = 12.06$ years.

This value is the period of the free libration in longitude. If we look at what E and K represent (3.43), we see that $T_{\bar{\psi}}$ is proportional to $\sqrt{C_m/(B-A)}$.

For example in the papers of D'Hoedt and Lemaître (2004, 2005), they chose $C_{22} = (B - A)/4 = 10^{-5}$ and they consider a rigid Mercury ($C_m = C = 0.34$) so that $T_{\bar{\psi}} = 15.85$ years.

With our analytical method, it is actually possible to have a very accurate expression for this formula. We have

$$T_{\bar{\psi}} = 2\pi\sqrt{\frac{L_o^{\star 6}}{3GM\mu^3 b_0}}\sqrt{\frac{C_m}{B-A}}, \tag{3.47}$$

with

$$b_0 = \frac{7}{2}e - \frac{123}{16}e^3 + \frac{489}{128}e^5 + \dots. \tag{3.48}$$

In Figure 3.4, we plot the fundamental period with respect to this moment ratio $(B-A)/C_m$. We emphasize 3 cases: the rigid case, the main case, standing for our principal values of C_{22} and C_m (hence $(B-A)/C_m$) chosen in this work and what we call the resonant case will be discussed in the next chapter.

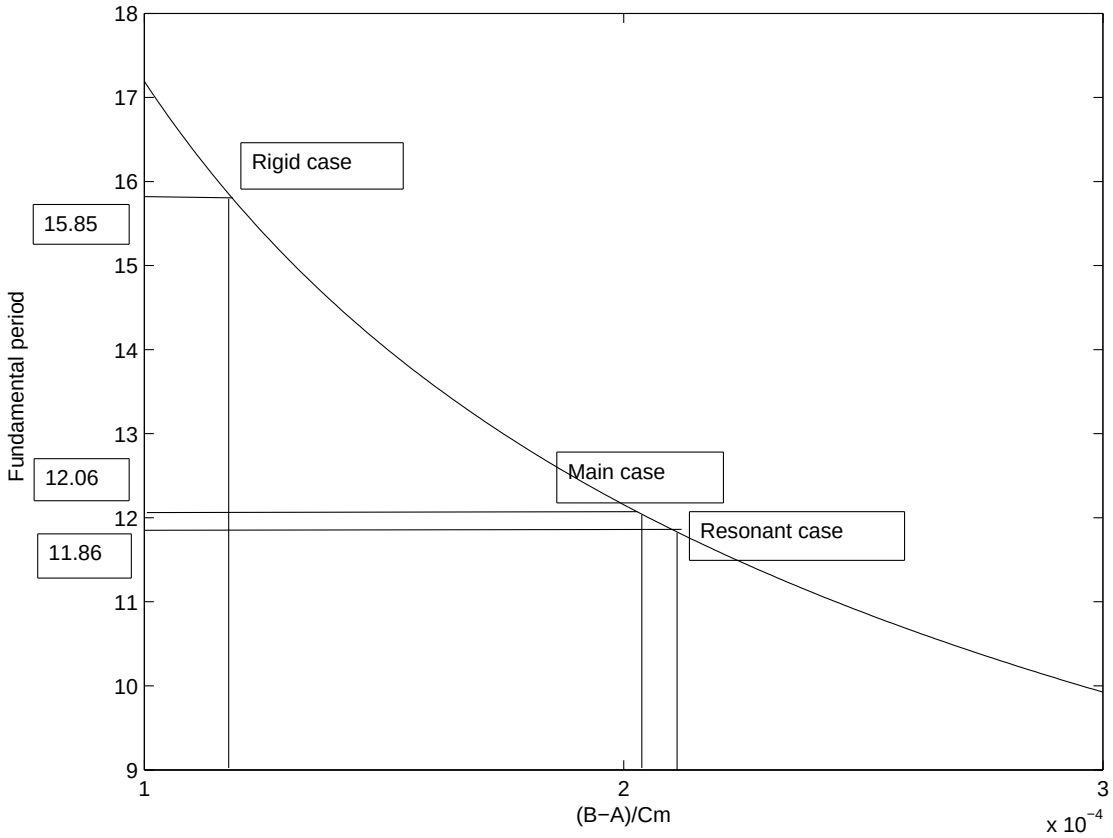

Figure 3.4: Plot of the fundamental period $T_{\bar{\psi}}$ in function of the moment ratio $(B-A)/C_m$. Three cases are highlighted, one corresponding to a rigid Mercury, the second corresponding to our main value adopted for this work, and finally what we call the resonant case, to be defined in the next chapter.

The generators of further orders are computed as described in Chapter 2, using the algorithm of the Lie triangle. Adding the 2nd order of the Lie triangle, the transformed Hamiltonian has the form:

$$\bar{H} = \omega'_{\bar{\psi}}\bar{J} + c\bar{J}^2, \tag{3.49}$$

with $\omega'_{\bar{\psi}}$ slightly different than $\omega_{\bar{\psi}}$ (second-order correction). As always with polar coordinates, when the radial component $\bar{J} = 0$, the angle $\bar{\psi}$ is not defined. To avoid this singularity, we introduce the averaged variables $\bar{x}_s$ and $\bar{y}_s$:

$$\begin{aligned} \bar{x}_s &= \sqrt{2\bar{J}}\ \sin(\bar{\psi}) \\ \bar{y}_s &= \sqrt{2\bar{J}}\ \cos(\bar{\psi}) \end{aligned}$$

to describe the averaged system and compute the equilibria. The Hamiltonian is then

$$\bar{H} = \omega'_{\bar{\psi}}(\bar{x}_s^2 + \bar{y}_s^2) + c(\bar{x}_s^2 + \bar{y}_s^2)^2, \tag{3.50}$$

and one of the solutions of Hamilton's equations for the equilibria is $(\bar{x}_s, \bar{y}_s) = (0, 0)$, implying that $\bar{J} = 0$, which is the solution corresponding to the Cassini equilibrium ($\Lambda_1^\star$). We also have

$$\dot{\bar{\psi}} = \frac{\partial \bar{H}}{\partial \bar{J}} = \omega'_{\bar{\psi}} + c\bar{J}, \tag{3.51}$$

giving the modified frequency (after evaluating $\bar{J} = 0$) for $\bar{\psi}$:

$$T_{\bar{\psi}} = \frac{2\pi}{\omega'_{\bar{\psi}}} = 12.057 \text{ years instead of } 12.06 \text{ years.} \tag{3.52}$$

The frequency of $\bar{l}_o$ is not modified.

④ The expression of the transformed variables is quite immediate. We have already computed that $\bar{J} = 0$, and the expressions of the angles are immediate:

$$\bar{l}_o = n_o t + l_{o,0} \tag{3.53}$$

and

$$\bar{\psi} = \omega'_{\bar{\psi}} t + \bar{\psi}_0. \tag{3.54}$$

Note that $\bar{\psi}$ is never present in the Poisson series since the angles that we are looking to reintroduce are the short-period angles (here only l_o). We actually change the variables to cartesian coordinates of our main degrees of freedom to avoid singularities since $\bar{J} = 0$.

3.2.4 Libration in longitude

⑤ The libration in longitude is the evolution of the resonant angle σ_1. To study that, we use the generators of the transformation and the expression of the transformed variables computed in the previous part along with the recurrence formula of the Lie triangle described in Chapter 2. We go back to our initial variables σ_1 and Λ_1 through the cartesian coordinates x_s and y_s (equation (3.44)):

$$\begin{aligned} \sigma_1 &= f_{\sigma_1}(x_s) = \sqrt[4]{\frac{K}{2E}}\ x_s \\ \Lambda_1 &= f_{\Lambda_1}(y_s) = \Lambda_1^\star + \sqrt[4]{\frac{2E}{K}}\ y_s. \end{aligned}$$

To compute the evolution of the variables using the generators of the averaging Lie transform, we consider the triangle

$$\begin{array}{llll} f_0^0 & & & \\ - & f_0^1 & & \\ - & f_1^1 & f_0^2 & \\ \dots & & & \end{array} \tag{3.55}$$

where we put either f_{σ_1} or f_{Λ_1} in f_0^0. The expression of σ_1 including short-period terms (with l_o and harmonics) lies in the diagonal of the triangle: $\sigma_1 = \sum_{i=0}^{n} \frac{f_0^i}{i!}$ where x_s and y_s in these expressions are evaluated at the transformed values: $\bar{x}_s = \bar{y}_s = 0$. The recurrence formula to compute the intermediate f_j^n is

$$f_j^n \;=\; f_{j+1}^{n-1} + \sum_{i=0}^{j} C_j^i\big(f_{j-i}^{n-1}; W_{1+i}\big),$$

and allows to compute the libration in longitude of Mercury.

Table 3.2 gives the libration in longitude using the Lie triangle until order 1 in the form $\sigma_1 = \sum_{i=1}^{2^*\text{order}} c_i \cos(i l_o)$. The largest contribution is the 88-day libration with an amplitude around 35 arcsec. Then come the harmonics of l_o, the 44-day, 29-day librations with amplitudes of about 3.8 arcsec and 0.38 respectively. The other ones are much smaller.
Going to the second order of Lie triangle, the changes are very small (numbers in brackets in table 3.2), of about 10^{-3} arcsec. The next orders bring of course even smaller contributions that we do not mention.

	Libration in longitude		
l_o	Period	Amplitude	Ratio
1	87.970 d	35.850 (35.848)	1.0000
2	43.985 d	3.7538 (3.7506)	0.1047
3	29.323 d	0.3859 (0.3860)	0.0108
4	21.992 d	0.0802 (0.0802)	0.0022
5	17.594 d	0.0139 (0.0139)	0.0004

Table 3.2: Longitudinal librations of Mercury, obtained analytically using the first-order generator of a Lie transform, from the resonant argument σ_1. The amplitudes are expressed in arcsec and the numbers in brackets are the contributions due to the second-order generator. The ratio is computed with respect to the 88-day contribution. Only the main contribution are given.

Similarly to Table 3.2, Table 3.3 gives the variation of the norm of the angular momentum in the form $\Lambda_1 = \sum_{i=0}^{2^*\text{order}} d_i \cos(i l_o)$, with $b_0 = 7.7035\ m\, R_e^2$ year^{-1} the mean value of Λ_1.

Figure 3.5 plots the libration in longitude angle σ_1 and its associated momentum, the norm of the angular momentum Λ_1 over one year. Since we put Mercury at the equilibrium ($\bar{\sigma_1} = 0$ and $\bar{\Lambda_1} = \Lambda_1^\star$) and we superpose small periodic terms using the generators afterwards, we have no free libration. The maximal amplitude of the forced libration is a little more than 38 arcsec.

		Variations of Λ_1	
l_o	Period	Amplitude	Ratio
constant term	-	7.7035	
1	87.970 d	0.89226×10^{-3} (0.89221×10^{-3})	1.0000
2	43.985 d	-0.18791×10^{-3}(-0.18776×10^{-3})	0.2106
3	29.323 d	-0.02850×10^{-3}(-0.02851×10^{-3})	0.0319
4	21.992 d	-0.00792×10^{-3}(-0.00792×10^{-3})	0.0089
5	17.594 d	0.00170×10^{-3} (0.00170×10^{-3})	0.0019

Table 3.3: Variations of Λ_1, the norm of the angular momentum. As in the previous table, these results are obtained analytically using the first-order generator of a Lie transform. The amplitudes are expressed in the units of the angular momentum, $m\,R_e^2$ year^{-1}. The numbers in brackets are the contributions due to the second-order generator.

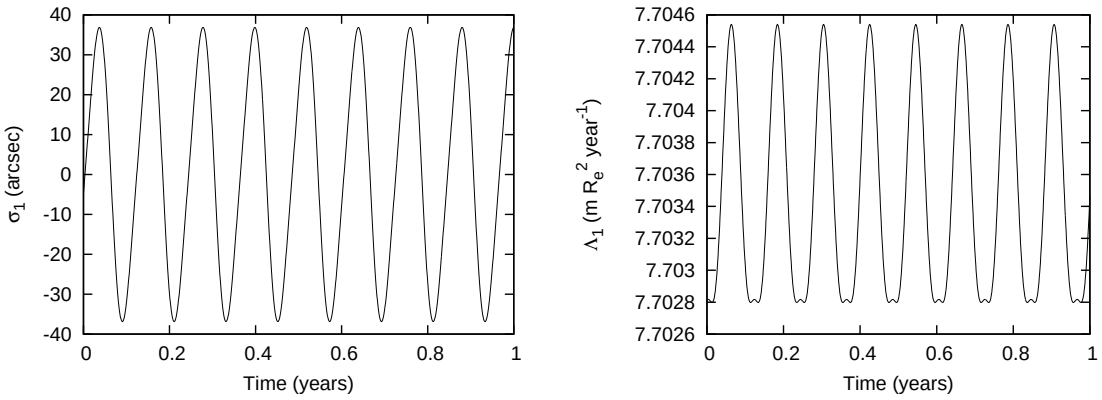

Figure 3.5: Left panel: evolution of the resonant angle σ_1 (the libration in longitude) over one year. With the parameters chosen, we obtain a maximal amplitude of 38.68 arcsec. Right panel: evolution of the associated momentum Λ_1 over one year around the mean value.

3.3 Latitudinal librations

3.3.1 Hypotheses

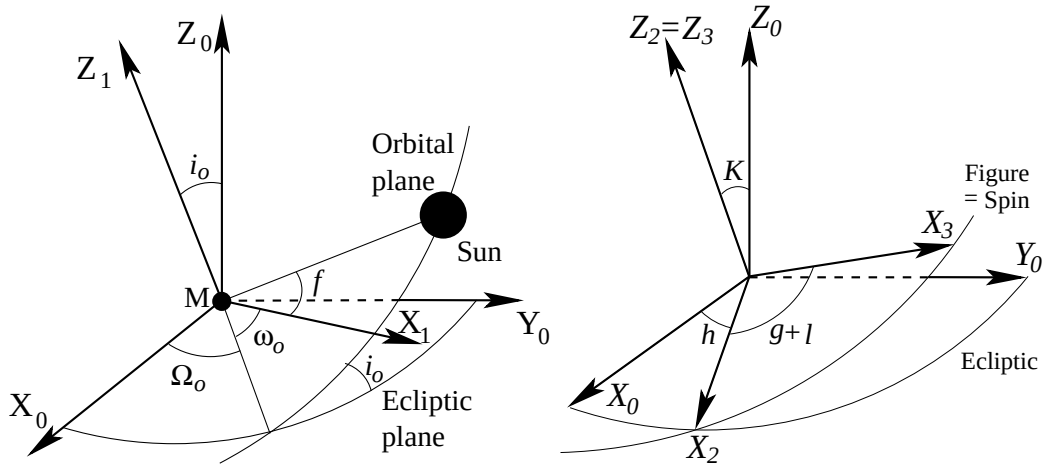

Figure 3.6: In this case, the orbital inclination i_o and the ecliptic obliquity K are not zero anymore. Orbit and rotation do not occur in the same plane anymore but the axis of greatest inertia still coincides with the spin axis.

In this 2-degree of freedom[1] model, almost everything from the complete model is added. The only simplification is that the wobble angle J is zero, implying that the Z-axes of the spin and the figure frames are equal. The hypotheses for this model are then:

- the inclination of the orbital plane i_o and the (ecliptic) obliquity are not 0,
- there is a precession of the ascending node and periherm,
- the wobble angle J between the spin axis and the axis of greatest inertia of the planet is still 0.

3.3.2 The Hamiltonian

Changes in V_G

The Keplerian contribution and the kinetic energy are the same as in our 1-degree of freedom Hamiltonian:

$$H_{2B} = n_o(\Lambda_o - 3\Lambda_1/2) \quad \text{and} \quad T = \frac{\Lambda_1^2}{2C_m}. \tag{3.56}$$

[1]When we mention 1, 2 or 3 degrees of freedom, we refer to what we call the main degrees of freedom, related to the rotational motion of the planet. Technically, the Hamiltonian used has more degrees of freedom if we take into account the mean anomaly l_o and its conjugated moment L for this chapter or the longitudes of the planets and their moments in the next one.

For the gravitational potential

$$V_G = -\frac{GM\mu^2}{L_o^{\star 6}} \left(\frac{r}{a}\right)^{-3} \left(\frac{-J_2}{2}(2-3(x^2+y^2)) + 3C_{22}(x^2-y^2)\right), \tag{3.57}$$

we must once again express (x, y, z), the vector pointing towards the Sun in the figure frame, in our set of variables. For that, we perform a series of rotations:

$$\begin{pmatrix} x \\ y \\ z \end{pmatrix} = R_3(g+l)R_1(K)R_3(h) \times \tag{3.58}$$

$$R_3(-\Omega_o)R_1(-i_o)R_3(-\omega_o) \begin{pmatrix} \cos f \\ \sin f \\ 0 \end{pmatrix}, \tag{3.59}$$

which gives in the modified Andoyer's variables

$$\begin{pmatrix} x \\ y \\ z \end{pmatrix} = R_3(\lambda_1+\lambda_2)R_1(K)R_3(-\lambda_2) \times \tag{3.60}$$

$$R_3(-\Omega_o)R_1(-i_o)R_3(-\omega_o) \begin{pmatrix} \cos f \\ \sin f \\ 0 \end{pmatrix}, \tag{3.61}$$

the rotation matrices being defined as

$$R_1(\phi) = \begin{pmatrix} 1 & 0 & 0 \\ 0 & \cos(\phi) & \sin(\phi) \\ 0 & -\sin(\phi) & \cos(\phi) \end{pmatrix} \quad \text{and} \quad R_3(\phi) = \begin{pmatrix} \cos(\phi) & \sin(\phi) & 0 \\ -\sin(\phi) & \cos(\phi) & 0 \\ 0 & 0 & 1 \end{pmatrix}. \tag{3.62}$$

The gravitational potential now depends on the variables $(r, f, i_o, \omega_o, \Omega_o, \lambda_1, \lambda_2, K)$ which is not a canonical set of variables. The inclination considered as constant in this model is evaluated at the value given in Table 3.1.
The first step to make this set canonical is, as in the previous case, the expansion of $(r/a)^{-3}$ and $\cos f$ and $\sin f$ in functions of e and l_o. With e also a constant in this model, we now have

$$V_G = V_G(l_o, \omega_o, \Omega_o, \lambda_1, \lambda_2, K) \tag{3.63}$$

Introducing the resonant angles $\sigma_1 = \lambda_1 - \frac{3}{2}l_o - \varpi_o$ expressing the 3:2 spin-orbit resonance and $\sigma_2 = \lambda_2 + \Omega_o$ representing the 1:1 commensurability between orbital and rotational nodes, and after adding the constant precessions, the Hamiltonian is

$$\begin{aligned} H &= n_o(\Lambda_o - 3\Lambda_1/2) + \dot{\varpi}_o(G'_o - \Lambda_1) + \dot{\Omega}_o(H''_o + \Lambda_2) + \frac{\Lambda_1^2}{2C_m} \\ &+ V_G(l_o, \varpi_o, \Omega_o, \sigma_1, \sigma_2, K). \end{aligned} \tag{3.64}$$

Changes of variables

The only problem remaining with the Hamiltonian (3.64) is the dependency on K in the gravitational potential, preventing the set of variables from being canonical. The relation between K and the canonical variables is pretty simple:

$$\Lambda_2 = \Lambda_1(1 - \cos K). \tag{3.65}$$

Since K was introduced with rotations, the occurences of K in V_G are through $\cos K$, $\sin K$ and their products and squares (since we use x^2 and y^2 in V_G). We must also remember that the MSNam requires Poisson series. For all these reasons we perform the change of variables

$$(l_o, \Lambda_o, \varpi_o, G'_o, \Omega_o, H''_o, \sigma_1, \Lambda_1, \sigma_2, K) \rightarrow (l_o, \Lambda'_o, \varpi_o, G''_o, \Omega_o, H'''_o, x_1, y_1, x_2, y_2) \tag{3.66}$$

with

$$\left\{\begin{array}{lcl} \Lambda_o &=& \Lambda_1^\star \Lambda'_o \\ G'_o &=& \Lambda_1^\star G''_o \\ H''_o &=& \Lambda_1^\star H'''_o \\ \sigma_1 &=& x_1 \text{ (Taylor expansion around } \sigma_1 = 0) \\ \Lambda_1 &=& \Lambda_1^\star(1 + y_1) \\ x_2 &=& \sqrt{\frac{2\Lambda_2}{\Lambda_1^\star}} \sin\sigma_2 \\ y_2 &=& \sqrt{\frac{2\Lambda_2}{\Lambda_1^\star}} \cos\sigma_2 \end{array}\right. \tag{3.67}$$

which is canonical with multiplier $1/\Lambda_1^\star$.
Since we do not want to get too technical (it is already enough), we explain the reasons for this particular change of variables in Appendix B. Let us also mention that even if it stands in a few lines in this thesis, implementing these changes of variables and verifying that it is actually correct and coherent is not such an easy task and should not be overlooked.
After these changes of variables and expansions, the Hamiltonian is

$$\begin{aligned} H \;=\; & \frac{1}{\Lambda_1^\star}\Bigg[n_o(\Lambda_1^\star \Lambda'_o - 3\Lambda_1^\star(1+y_1)/2) + \frac{\Lambda_1^{\star 2}(1+y_1)^2}{2C_m} \\ & + \dot{\varpi}_o\left(\Lambda_1^\star G''_o - \Lambda_1^\star(1+y_1)\right) + \dot{\Omega}_o\left(\Lambda_1^\star H'''_o + \frac{\Lambda_1^\star}{2}(x_2^2+y_2^2)\right) \\ & + V_G(l_o, \varpi_o, \Omega_o, x_1, y_1, x_2, y_2)\Bigg]. \end{aligned} \tag{3.68}$$

There are several simplifications that we wish to make on this Hamiltonian:

- Similarly to the previous case, the linear term in y_1 in the kinetic energy is cancelled by the term in y_1 in the Keplerian contribution, using $\Lambda_1^\star = \frac{3}{2} n_o C_m$,
- All the constant terms are dropped,
- Since in this chapter we are interested in very short-periodic terms (the only periods that we will find are 88 days and harmonics), we evaluate ϖ_o and Ω_o (very slow angles) at their values at J2000 (see Table 3.1). However we keep the precessions. Without them we actually would not have any latitudinal libration.

The Hamiltonian finally becomes

$$\boxed{H = n_o\Lambda'_o + \frac{\Lambda_1^\star y_1^2}{2C_m} + \dot{\varpi}_o\left(G''_o - y_1\right) + \dot{\Omega}_o\left(H'''_o + \frac{x_2^2+y_2^2}{2}\right) + \frac{1}{\Lambda_1^\star}V_G(l_o, x_1, y_1, x_2, y_2)} \tag{3.69}$$

Using Hamilton's equations for the orbital motion, we find

$$\frac{dl_o}{dt} = \frac{\partial H}{\partial \Lambda'_o} = n_o \tag{3.70}$$

$$\frac{d\varpi_o}{dt} = \frac{\partial H}{\partial G''_o} = \dot{\varpi}_o \tag{3.71}$$

$$\frac{d\Omega_o}{dt} = \frac{\partial H}{\partial H'''_o} = \dot{\Omega}_o, \tag{3.72}$$

showing that at our level of truncation and our simplifications, the shape of the planet has no influence on the orbital motion.

3.3.3 Equilibria and fundamental periods

Now that we finally have our Hamiltonian with canonical variables, and expressed as Poisson series, we want to use our perturbation theory in order to compute the evolution of several variables such as the libration in longitude angle σ_1, the other resonant angle σ_3 and the ecliptic obliquity K. As in the previous case we use the same 5 steps to compute the evolution of these variables.

① We would like to put in H_0^0 the terms without short-periodic contributions in such a way that it is easy to compute the fundamental periods of our 2 degrees of freedom. The Hamiltonian without angle dependencies or orbital terms can be viewed as

$$H_0 = \sum_{i,j,k,l=0}^{ordexp} a_{ijkl} x_1^i x_2^j y_1^k y_2^l, \tag{3.73}$$

where *ordexp* is the order of the expansions in the different variables (we chose 5). Bearing in mind that these variables are supposed to be small, an expansion to order 5 is enough at our level of truncation as confirmed by computational investigations (see Appendix B for more details). To use the Lie triangle procedure, the periods associated with the degrees of freedom called the **fundamental periods**[2] must be computed in order to get the generators. For this, we must first get rid of the linear terms in y_1 and y_2 (due to our construction of the Hamiltonian, there are no linear terms in x_1 and x_2) and we simply perform an expansion around the equilibrium values of y_1 and y_2. To find these equilibria, we use the Hamiltonian (3.73) in which we put $x_1 = x_2 = 0$, since at the Cassini equilibrium (at the exact spin axis and node resonances) we have $\sigma_1 = \sigma_3 = 0$:

$$H_{\text{eq}}(y_1, y_2) = \frac{1}{\Lambda_1^\star}\left(\sum_{k,l=0}^{ordexp} a_{kl} y_1^k y_2^l\right). \tag{3.74}$$

[2] In this text they are also referred to as free or proper periods and a similar vocabulary is used for the associated frequencies

With a simple iterative process, it is now possible to find the equilibria for y_1 and y_2:

$$\begin{aligned} y_1^\star &= -7.0428745\ 10^{-7} \\ y_2^\star &= 0.12244729 \end{aligned}$$

giving

$$K^\star = \arccos\left(1 - \frac{x_2^{\star 2} + y_2^{\star 2}}{2(1+y_1^\star)}\right) = 7.0201^\circ = 7^\circ\ \ 1.206 \text{ arcmin.} \tag{3.75}$$

and

$$\Lambda_1^\star = 7.70349 m R_e^2 \text{ years}^{-1} \tag{3.76}$$

The usual obliquity (as opposed to the ecliptic obliquity K), denoted by θ is the angle between the orbital and spin plane (between Z_2 and Z_1). The relation between θ, K and σ_2 is given by

$$\cos\theta = \cos i_o \cos K + \sin i_o \sin K \cos\sigma_2. \tag{3.77}$$

Using this formula, we easily find the equilibrium value of the usual obliquity ($i_o = 7.005^\circ$, Table 3.1):

$$\theta^\star = 0.907 \text{ arcmin.} \tag{3.78}$$

Let us note that in order to have consistent values for the equilibria $K^\star$ and $\theta^\star$, they should be computed using a rigid model (C instead of C_m in the kinetic energy). Indeed, on long time scales we do not expect Mercury's core and mantle to be dissociated. This will be discussed in the next chapter.

We perform a translation to put these equilibria at the centre of our coordinates and as a consequence, the new linear terms in y_1 and y_2 vanish. We note that these variables are in fact not y_1 and y_2 anymore since we performed a translation, but we decide to keep their names to avoid heavier notations.

To find the fundamental periods we take the quadratic unperturbed Hamiltonian:

$$\begin{aligned} H^{(2)}(x_1, y_1, x_2, y_2) &= 0.34466 \times 10^{-2} x_1^2 + 0.40274 \times 10^{-3} x_1 x_2 + 0.50814 \times 10^{-2} x_2^2 \\ &+ 19.566 y_1^2 - 0.61460 \times 10^{-3} y_1 y_2 + 0.49220 \times 10^{-2} y_2^2. \end{aligned}$$

We notice that the two degrees of freedom are linked and we need to dissociate them, i.e. perform another canonical transformation that removes the mixed terms in $x_1 x_2$ and $y_1 y_2$. For this, we use the untangling transformation (Henrard & Lemaitre, 2005). After another canonical transformation to have the same coefficients for the variable and moment of the same degree of freedom and a last change to action-angle variables

$$\begin{cases} x_1 = \sqrt{2U}\sin(u) & y_1 = \sqrt{2U}\cos(u) \\ x_2 = \sqrt{2V}\sin(v) & y_2 = \sqrt{2V}\cos(v), \end{cases} \tag{3.79}$$

the quadratic Hamiltonian is now

$$H^{(2)}(-,-,U,V) = n_u U + n_v V, \tag{3.80}$$

with n_u and n_v the free frequencies of the degrees of freedom 1 and 2. The corresponding free periods are:

$$\begin{aligned} T_1 &= 2\pi/n_u = 12.06 \text{ years}, \\ T_2 &= 2\pi/n_v = 616.26 \text{ years}. \end{aligned}$$

The same changes of variables are performed for the rest of the Hamiltonian as well and it now reads

$$H = n_o\Lambda_o + n_u U + n_v V + P(l_o, u, U, v, V), \tag{3.81}$$

where we did not write the terms in H_o''' and G_o'', now constants since we evaluated their conjugated variables ϖ_o and Ω_o at their J2000 values (Table 3.1).

3.3.4 Libration in latitude

Applying a procedure with canonical Lie transforms similar to the planar case, it is possible to compute both the librations in longitude and latitude.

We choose to put in H_0^0 the quadratic Hamiltonian and the 2-body problem part $n_o\Lambda_o$, and in H_1^0 the perturbation with the periodic terms in l_o and the higher-order terms in $\sqrt{2U}$ and $\sqrt{2V}$:

$$H_0^0 = n_o\Lambda_o + n_u U + n_v V \quad \text{and} \quad H_1^0 = P(l_o, u, U, v, V). \tag{3.82}$$

We then compute the transformed Hamiltonian and the generators as previously ②.

③ Note that the frequency is barely modified when pushing the procedure to higher orders of the Lie triangle. We have $\bar{T}_2 = 616.31$ years at the second order compared to 616.26 years for T_2. The next orders bring even less changes.

④ As in the previous case, we expect Mercury to be at the Cassini equilibrium, and similar computations lead to the expression of the transformed variables: $\bar{x}_1 = \bar{x}_2 = \bar{y}_1 = \bar{y}_2 = 0$ and the angles are linear functions of time.

⑤ From there, the technique is similar to the computation of the libration in longitude in the planar case and we do not explain it again.

The introduction of another degree of freedom does not modify the librations in longitude significantly (relative change of 10^{-6}, very weak coupling between these degrees of freedom) and we do not write them again in this section. The variations around the ecliptic obliquity $K^\star$ and the second resonant angle σ_2 are shown in Table 3.4 and 3.5, with the amplitudes in milliarcsec. These variations are way below the arcsec level and will not be observed by any space mission. In brackets is the contribution due to the second-order generator. In this case, the relative corrections are a lot larger than for the longitudinal librations. The third-order generator brings much smaller relative corrections (10^{-4}).

Finally, note that the variations around the ecliptic obliquity $K^\star$ or around the usual obliquity $\theta^\star$ are almost the same and are referred to as latitudinal librations. Indeed, taking a look at the equation (3.77)

$$\cos\theta = \cos i_o \cos K + \sin i_o \sin K \cos\sigma_2, \tag{3.83}$$

and since σ_2 is of order 10^{-6}, $\cos\sigma_2 = 1 - \sigma_2^2/2 = 1 + O(10^{-12})$, 10^{-12} being our truncation level. Hence we put $\cos\sigma_2 = 1$ and we have $\cos\theta = \cos(K - i_o)$. With i_o a constant, the variations around $K^\star$ or $\theta^\star$ are almost the same.

Latitudinal librations (angle K)			
l_o	Period	Amplitude (in milli as)	Ratio
2	43.985 d	8.9801 (9.2406)	2.0634
3	29.323 d	5.6837 (5.6670)	1.3060
1	87.970 d	4.3521 (4.4199)	1.0000
4	21.992 d	1.8267 (1.8308)	0.4197
5	17.594 d	0.5719 (0.5728)	0.1314

Table 3.4: Short-period variations around the equilibrium value of the ecliptic obliquity of Mercury, obtained analytically using the first-order generator of a Lie transform, from the ecliptic obliquity K. The amplitudes are expressed in milliarcsec and the numbers in brackets are the contributions due to the second-order generator. The ratio is computed with respect to the 88-day contribution.

Variations of σ_2			
l_o	Period	Amplitude (milli as)	Ratio
1	87.970 d	152.15	1.0000
2	43.985 d	53.990	0.3549
3	29.323 d	42.178	0.2772
4	21.992 d	13.856	0.0910
5	17.594 d	4.4484	0.0292

Table 3.5: Variations of the resonant angle σ_2, representing the commensurability between the orbital and rotational precessions. The amplitudes are expressed in milliseconds of arc. The ratio is computed with respect to the 88-day contribution.

3.4 The wobble motion

3.4.1 Hypotheses

The addition of the last degree of freedom (the wobble) forms the complete model. The

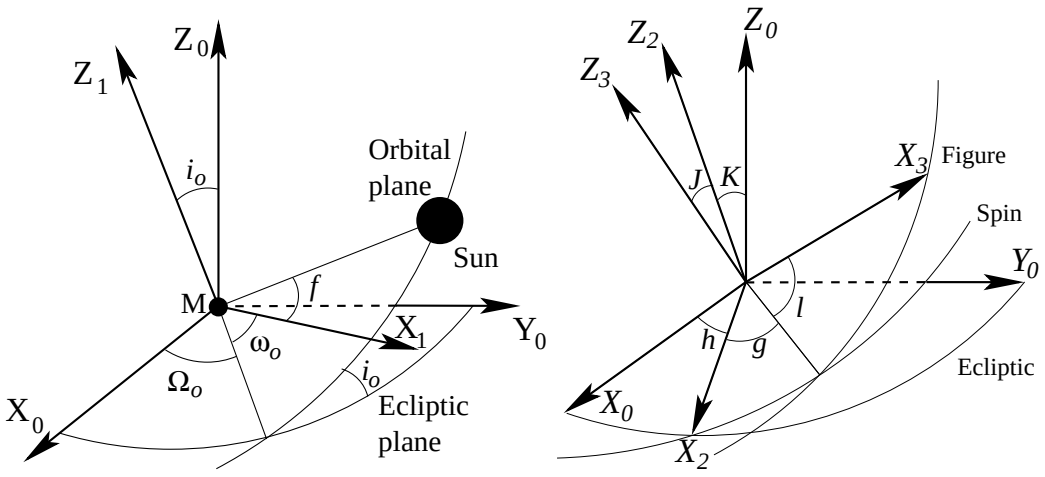

Figure 3.7: Situation with 3 degrees of freedom: the longitude $\lambda_1 = l + g + h$, the latitude K and the wobble J. We also consider an orbital inclination.

hypotheses are:

- the inclination of the orbital plane i_o, the (ecliptic) obliquity K and the wobble angle J are not 0,
- there is a precession of the ascending node and periherm.

3.4.2 Hamiltonian

The 2-body problem contribution is of course the same as in the previous cases. However, since the angle J is not zero anymore, there are no simplifications on the kinetic energy and T is the complete equation (3.4).

For the gravitational potential, compared to the 2-degree of freedom case, we have one more rotation of angle J. The vector (x, y, z) pointing towards the Sun in the figure frame is

$$\begin{pmatrix} x \\ y \\ z \end{pmatrix} = R_3(l)R_1(J)R_3(g)R_1(K)R_3(h) \times \tag{3.84}$$

$$R_3(-\Omega_o)R_1(-i_o)R_3(-\omega_o) \begin{pmatrix} \cos f \\ \sin f \\ 0 \end{pmatrix}, \tag{3.85}$$

or, with the modified Andoyer's variables:

$$\begin{pmatrix} x \\ y \\ z \end{pmatrix} = R_3(-\lambda_2)R_1(J)R_3(\lambda_1+\lambda_2+\lambda_3)R_1(K)R_3(-\lambda_2)\times \tag{3.86}$$

$$R_3(-\Omega_o)R_1(-i_o)R_3(-\omega_o)\begin{pmatrix} \cos f \\ \sin f \\ 0 \end{pmatrix}. \tag{3.87}$$

The gravitational potential thus reads

$$V_G = V_G(r, f, \lambda_1, \lambda_2, \lambda_3, J, K). \tag{3.88}$$

To have the complete Hamiltonian, we go through steps similar to the 2-degree of freedom case:

- expansions of the ratio $(r/a)^{-3}$, $\cos f$ and $\sin f$ until order 5 in eccentricity and mean anomaly,
- introduction of the resonant angles σ_1 and σ_2, and of the precessions of the longitude of the periherm and the ascending node,
- changes to the associated moments,
- changes of variables to

  $$(l_o, \Lambda_o, \varpi_o, G'_o, \Omega_o, H''_o, \sigma_1, \Lambda_1, \sigma_2, K, \lambda_3, J) \to (l_o, \Lambda'_o, \varpi_o, G''_o, \Omega_o, H'''_o, x_1, y_1, x_2, y_2, x_3, y_3) \tag{3.89}$$

  with

$$\begin{cases} \Lambda_o &= \Lambda_1^\star \Lambda'_o \\ G'_o &= \Lambda_1^\star G''_o \\ H''_o &= \Lambda_1^\star H'''_o \\ \sigma_1 &= x_1 \text{ (Taylor expansion around } \sigma_1 = 0) \\ \Lambda_1 &= \Lambda_1^\star (1+y_1) \\ x_2 &= \sqrt{\frac{2\Lambda_2}{\Lambda_1^\star}}\sin\sigma_2 \\ y_2 &= \sqrt{\frac{2\Lambda_2}{\Lambda_1^\star}}\cos\sigma_2 \\ x_3 &= \sqrt{\frac{2\Lambda_3}{\Lambda_1^\star}}\sin\lambda_3 \\ y_3 &= \sqrt{\frac{2\Lambda_3}{\Lambda_1^\star}}\cos\lambda_3 \end{cases} \tag{3.90}$$

  which is a canonical set with multiplier $1/\Lambda_1^\star$.

The final Hamiltonian is similar to the 2-degree of freedom Hamiltonian:

$$\boxed{H = n_o\Lambda'_o + T(y_1, x_3, y_3) + \dot{\varpi}_o\,(G''_o - y_1) + \dot{\Omega}_o\left(H'''_o + \frac{x_2^2+y_2^2}{2}\right) + \frac{1}{\Lambda_1^\star}V_G(l_o, x_1, y_1, x_2, y_2, x_3, y_3)} \tag{3.91}$$

Unlike the previous cases in one or two degrees of freedom, the kinetic energy now depends on 3 variables: y_1, x_3 and y_3.

The procedure is once again similar to the previous sections and we use the same numbers for the steps of the method.

3.4.3 Fundamental periods

① Using Hamilton's equations and seeing that there are only quadratic terms in x_3 and y_3 in the unperturbed Hamiltonian, we easily deduce the equilibrium $x_3^\star = y_3^\star = 0$, implying that $\Lambda_3^\star = 0$ and $J^\star = 0$. As a consequence the equilibria of y_1 and y_2 are computed in the same way as in the previous section and we have the same equilibria for K and Λ_1.

To get the fundamental periods, we once again take the quadratic unperturbed Hamiltonian:

$$\begin{aligned} H^{(2)} &= 0.34466 \times 10^{-2} x_1^2 + 0.40274 \times 10^{-3} x_1 x_2 + 0.50814 \times 10^{-2} x_2^2 + 0.17078 \times 10^{-1} x_3^2 \\ &+ 19.566 y_1^2 - 0.61460 \times 10^{-3} y_1 y_2 + 0.49220 \times 10^{-2} y_2^2 + 0.50700 \times 10^{-2} y_3^2. \end{aligned}$$

The 3rd degree of freedom is completely dissociated with the two others.
The next steps are then similar to the 2-degree of freedom case: untangling transformation, transformation to have the same coefficient for variables and moments of the same degree of freedom and action-angle variables

$$\begin{cases} x_1 = \sqrt{2U}\sin(u) & y_1 = \sqrt{2U}\cos(u), \\ x_2 = \sqrt{2V}\sin(v) & y_2 = \sqrt{2V}\cos(v), \\ x_3 = \sqrt{2W}\sin(w) & y_3 = \sqrt{2W}\cos(w), \end{cases} \tag{3.92}$$

and the quadratic Hamiltonian is

$$H^{(2)}(-,-,-,U,V,W) = n_u U + n_v V + n_w W, \tag{3.93}$$

with n_u, n_v, and n_w the free frequencies of the degrees of freedom 1, 2 and 3, corresponding to the fundamental periods

$$\begin{aligned} T_1 &= 2\pi/n_u = 12.06 \text{ years}, \\ T_2 &= 2\pi/n_v = 616.26 \text{ years}, \\ T_3 &= 2\pi/n_w = 337.62 \text{ years}. \end{aligned}$$

In the rigid case, this 3-degree of freedom model was first studied by D'Hoedt & Lemaître (2005) and the periods found were $T_1 = 15.857$ years, $T_2 = 1065.05$ years and $T_3 = 583.989$ years.

② With these free frequencies, it is now possible to compute the generators of the averaging transformation over l_o, with

$$H_0^0 = n_o \Lambda_o + n_u U + n_v V + n_w W \quad \text{and} \quad H_1^0 = P(l_o, u, U, v, V, w, W). \tag{3.94}$$

where we put in P all the terms depending on l_o and the terms in $\sqrt{2U}$,$\sqrt{2V}$ and $\sqrt{2W}$ of order higher than 2.

③ The correction to the frequency is also very small for the 3rd degree of freedom. The periods, using the generators to until order 2, are:

$$\begin{aligned} T_1 &= 2\pi/n_u = 12.057 \text{ years instead of } 12.06, \\ T_2 &= 2\pi/n_v = 616.31 \text{ years instead of } 616.26, \\ T_3 &= 2\pi/n_w = 337.77 \text{ years instead of } 337.62. \end{aligned}$$

3.4.4 Wobble and pole motion

④ ⑤ To compute the evolution of the wobble and the pole motion, we use once again the same procedure as for the other cases, without any notable change. With the generators, it is now theoretically possible to compute any analytic function of x_1, x_2, x_3, y_1, y_2, y_3 with short-period terms. However, since these variables are in Poisson series form, it is sometimes very tricky to compute a function of these variables.
To compute the series of K, we have

$$K = \arccos\left(1 - \frac{x_2^2 + y_2^2}{2\Lambda_1^\star(1+y_1)}\right), \tag{3.95}$$

with y_1, x_2 and y_2 being Poisson series of several thousands of terms...
We managed to compute the Poisson series of K through series expansions around $y_2^\star$ and $y_1^\star$.
The expression of J is very similar:

$$J = \arccos\left(1 - \frac{x_3^2 + y_3^2}{2\Lambda_1^\star(1+y_1)}\right). \tag{3.96}$$

However, since $y_3^\star = 0$, it is a lot trickier to get the Poisson series expression of the variable J (because the equation above would give 0 at the equilibrium and no expansions are possible).

The variations of this angle are expressed in Table 3.6 in the form $J = \sum_i c_i \cos(\frac{2i-1}{2} l_o)$. Note that, unlike all the other variables analysed until here, the periods in the angle J are odd harmonics of the sidereal Hermean day (176 days). The values of the other librations of the problem are the same as in the previous cases.

Wobble angle J		
l_o	Period	Amplitude
1/2	175.93 d	106.12
3/2	58.646 d	49.368
5/2	35.187 d	7.1940
7/2	25.134 d	10.537
9/2	19.549 d	8.5522

Table 3.6: Variations of the wobble angle J. These results obtained analytically using a second-order Lie transform. The amplitudes are expressed in milliarcsec.

Let us explain how we got this series. Since we expect J to be extremely small, we make the approximation that $\cos J = 1 - J^2/2$. Using the relation $\Lambda_3 = \Lambda_1(1 - \cos J)$ we have

$$1 - \frac{J^2}{2} = 1 - \frac{\Lambda_3}{\Lambda_1} \tag{3.97}$$

$$\Leftrightarrow \qquad J^2 = 2\frac{\Lambda_3}{\Lambda_1}. \tag{3.98}$$

The series of Λ_3 is easily computable and it is possible to divide it by the series of Λ_1, we expand it around the mean value $\Lambda_1^\star$. The result of the division (hence J^2) is another Poisson

series. It is actually required to use the Lie triangle procedure until the second order and to lower our level of truncation to get small variations for this degree of freedom. For all the other variables, the order 2 and higher only brought minor corrections on the amplitudes computed with the first order. However the Poisson series of J^2 has such a small constant term that it is not possible to use expansions to determine its square root (and get the angle J). To bypass this difficulty, we look for a solution a priori, compute the square of this solution and compare the coefficients obtained with the actual ones, from the series J^2. This comparison pushes us to use Newton method to solve non-linear equations and we verify that the square of the solution J obtained with this method is indeed very close to J^2. This procedure is extremely heavy to implement and to use and works because we have only one angle and just 13 terms in J^2.

In this chapter we computed the effect of the non-sphericity of Mercury on the three degrees of freedom of the rotation: the longitude, the latitude and the wobble motions. For a fairly large core (as expected by the high density of the planet and the radar observations of Margot et al. (2007)), the largest oscillations were found on the libration in longitude with an amplitude of the 88-day period contribution close to 40 arcsec. The latitudinal as well as the wobble librations are well below the arcsec threshold and should not be observed by either of the space missions.

4

The indirect planetary perturbations on the rotation

After studying the effect of the non-sphericity of Mercury, this chapter deals with the indirect influence of the planets on the rotation. By indirect influence we mean that the planets affect the orbit of Mercury and these changes in the orbital elements will in turn have an effect on the rotation, mainly through the 3:2 spin-orbit resonance and the non-sphericity of the planet. As a matter of fact planetary perturbations were already introduced in the previous chapter: the precessions of the ascending node and of the perihelion are actually caused by the other planets. However in this chapter, we complete these precessions by expressing each of the orbital elements of Mercury as functions of the mean longitudes of all the other planets.

We start by explaining what is the form of the planetary theory used and how we introduce it in our problem.

Then, we state and explain the results obtained with the introduction of the indirect planetary perturbations. These results were published in two of our papers (Dufey et al. (2008) and Dufey et al. (2009)), hereafter referred to as Paper I and Paper II. We report these results chronologically, explaining the different steps that led us to several comparisons and refinements of our model. From a rigid model at first, we passed by a 1-degree of freedom model with a spherical liquid core to eventually get to a 2-degree of freedom model with a constrained size of the core. In the process we were able to detect a mistake in Peale et al. (2007), ensure that our results were absolutely correct and analyse a couple of potential resonant forcings on both the longitudinal and latitudinal librations.

4.1 Inserting the planetary perturbations

4.1.1 The planetary theory

The planetary theory that we have used was kindly given by Jean-Louis Simon from the IMCCE in Paris. It is the solution VSOP (Variations Séculaires des Orbites Planétaires) obtained at the end of 2004 and adjusted to the ephemerides DE405 (for a reference for the VSOP

coefficients, see Fienga and Simon, 2004). It gives the Poisson series of the elliptic elements:

$$\left\{\begin{array}{l} a \text{ the semi-major axis of Mercury} \\ l_M \text{ the mean longitude} \\ k = e\cos\varpi_o, \text{ with } e \text{ the eccentricity and } \varpi_o \text{ the longitude of the perihelion} \\ h = e\sin\varpi_o \\ q = \gamma\cos\Omega_o, \text{ with } \gamma = \sin i_o/2,\ i_o \text{ the inclination and } \Omega_o \text{ the longitude of the ascending node} \\ p = \gamma\sin\Omega_o. \end{array}\right. \tag{4.1}$$

Note that we have the relation $l_M = l_o + \varpi_o$, with l_o the mean anomaly. Each variable is expressed as

$$X = \sum_{i=0}^{3} t^i X_i, \tag{4.2}$$

with t the time and X_i Fourier series the arguments of which are linear combinations of the longitudes of all the planets:

$$X_i = \sum_{\substack{i_M,i_V,i_E,i_{Ma} \\ i_J,i_S,i_U,i_N}} a^{i_M,i_V,i_E,i_{Ma}}_{i_J,i_S,i_U,i_N} \left\{\begin{array}{c}\sin\\ \cos\end{array}\right\} (i_M l_M + i_V l_V + i_E l_E + i_{Ma} l_{Ma} + i_J l_J + i_S l_S + i_U l_U + i_N l_N), \tag{4.3}$$

with $l_M, l_V, l_E, l_{Ma}, l_J, l_S, l_U, l_N$ respectively being the longitudes of Mercury, Venus, the Earth, Mars, Jupiter, Saturn, Uranus and Neptune. The so-called Poisson terms are the terms of (4.2) containing the time, i.e. $\sum_{i=1}^{3} t^i X_i$,.

Only the terms giving a contribution larger than 10^{-12} after 100 years are kept in these series. The 6 series total a number of 17520 terms together, the largest one being the longitude of Mercury with almost 5000 terms.

This solution also provides the phases and mean motions of the different planets at J2000.

We finally note that, besides the 5 biggest asteroids (Vesta, Iris, Bamberga, Ceres and Pallas) taken into account in these series, the solution contains relativistic contributions as well as contributions due to the Solar J_2 and 295 minor asteroids included in the coefficients of the terms.

Now that we are a little more familiar with this planetary theory, let us explain how we use it. The first thing to do is to express the elliptic variables in our usual orbital variables. We note that each one of the variables var_i actually has a large constant and linear contribution (corresponding to the Keplerian contribution), with small contributions (perturbations) aside:

$$var_i = \underbrace{var_{i,0} + n_i t}_{var_i^\star} + f_{var}(l_M, l_V, l_E, l_{Ma}, l_J, l_S, l_U, l_N), \tag{4.4}$$

with the functions f_{var} at least 10^4 times smaller than the Keplerian contributions $var_i^\star$. With some background work, our software MSNam allows us to compute expansions around these values $var_i^\star$ to have the expressions of the orbital elements $a, e, i_o, l_o, \Omega_o, \varpi_o$.

These series however contain several thousands of terms. Since we must introduce them in our Hamiltonian, once again as series expansions and multiplied by other Poisson series, we

do not want such large series for the orbital elements and must somehow cut them. We are interested in the behaviour of Mercury on short timescales (a few dozens of years at most). Taking a look at our series we note that the Poisson terms are at least 100 times smaller than the periodic contributions over 100 years. As a consequence we simply cut these Poisson terms. Verifications will be performed later on to check if this cut is legitimate. Without these Poisson terms, the size of the series is divided by a factor two but is still too large for a practical use of the MSNam. We then decide to analyse the angle combinations in the series appearing with the largest coefficients and we select only 13 of them, implying only 4 other planets, Venus (closest planet), Jupiter and Saturn (most massive planets) and the barycenter Earth-Moon (decent ratio mass/distance). These 13 contributions are listed in Table 4.1.

Main planetary contributions					
Jupiter	l_J	Venus	$2l_M - 5l_V$	Saturn	$2l_S$
Jupiter	$2l_J$	Earth	$l_M - 4l_E$	Venus	$l_M - 2l_V$
Venus	$l_M - 3l_V$	Jupiter-Saturn	$2l_J - 5l_S$	Venus	$l_M - l_V$
Venus	$2l_M - 4l_V$	Mercury	l_M	Jupiter	$3l_J$
Mercury	$2l_M$				

Table 4.1: Angle combinations (in no particular order) selected in the expressions of the orbital elements from the planetary theory VSOP.

This selection is actually the result of a lot of back and forth comparisons between numerical and analytical methods, to be absolutely sure that no relevant contribution was omitted.

We can now write down a simple formulation for our orbital elements:

$$a = a^\star + f_a(l_M, l_V, l_E, l_J, l_S) \qquad e = e^\star + f_e(l_M, l_V, l_E, l_J, l_S)$$
$$i_o = i_o^\star + f_{i_o}(l_M, l_V, l_E, l_J, l_S) \qquad l_M = l_M^\star + f_l(l_M, l_V, l_E, l_J, l_S)$$
$$\Omega_o = \Omega_o^\star + f_\Omega(l_M, l_V, l_E, l_J, l_S) \qquad \varpi_o = \varpi_o^\star + f_\varpi(l_M, l_V, l_E, l_J, l_S),$$

with l_M, l_V, l_E, l_J, l_S the mean longitudes of Mercury, Venus, the barycenter Earth-Moon, Jupiter, and Saturn, and the functions f_{var} at least 10^4 times smaller than the first Keplerian contributions. These series have 28 terms: 2 for the Keplerian contribution and 26 for the sines and cosines of the angle combinations chosen.

4.1.2 Introduction of the planetary perturbations in the Hamiltonian

Coming back to our problem, these series of the orbital elements are inserted in the Hamiltonian (in the second-order gravitational potential) right before the introduction of the resonant angles:

$$H = H_{2B}(L_o) + T(\Lambda_1, \lambda_3, \Lambda_3) + V_G(l_o, L_o, \omega_o, \Omega_o, \lambda_1, \Lambda_1, \lambda_2, \Lambda_2, \lambda_3, \Lambda_3), \qquad (4.5)$$

where only the dependencies on canonical variables are written. We recall that this gravitational potential is obtained after a series of rotations around (among others) $\omega_o = \varpi_o - \Omega_o$, the argument of the perihelion, i_o and Ω_o. Also, it was expanded as functions of the mean anomaly

$l_o = l_M - \varpi_o$ and the eccentricity e. Finally V_G also depends on the semi-major axis a through $L_o = \sqrt{\mu a}$. Hence the dependencies of the second-order gravitational potential are

$$V_G = V_G(e, i_o, \Omega_o, \varpi_o, l_o, L_o(a), \lambda_1, \Lambda_1, \lambda_2, \Lambda_2, \lambda_3, \Lambda_3). \tag{4.6}$$

This gravitational potential is in a Poisson series form and e and a (through L_o) are present as polynomial variables. As a consequence, it is quite simple to introduce the planetary dependencies of these variables: simple substitutions and expansions around their Keplerian parts $e^\star$ and $a^\star$ are performed.

It is slightly more complicated for the other variables as they are brought into play as sines and cosines in V_G. We explain with an example how we proceed for the mean longitude $l_M = l_M^\star + \epsilon$, with $l_M^\star$ the Keplerian contribution and ϵ the perturbation. Suppose that the term $\cos(il_M + x)$ belongs to our Hamiltonian (4.5), with i, j integers and x a linear combination of other angular variables. We express it as

$$\begin{aligned}
\cos(il_M + x) &= \cos(il_M)\cos(x) - \sin(il_M)\sin(x) && (4.7)\\
&= \cos(i(l_M^\star + \epsilon))\cos(x) - \sin(i(l_M^\star + \epsilon))\sin(x) && (4.8)\\
&= \cos(x)[\cos(il_M^\star)\cos(i\epsilon) - \sin(il_M^\star)\sin(i\epsilon)] && (4.9)\\
&\quad - \sin(x)[\sin(il_M^\star)\cos(i\epsilon) + \cos(il_M^\star)\sin(i\epsilon)], && (4.10)
\end{aligned}$$

and we expand $\cos(i\epsilon)$ and $\sin(i\epsilon)$ to the second order around $i\epsilon = 0$: $\cos(i\epsilon) = 1 - (i\epsilon)^2/2$ and $\sin(i\epsilon) = i\epsilon$. This expansion is sufficient since ϵ is of order 10^{-4} at most and we also must remember that it is introduced in the perturbation V_G, already small.
A similar procedure is used for the other angular variables i_o, ϖ_o and Ω_o.

With the introduction of 4 new variables in the problem (l_V, l_E, l_J, l_S), we must artificially add their corresponding conjugated momenta in order to keep a canonical set of variables. Finally, after the introduction of the resonant angles and the precessions, our general Hamiltonian is the following:

$$\begin{aligned}
H &= n_o(\Lambda_o - 3\Lambda_1/2) + n_V\Lambda_V + n_E\Lambda_E + n_J\Lambda_J + n_S\Lambda_S + \dot{\varpi}_o(G'_o - \Lambda_1) + \dot{\Omega}_o(H''_o + \Lambda_2)\\
&\quad + T(\Lambda_1, \lambda_3, \Lambda_3) - \frac{GM\mu^3}{\left(\Lambda_o - \frac{3\Lambda_1}{2}\right)^6} P(l_o, \varpi_o, \Omega_o, \sigma_1, \Lambda_1, \sigma_2, \Lambda_2, \lambda_3, \Lambda_3, l_V, l_E, l_J, l_S), \qquad (4.11)
\end{aligned}$$

with $\Lambda_V, \Lambda_E, \Lambda_J, \Lambda_S$ the moments associated with l_V, l_E, l_J, l_S.

Before going to the results we must say a few words on how we compute them de facto. We use the same technique as in the previous chapter, with the only difference being that we have a larger number of variables. The transformation is performed such that the averaged Hamiltonian does not depend on any fast angular variable. By fast we mean the longitudes of the planets and of the Sun in the hermeocentric frame. As a consequence, the generators of the transformation only contain terms with these fast variables. Just like the mean motion n_o was not modified during the averaging process, the frequencies of the planets (mean motions) are not modified either which was to be expected. Indeed, it would be quite foolish to think that the shape of Mercury actually has a significant effect on the orbital motion of other planets. To sum up, the perturbation by canonical Lie transforms is similar to our previous use in each of the five

steps. The only differences are that the Poisson brackets are computed with 4 more variables and the generators depend on 4 more longitudes, which will allow us to have the influence of planetary perturbations in any analytic function of the variables.

4.2 Paper I: the longitudinal librations

We first deal with the longitudinal librations in a 1-degree of freedom model. These librations were also studied in the first part of Paper II with a different value of the ratio C_m/C and from a 2-degree of freedom model.

The purpose of Paper I was to build this theory and get the amplitudes of the planetary perturbations in a very cautious way, ensuring that all our steps were correct. We were not adventuring completely in the dark, Peale et al. (2007) had just published a paper about long-period forcing of Mercury's libration in longitude. Their model was also a 1-degree of freedom one, but their method was completely different than ours. They numerically integrated the equations of motions from the Lagrangian, adding non-conservative forces in order to dissipate any free amplitudes, as Mercury should be in a Cassini equilibrium. Their planetary theory was DE408 and they used a fast Fourier transform on the power spectrum of the libration in order to get the amplitudes and frequencies of the different effects.

On the other hand, we used a Hamiltonian analysis with the planar case described in Section 3.2 and we compared our results with those obtained by the SONYR model (described hereafter) and by Peale et al. (2007). These comparisons (especially those obtained with the SONYR model) allowed us to have a complete trust in our planetary theory and our method.

SONYR is the acronym of Spin-Orbit N-bodY Relativistic model, it is a dynamical model of the Solar system including the coupled spin-orbit motion of the terrestrial planets and of the Moon (see Rambaux and Bois (2004) and references therein).

As a consequence to the planar case used for this model, no planetary perturbations are included in the longitude of the ascending node and the inclination since these angles are undefined. We also did not compute the phases of the various contributions.

In the first part we state the results obtained with our analytical method. Then, we compare them with the results obtained with three different numerical methods:

1. the results from the SONYR (Spin-Orbit N-bodY Relativistic) model using the series of the analytical method (Simon, 2004, Fienga and Simon, 2004) as orbital solutions;

2. the results from the SONYR model with the orbital motion resulting from the numerical integration of the N-body problem;

3. the results from Peale et al. (2007) using the JPL Ephemeris DE 408.

The first comparison guarantees that our method is correct, the second that our planetary series are accurate enough and the last one analyses the results of two methods fundamentally different.

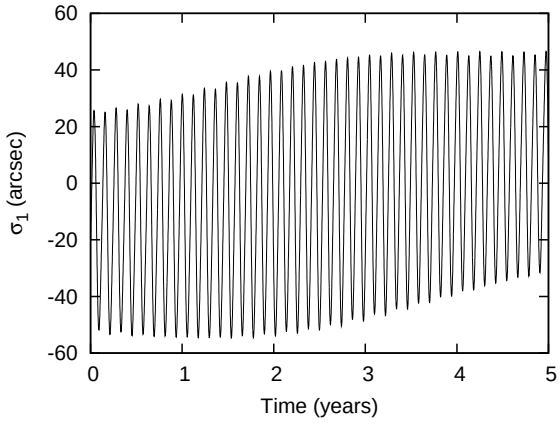

Figure 4.1: Evolution of the resonant angle σ_1 (libration in longitude) over 5 years with planetary perturbations included. We detect the same 88-day-period effect that we observed in the case without planetary perturbations (amplitude of 40 arcsec), but we now see that the whole curve is oscillating, showing the longer period influence of the planetary perturbations.

4.2.1 Results from the analytical method

The value of C_m is 0.17. It corresponds to $C_m/C = 0.5$, and was chosen to match that of Peale et al. (2007) for comparisons sake, even if we expect this value to be larger. Applying the same method as in the previous chapter, we are able to compute the evolution of σ_1 and Λ_1, using the first-order generator (the other orders do not bring relevant changes in the results).

First of all, we notice that planetary perturbations have a very faint influence on the norm of the angular momentum Λ_1. The oscillations are approximately 100 times smaller than the 88-day variation plotted in the previous chapter.

For σ_1 however, the influence of the planetary perturbations are much larger (Figure 4.1). The amplitude (around 40 arcsec) is the same that we observed without planetary perturbations but the whole curve is now oscillating according to planetary perturbations. Figure 4.2 shows the evolution of σ_1 on a larger timescale.

Analytical method			
Effect of (angle combination)	Period (years)	Amplitude (arcsec)	Relative amplitude
Mercury (l_o)	0.24084	40.693	1
Jupiter (l_J)	11.86200	13.270	0.326110
Mercury ($2l_o$)	0.12042	4.5371	0.111496
Venus ($2l_o - 5l_V$)	5.66608	4.3504	0.106910
Jupiter ($2l_J$)	5.93100	1.6730	0.041112
Saturn ($2l_S$)	14.7285	1.2332	0.030306
Earth ($l_o - 4l_E$)	6.57966	0.7160	0.017595

Table 4.2: The main planetary contributions on the libration in longitude angle σ_1 obtained with our planar first order generator.

Table 4.2 presents the main planetary perturbations on the resonant angle σ_1. The five main effects are Mercury's orbital motion (l_o and $2l_o$), Jupiter (l_J and $2l_J$), Venus ($2l_o - 5l_V$), Saturn ($2l_S$) and the Earth ($l_o - 4l_E$). We give for each of them the amplitude in arcsec and the relative amplitude with respect to the 88-day contribution.

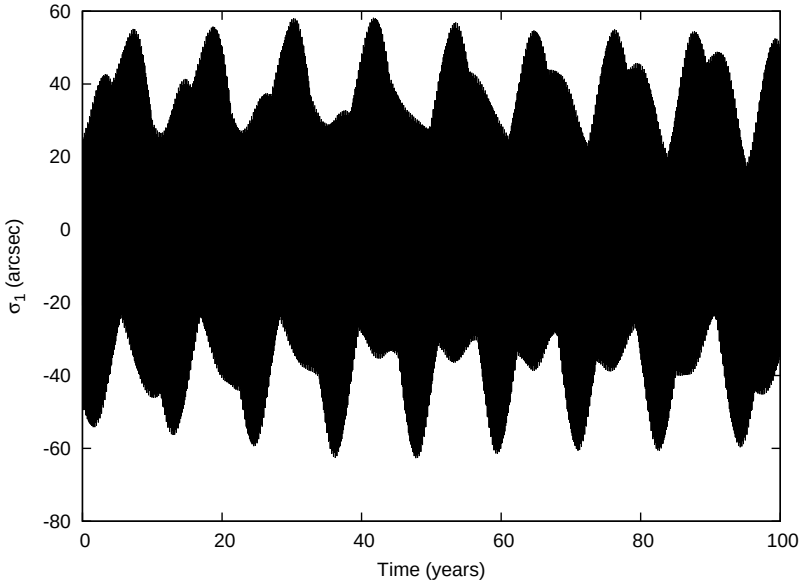

Figure 4.2: Evolution of σ_1 over 100 years. The perturbations acting on the resonant angle are listed in Table 4.2

We notice that the largest contribution (after Mercury's orbital motion) comes from Jupiter. This is due to our choice of $C_{22} = (B - A)/4 = 10^{-5}$ and $C_m/C = 0.17$, giving a period of 11.21 years for the free libration. This period being close to Jupiter's orbital period explains the significant contribution of Jupiter in the libration in longitude. As also mentioned in Margot et al. (2007), given the large uncertainty on C_{22} and the moment of inertia of the mantle C_m there could be an even stronger resonant effect between Jupiter and the free libration. This resonant forcing will be highlighted in the results of Paper II as well as in the Chapter 6.

4.2.2 Comparison with SONYR using the same planetary theory

To validate our analytical results, we compare them with the results of the SONYR model. For the purpose of this work, we assume that all planets move in the same plane defined by the orbital plane of Mercury (all the initial inclinations of the planets are taken equal to zero). In addition, we eliminate the libration in latitude by choosing an initial obliquity equal to zero. Therefore the rotational motion of Mercury is described by only one angle, the libration in longitude, which oscillates in the equatorial plane of Mercury. As the obliquity is zero, the equatorial plane of Mercury coincides with its orbital plane and the spin-orbit motion can be described by two degrees of freedom, one for the orbit and one for the rotation. We call this system the planar case. The libration in longitude is then treated by frequency analysis in order to compare with the series of the analytical method.
In this first comparison with the SONYR model, we integrate numerically the rotational motion of Mercury with the orbital motion described by the VSOP analytical series of Simon (Fienga and Simon, 2004), i.e. the same ephemeris used in the analytical solution. The solutions are listed in Table 4.3.

Tables 4.2 and 4.3 show very similar results as a consequence of the use of the same orbital model. The main frequencies acting on σ_1 are identified and their relative contribution is quantifiable: the main oscillation is the annual period of Mercury, then come the influence of Jupiter (l_J), Venus ($2l_o$-$5l_V$), the semi-annual period of Mercury ($2l_o$), Jupiter ($2l_J$), Saturn ($2l_S$) and finally the effect of the Earth (l_o-$4l_E$).

SONYR with the VSOP planetary theory				
Effect of (angle combination)	Period (years)	Amplitude (arcsec)	Relative amplitude	Relative amplitude (from Table 4.2)
Mercury (l_o)	0.24084	41.487	1	1
Jupiter (l_J)	11.86200	13.057	0.314721	0.326110
Mercury ($2l_o$)	0.12042	4.0278	0.097085	0.111496
Venus ($2l_o - 5l_V$)	5.66608	4.3617	0.105134	0.106910
Jupiter ($2l_J$)	5.93100	1.6776	0.040436	0.041112
Saturn ($2l_S$)	14.7285	1.2183	0.029365	0.030306
Earth ($l_o - 4l_E$)	6.57966	0.7183	0.017314	0.017595

Table 4.3: The main planetary contributions obtained with SONYR with a forced analytical orbital motion.

4.2.3 Comparison with SONYR using the N-body integration

In this second comparison, we use a full numerical integration to solve for the orbital and rotational motions in the $N-$body problem. The initial inclinations of the orbital planes of the planets are fixed to zero in order to obtain the planar problem. The frequency analysis is performed over a time span of 1000 years and we present in Table 4.4 the solution for this case. When we compare the Tables 4.2 and 4.4 we notice that the differences are more important than in the previous section. However, the amplitudes of the annual oscillation, the semi-annual oscillation and of the oscillations containing the mean longitude of Jupiter, Venus and Saturn give very satisfying results for such a simple model. The first contribution of the Earth of 6.57 years is too faint to be detected by the frequency analysis in SONYR results.

4.2.4 Comparison with Peale et al. (2007)

Finally we compare our amplitudes with the results given in Table I of Peale et al. (2007), based on numerical ephemeris valid for much longer timescales than the analytical series that we used (comparison in Table 4.5). In order to match the value of C_{22} taken in their paper, our analytical results in Table 4.5 are now calculated with $C_{22} = 1.5 \times 10^{-5}$. This change of the C_{22} does not affect the good agreement of the solutions obtained between our analytical approach and SONYR.

Concerning the comparison itself, the amplitudes of the terms induced by Mercury's orbital motion and Venus are similar to our results but the term in $2l_J$ is completely different. Although

SONYR with its own orbital motion				
Effect of (angle combination)	Period (years)	Amplitude (arcsec)	Relative amplitude	Relative amplitude (from Table 4.2)
Mercury (l_o)	0.24084	41.484	1	1
Jupiter (l_J)	11.86200	13.661	0.329313	0.326110
Mercury ($2l_o$)	0.12042	4.1839	0.100856	0.111496
Venus ($2l_o - 5l_V$)	5.66608	4.4623	0.107566	0.106910
Jupiter ($2l_J$)	5.93100	1.8045	0.043499	0.041112
Saturn ($2l_S$)	14.7285	1.2672	0.030546	0.030306
Earth ($l_o - 4l_E$)	6.57966	undetected	/	/

Table 4.4: The main planetary contributions obtained with SONYR.

Peale et al. (2007)			
Effect of (angle combination)	Period (years)	Relative amplitude	Our relative amplitude (with $C_{22} = 1.5 \times 10^{-5}$)
Mercury ($l_M - \varpi = l_o$)	0.24084	1	1
Venus ($2l_o - 5l_V + 3\varpi$)	5.66608	0.1427	0.1289
Mercury ($2(l_M - \varpi) = 2l_o$)	0.12042	0.1028	0.1115
Jupiter (l_J)	11.86200	not listed ($\simeq 0.04$)	0.0571
Jupiter ($2l_J - 2\varpi$)	5.93100	0.3483	0.0509
Saturn ($2l_S$)	14.7285	not listed ($\simeq 0.02$)	0.0138
Earth ($l_o - 4l_E$)	6.57966	not listed ($\simeq 0.01$)	0.0239

Table 4.5: Results extracted from Peale et al. (2007).

Peale et al. (2007) did not list the amplitude of the contribution of l_J, $2l_S$ and $l_o - 4l_E$ in their Table I, it appears from their figure 6 that these contributions are respectively around 4%, 2% and 1% of the contribution of the orbital motion of Mercury, which are quite close to our own values.

Although the orders of magnitude of the different contributions are similar in the analytical and Peale's theories, the agreement is far from that obtained by the comparison with SONYR. We directly thought that the differences came from the fact that we introduce perturbations on different orbital elements (Peale et al. (2007) do not consider perturbations on the mean anomaly). We tried removing these perturbations, without a better agreement.
Another possibility was the differences in the ephemerides and time spans. We used simplified ephemeris, cutting the Poisson terms. However, even with these ephemerides, we have a good agreement with the results of SONYR using the full N-body integration.

It turned out that the omission of the planetary perturbations of the anomaly of Peale et al. (2007) was critical and provoked all these differences. In their next paper, Peale et al. (2009) computed these amplitudes again, this time with perturbations on the anomaly and obtained ratios in good agreement with our results. However, they chose a value of the ratio $C_m/C = 0.579$, consistent with the radar observations of Margot et al. (2007), also corresponding to the value of Paper II described in the next section.

4.3 Paper II: Longitudinal and latitudinal forced librations

In Paper II, we used a 2-degree of freedom model to compute longitudinal and latitudinal librations. The numerical method implemented for the comparisons is different than before and is described in the first subsection.

The part of Paper II concerning the longitudinal librations has a double use: validate the cut that we made in our planetary theory and use a value of the ratio C_m/C accepted in the literature as the most likely (Margot et al., 2007): $C_m/C = 0.579$. This new value allows us to see that our results are perfectly coherent with those from Peale et al. (2009), highlighting the resonant forcing between the Jovian period and the free period linked to the longitudinal degree of freedom.

To our knowledge, the planetary perturbations on the latitudinal motion have only been computed in this work and we show that they should be too small to be detected by the space missions. However, for particular values of the ratio C_m/C and the 2nd degree harmonic coefficients falling within the 1σ-range uncertainty of these values, there might be another long-period resonant forcing between the great inequality period and the free period linked to the latitudinal degree of freedom. The amplitude associated with the great inequality might then grow well over the arcsec level. However, because of its very long period (883 years) compared to a couple of years for the nominal missions, this contribution, should it be detected, would only be viewed as a shift on the latitudinal librations, not as oscillations.

We also add the phases of each contribution in this study.

4.3.1 The numerical method

The numerical method used here is different than in the previous section. Instead of the SONYR integration of the Solar System, we integrate the equations derived from the Hamiltonian (4.11). This numerical study is similar to the one in Noyelles et al. (2008), where after the numerical integration, we give synthetic representations of the variables by frequency analysis.

The frequency analysis algorithm used is named NAFF for Numerical Analysis of the Fundamental Frequencies and is based on Laskar (1993). It is improved with some refinements such as the use of different time steps in the analysis, to detect high frequencies (see Laskar (2003)) and an iterative determination of the frequencies, taking into account the frequencies previously detected (see Champenois (1998)).

The frequency analysis aims at writing a complex signal $f(t)$ under the form

$$f(t) \approx \sum_{k=1}^{n} a_k \exp(\sqrt{-1}\omega_k t), \tag{4.12}$$

where ω_k are real frequencies and a_k complex coefficients. If the signal $f(t)$ is real, its frequency spectrum is symmetric and the complex amplitudes associated with the frequencies ω_k and $-\omega_k$ are complex conjugates. This algorithm is very efficient, except when two frequencies are too close to each other. In that case the algorithm is not confident in its accuracy and stops. When the difference between two frequencies is larger than twice the frequency associated with the length of the total time interval, the determination of each fundamental frequency is not perturbed by the other ones. Although the iterative method suggested by Champenois (1998) allows to reduce this distance, some troubles still remain when the frequencies are too close to each other.

The integrated equations are

$$\begin{aligned} \frac{d\lambda_1}{dt} &= \frac{\partial H}{\partial \Lambda_1}, \qquad \frac{d\Lambda_1}{dt} = -\frac{\partial H}{\partial \lambda_1}, \\ \frac{d\lambda_2}{dt} &= \frac{\partial H}{\partial \Lambda_2}, \qquad \frac{d\Lambda_2}{dt} = -\frac{\partial H}{\partial \lambda_2}. \end{aligned} \tag{4.13}$$

The variables λ_0 and Λ_0 do not appear here because the orbital motion of Mercury is determined by ephemerides and not by integration of the system. The integrations are performed with the Adams-Bashforth-Moulton 10^{th} order predictor-corrector integrator.

One of the critical points is the initial conditions. As suggested by Peale (2005), the amplitudes associated with the free librations should be negligible. Unfortunately, when choosing initial conditions even very close to the exact equilibrium, we always get a free part in the solution, that is often predominant. Several methods exist to drop this free part. For instance, Bois & Rambaux (2007) proposed to fit the mean initial conditions in order to locate the spin-orbit system at its center of libration. Another possibility is to add a damping in the equations that will reduce the amplitudes of the free librations, as done for instance by Peale et al. (2007) for the behavior of Mercury's spin. Yseboodt & Margot (2006) explored a third way, starting from the

equilibrium related to a simplified problem and slowly switching on the planetary perturbations, to induce an adiabatic deviation of the equilibrium without apparition of free librations.

In this work we use an iterative method, with a synthetic representation of the solutions. It consists of three steps:

1. Numerical integrations of the system over 8,000 years with initial conditions "cleverly" chosen. "Cleverly" means here that we choose initial conditions as close to the expected equilibrium as possible.

2. Quasi-periodic decomposition and identification of the solutions. Since some of the solutions are diverging over the integration timespan because of very long-period contributions (especially the regression period of Mercury's orbital node, i.e. 235000 years), we fit and remove a polynomial to get a quasi-periodic signal. After analysis, the free part is easy to identify because the analytical study gives us a very good approximation of the frequencies of the free librations. We extract the value of this free part at the time origin of the numerical simulation. The difficulty at this stage comes from the very long-period contributions. They tend to distort the quasi-periodic contributions and their period might change significantly over the integration. This alters the accuracy of the determination of the free solution at the time origin. The solution that we have found is to use the full integration to determine the polynomial to remove, but a shorter timespan to analyze the signal. The free solution can then be evaluated efficiently.

3. Removal of the free part at the time origin from the initial conditions. With that last step, we get the new initial conditions that we use in a numerical integration.

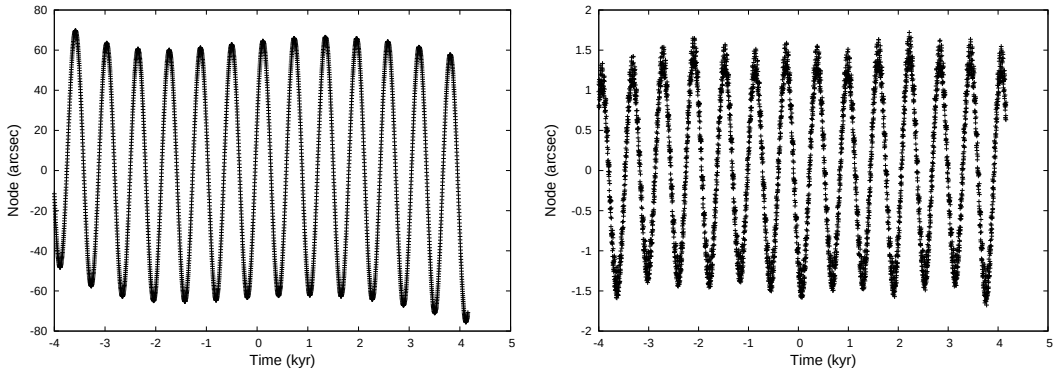

Figure 4.3: Two numerical integrations giving the rotational node λ_2: the second integration has been obtained by removing the free solution extracted from the first one by frequency analysis. This free term, with a period about 616 years, is still predominant but with an amplitude about 50 times smaller.

Figure 4.3 gives an example of use of this algorithm on the variable λ_2 (the longitude of the rotational node), with sinusoidal planetary perturbations. A fourth-degree polynomial has been fitted on the evolution of λ_2, then removed from it. The left panel gives the result. We can see a free sinusoidal term (v) with an amplitude of about 50 arcsec and a period around 616 years. The frequency analysis algorithm gives an estimation of the phase and the amplitude of

this term at the time origin. We removed it from the initial conditions to get the right panel, on which the free term v is still predominant, but with an amplitude of only 1.3 arcsec. A third iteration was used to analyse the evolution of this variable properly. In this third iteration, a free contribution still remains and is actually detected, but its amplitude is very small and is not considered as an obstacle in the quasi-periodic decomposition of the forced rotational motion.

4.3.2 Analytical results

The analytical study is performed in a similar way as in Paper I and the previous chapter. The introduction of the planetary perturbations does not modify the free periods: $T_1 = 12.057$ years and $T_2 = 616.31$ years.

We also mention that (similarly to the previous paper), the resonant arguments are defined using the proper modes of the system. So, in the definition of $\sigma_1 = \lambda_1 - 3/2 l_o - \varpi_o$ and $\sigma_2 = \lambda_2 + \Omega_o$, the mean anomaly l_o and the longitudes of the perihelion ϖ_o and of the ascending node Ω_o are linear functions of time, i.e. $l_o(t) = n_o t + \phi_{l_o}$, $\varpi_o(t) = \dot{\varpi}_o t + \phi_{\varpi_o}$ and $\Omega_o(t) = \dot{\Omega}_o t + \phi_{\Omega_o}$ where n_o, $\dot{\varpi}_o$, and $\dot{\Omega}_o$ are constants, and ϕ_{l_o}, ϕ_{ϖ_o}, and ϕ_{Ω_o} are the initial phases at J2000.

In the following tables, we display the amplitude and the phase of each contribution in the form $A\cos(nt + \phi)$, where A is the amplitude of the contribution, n its frequency and ϕ its phase. After applying the analytical method, σ_1 is a series expressed as:

$$\begin{aligned}\sigma_1 = \sum_{ijkmn} \quad & a_{ijkmn} \quad \cos(i l_o + j l_V + k l_E + m l_J + n l_S - p\varpi_o) \\ + \quad & b_{ijkmn} \quad \sin(i l_o + j l_V + k l_E + m l_J + n l_S - p\varpi_o).\end{aligned}$$

Unlike Paper I, we pay attention that each contribution verifies the rotational invariance, i.e. in the previous formula we have $p = j + k + m + n$. We remind the reader that l_o is the mean anomaly of Mercury and not its mean longitude, while l_V, l_E, l_J, l_S are respectively the longitudes of Venus, the barycenter Earth-Moon, Jupiter and Saturn.

We illustrate how to compute the amplitude and phase of a contribution with an example. Let us take the 11.86-year contribution: $a\cos(l_J - \varpi_o) + b\sin(l_J - \varpi_o)$. The amplitude A is $A = \sqrt{a^2 + b^2}$ and the phase is the sum of two parts: $\phi = \phi_1 + \phi_2$. The first one is $\phi_1 = \arctan(-b/a)$ and the second is the sum of the initial phases: $\phi_2 = \phi_{l_J} - \phi_{\varpi_o}$.

The short-period longitudinal librations are gathered in Table 4.6, while the latitudinal librations (in the ecliptic obliquity K) are in Table 4.8. Table 4.7 gives the short-period librations of the resonant angle σ_2, related to the precessional motion of Mercury. Its dynamics is strongly linked to K, because they belong to the same canonical degree of freedom (σ_2, λ_2), with $\lambda_2 = \Lambda_1(1 - \cos K)$.

We already indicated that the value of the ratio $C_m/C = 0.579$ is different than in Paper I, in order to compare with the numerical study of Peale et al. (2009). As they mention, the 11.862-year contribution, i.e. the orbital period of Jupiter is predominant, because of the proximity of the resonance to the free libration in longitude. Let us mention that this amplitude is strongly related to the value of the moment ratio $(B - A)/C_m$ (hence to the free period). In Table 4.6, the value chosen is $(B - A)/C_m = 2.0319 \times 10^{-4}$. This value is consistent with the interval given by Margot et al. (2007), i.e. $(B - A)/C_m = (2.03 \pm 0.12) \times 10^{-4}$. Should we choose

the inferior bound of the interval we would find an amplitude of 14.32 arcsec for the 11.86-year contribution. With the superior bound, this amplitude would be 56.94 arcsec. By analysis of our series, we were able to get a (semi-)analytical formula for the Jovian contribution. The formula for the amplitude ϕ_J is

$$\phi_J = \frac{\frac{B-A}{C_m}}{m_{1B}\frac{B-A}{C_m} - n_J^2}\sqrt{m_{2B}^2 + m_{3B}^2}, \tag{4.14}$$

where $m_{1B} = 0.133586 \times 10^4$, $m_{2B} = 0.633298 \times 10^{-2}$, $m_{3B} = 0.656925 \times 10^{-2}$. These coefficients depend on the eccentricity only. The first term of the denominator is in fact the square of the fundamental frequency associated with the longitudinal motion. When it comes really close to n_J, the orbital frequency of Jupiter, the amplitude raises extremely fast.

σ_1 with the analytical method										
N	l_o	l_V	l_E	l_J	l_S	ϖ_o	Period	Amplitude	Ratio	Phase
1	-	-	-	1	-	-1	11.862 y	43.712 as	1.2193	-9.54°
2	1	-	-	-	-	-	87.970 d	35.849 as	1.0000	84.80°
3	2	-	-	-	-	-	43.985 d	3.754 as	0.1047	79.59°
4	2	-5	-	-	-	5	5.664 y	3.597 as	0.1003	-92.80°
5	-	-	-	-	2	-2	14.729 y	1.568 as	0.0437	35.79°
6	-	-	-	2	-	-2	5.931 y	1.379 as	0.0385	-176.10°
7	1	-	-4	-	-	4	6.575 y	0.578 as	0.0161	152.24°
8	3	-	-	-	-	-	29.323 d	0.386 as	0.0108	-105.62°
9	1	-	-	-2	-	2	91.692 d	0.201 as	0.0056	-8.12°
10	1	-	-	2	-	-2	84.537 d	0.191 as	0.0053	-2.29°
11	-	-	-	2	-5	3	883.28 y	0.103 as	0.0029	101.73°
12	2	-	-	-1	-	1	44.436 d	0.069 as	0.0019	105.17°
13	2	-	-	1	-	-1	43.541 d	0.067 as	0.0019	112.43°
14	1	-	-	-1	-	1	89.793 d	0.044 as	0.0012	-166.52°
15	1	-	-	1	-	-1	86.217 d	0.043 as	0.0012	154.23°
16	2	-	-	-2	-	2	44.897 d	0.041 as	0.0011	-13.32°
17	2	-	-	2	-	-2	43.110 d	0.040 as	0.0011	-7.50°

Table 4.6: Longitudinal librations of Mercury, obtained analytically, from the resonant argument σ_1. Each contribution has the form $A\cos(nt + \phi)$, with A the amplitude, n the frequency and ϕ the phase computed at J2000.

The librations related to the latitudinal motion (Tables 4.7 and 4.8) are dominated by a very long-period contribution ($\approx 63,315$ years) corresponding to twice the argument of the perihelion (2 ω_o). It results in an adiabatic oscillation of Mercury's spin axis, beyond the work on short-period oscillations only. Moreover, as mentioned by Peale (2006), the adiabatic deviation of Mercury's spin axis is followed by the mantle and by the molten core, so our decoupling hypotheses are not valid for low frequencies. As a consequence, the amplitude that we indicate for this contribution should not be considered as reliable, but only as an indication that long-period effects might alter the determination of some variables. However, we are confident in the amplitudes associated with the other contributions.

σ_2 with the analytical method											
N	l_o	l_V	l_E	l_J	l_S	ϖ_o	Ω_o	Period	Amplitude	Ratio	Phase
1	-	-	-	-	-	*2*	*-2*	*63315 y*	*3.74 as*	*26.128*	*-56.84°*
2	1	-	-	-	-	-	-	87.970 d	143.06 mas	1.0000	84.80°
3	2	-	-	-	-	2	-2	43.985 d	67.31 mas	0.4705	-67.25°
4	-	-	-	2	-5	3	-	883.280 y	65.44 mas	0.4574	15.01°
5	3	-	-	-	-	2	-2	29.323 d	45.02 mas	0.3147	107.55°
6	4	-	-	-	-	2	-2	21.992 d	14.71 mas	0.1028	-77.66°
7	-	-	-	2	-	-2	-	5.931 y	14.64 mas	0.1023	-117.10°
8	2	-	-	-	-	-	-	43.985 d	12.91 mas	0.0902	-100.41°
9	1	-	-	-	-	2	-2	87.970 d	8.20 mas	0.0573	-62.04°
11	-	-	-	1	-	-1	-	11.862 y	7.83 mas	0.0547	-148.63°
10	2	-5	-	-	-	5	-	5.664 y	6.00 mas	0.0420	100.24°
12	-	-	-	-	2	-2	-	14.729 y	4.43 mas	0.0309	-157.27°
13	1	-	-4	-	-	4	-	6.575 y	1.93 mas	0.0135	-66.00°

Table 4.7: Librations of σ_2, related to the precessional motion. The first line, written in italic, represents the amplitude of the librations due to the precessional motion. Since it is a long-period perturbation, a model studying both the core and the mantle of Mercury would be more appropriate than ours. As a consequence, this line is just an indication that long-period effects might alter the determination of some variables. Each contribution has the form $A\cos(nt+\phi)$, with A the amplitude, n the frequency and ϕ the phase computed at J2000.

Peale (2006) has already suggested that the short-period oscillations of Mercury's obliquity would be smaller than 1 arcsec. Table 4.8 confirms this result by giving amplitudes smaller than 10 mas. We can notice that the 44-day and 29-day contributions, i.e. twice and thrice Mercury's orbital frequency, are larger than the 88-day one. More interesting is the 883-year contribution, due to the Jupiter-Saturn great inequality. This contribution is due to the proximity of the Jupiter-Saturn system to the $5:2$ orbital resonance. It has a significant dynamical effect on the Solar System bodies, on the planets themselves, on the Asteroidal Belt (Ferraz-Mello et al. (1997), Henrard (1997)) and also on the irregular satellites of the outer planets (Cuk & Burns, 2004). In addition to this effect, one can notice contributions of Jupiter (5.931 and 11.862 years), Saturn (14.723 years), Venus (5.664 years) and the Earth (6.575 years).

4.3.3 Numerical results

We give here our numerical results, obtained after removal of the free librations. Three analyses have been made, named as Models 1, 1b, and 2.

- In Model 1, the frequency analyses have been performed over 262144 points with a timestep of 10.5192 days, the starting point being JD 990559.4639 (i.e. $\approx$ 4000 years before J2000), and the time interval $\approx$ 7500 years. The ephemerides are modeled with the series of 28 terms used in the analytical study.

K with the analytical method											
N	l_o	l_V	l_E	l_J	l_S	ϖ_o	Ω_o	Period	Amplitude	Ratio	Phase
1	-	-	-	-	-	*2*	*-2*	*63315 y*	*457.230 mas*	*127.0400*	*33.16°*
2	2	-	-	-	-	2	-2	43.985 d	8.213 mas	2.2820	22.75°
3	3	-	-	-	-	2	-2	29.323 d	5.551 mas	1.5304	-162.45°
4	-	-	-	2	-5	3	-	883.280 y	4.676 mas	1.2991	134.22°
5	1	-	-	-	-	-	-	87.970 d	3.599 mas	1.0000	174.79°
6	4	-	-	-	-	2	-2	21.992 d	1.798 mas	0.4996	12.34°
7	-	-	-	2	-	-2	-	5.931 y	1.624 mas	0.4511	144.13°
8	2	-	-	-	-	-	-	43.985 d	1.483 mas	0.4120	169.59°
9	-	-	-	1	-	-1	-	11.862 y	1.259 mas	0.3499	108.13°
10	1	-	-	-	-	2	-2	87.970 d	0.991 mas	0.2754	27.96°
11	2	-5	-	-	-	5	-	5.664 y	0.523 mas	0.1452	-24.59°
12	-	-	-	-	2	-2	-	14.729 y	0.477 mas	0.1325	100.25°
13	1	-	-4	-	-	4	-	6.575 y	0.185 mas	0.0515	-171.72°

Table 4.8: Latitudinal librations, i.e. librations around the equilibrium of the ecliptic obliquity $\bar{K} = 7.0201°$. Each contribution has the form $A\cos(nt+\phi)$, with A the amplitude, n the frequency and ϕ the phase computed at J2000.

- In Model 1b, the frequency analyses are performed over 65536 points with a timestep of 21.0384 days, the starting point being JD 2358265.8476 (i.e. $\approx$ 255 years before J2000), and the time interval $\approx$ 3,800 years. Since the time interval is shorter than in Model 1, we expect to detect less frequencies. The ephemerides are the same as in Model 1.

- In Model 2, the frequency analyses are the same as in Model 1, but the ephemerides are modelized with more than 10000 terms. These terms are all the quasi-periodic terms present in the VSOP ephemerides.

Model 1 aims at comparing a numerical and an analytical study of the same model. Model 1b, with a different starting date, shows the time-dependency of the amplitudes. Since the slow variations of g_o cannot be isolated by frequency analysis, the amplitudes found are likely to be time-dependent. The aim of Model 2 is to validate the choice of the 28 terms used in the analytical study. If the frequency analyses of the results of Model 2 show contributions that are not included in the series, a new Model 1 is elaborated to include these contributions. The frequencies are estimated independently for each model.

The longitudinal librations (Table 4.9) are obtained after subtraction of a polynomial from the spin angle λ_1, to remove the mean spin rate of Mercury (≈ 39.13 rad.y^{-1}) and the contributions due to the very long periods. Then we obtain a signal that we assume to be quasi-periodic, and, using the method described in the section 4.3.1, we analyze it. As explained earlier, the frequency analysis algorithm determines first the contributions associated with the highest frequency, then the next one, and so on, until the detected frequency is very close to one already determined. The detection of such a frequency is generally due to a lack of accuracy in the determination of the frequencies. Here, the slow variations of g_o induce time variations of the

detected frequencies, hence a loss of accuracy in the determination of frequencies. That is the reason why the determination stops before the detection of the smaller contributions.

We still find a very good agreement between numerical and analytical results. When we compare Models 1, 1b and 2, we can notice a large change of the amplitude associated with l_J, i.e. the 11.862-year contribution. The closeness to the resonance makes this amplitude very sensitive to the parameters of the system, as shown by Peale et al. (2009). This explains a lack of accuracy in its determination.

σ_1 with the numerical method										
N	l_o	l_V	l_E	l_J	l_S	ϖ_o	Period	Model 1	Model 2	Model 1b
1	-	-	-	1	-	-1	11.862 y	42.443 as	41.786 as	47.557 as
2	1	-	-	-	-	-	87.970 d	35.834 as	35.864 as	35.671 as
3	2	-	-	-	-	-	43.985 d	3.772 as	3.772 as	-
4	2	-5	-	-	-	5	5.664 y	3.565 as	3.593 as	-
5	-	-	-	-	2	-2	14.729 y	-	1.572 as	-
6	-	-	-	2	-	-2	5.931 y	-	1.377 as	-

Table 4.9: Longitudinal librations obtained numerically from σ_1, defined as λ_1 from which a polynomial has been removed.

The librations associated with the latitudinal motion (Tables 4.10 & 4.11) have been obtained in a similar way. They tend to confirm the analytical results, especially for the presence of the 883-year contribution. However, the comparison between the Models 1 and 1b shows significant differences for the amplitudes associated with the l_o and $2l_o$ contributions (respectively 87.97 and 43.98 days). This can be explained by the presence, in the analytical results (Tables 4.7 & 4.8), of significant contributions in l_o, l_o+2g_o, $2l_o$ and $2l_o+2g_o$ that the frequency analysis is unable to distinguish. So, the variation of the amplitude that is numerically derived is due to the slow evolution of g_o. In Model 1b, the 883-year contribution might be quite difficult to determine because the time length of the interval of study is not large compared to 883 years. Moreover, this contribution has to be distinguished from a 616-year one, i.e. a residual of the free precession.

σ_2 with the numerical method										
N	l_o	l_V	l_E	l_J	l_S	ϖ_o	Period	Model 1	Model 2	Model 1b
1	1	-	-	-	-	-	87.970 d	143.59 mas	143.63 mas	146.67 mas
2	2	-	-	-	-	-	43.985 d	68.65 mas	68.65 mas	71.85 mas
3	-	-	-	2	-5	3	883.280 y	65.30 mas	65.30 mas	65.93 mas
4	3	-	-	-	-	-	29.323 d	47.57 mas	47.57 mas	48.82 mas
5	4	-	-	-	-	-	21.992 y	15.41 mas	15.41 mas	-
6	-	-	-	2	-	-2	5.931 y	14.95 mas	14.65 mas	-
7	2	-5	-	-	-	5	5.664 y	5.71 mas	5.83 mas	-

Table 4.10: Numerical computation of the librations of σ_2, associated with the precessional motion.

K with the numerical method										
N	l_o	l_V	l_E	l_J	l_S	ϖ_o	Period	Model 1	Model 2	Model 1b
1	2	-	-	-	-	-	43.985 d	9.617 mas	9.617 mas	9.466 mas
2	1	-	-	-	-	-	87.970 d	6.428 mas	6.428 mas	5.727 mas
3	3	-	-	-	-	-	29.323 d	6.104 mas	6.104 mas	6.078 mas
4	-	-	-	2	-5	3	883.280 y	4.706 mas	4.706 mas	4.997 mas
5	-	-	-	2	-	-2	5.931 y	1.659 mas	1.631 mas	-
6	-	-	-	1	-	-1	11.862 y	1.261 mas	1.262 mas	-

Table 4.11: Latitudinal librations, obtained after numerical studies of the ecliptic obliquity K.

As a conclusion we note a very good agreement between the Models 1 and 2. It validates the choice of the 28 terms used in the Model 1 and the analytical model.

Analysis of the residuals

The analytical results give more frequencies than the numerical ones. To find the missing contributions, we compute the Fourier spectra of the residuals of our numerical solutions. We obtain the residuals by removing the series given by the tables 4.9 to 4.11 from the solutions obtained after the numerical integrations.

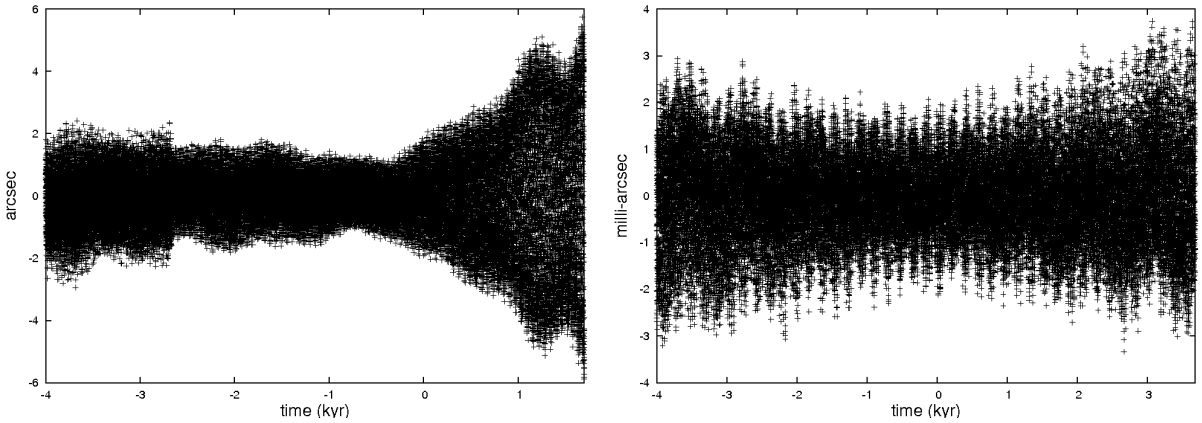

Figure 4.4: Two examples of residuals of the frequency analysis, for the longitudinal librations (left), and for the latitudinal librations (right) of Model 1.

First, the Fourier spectra indicate significant amplitudes for the contributions with periods close to harmonics of the mean motion, i.e. 87.97 days , 43.98 days, 29.32 days, and so on. Unfortunately, it is impossible to isolate all these contributions to identify them. So, the Fourier spectra at this range of periods does not give much information.

On the contrary, plotting them on a longer timescale allows to estimate the contribution of several planetary perturbations that the frequency analysis failed to detect. The Fourier spectra of Models 1 and 1b are given in Figure 4.5 and Table 4.12. Here, we detect for instance the

6.6-year (due to the Earth) and 3.9-year ($3l_J$) contributions that are detected analytically but not numerically.

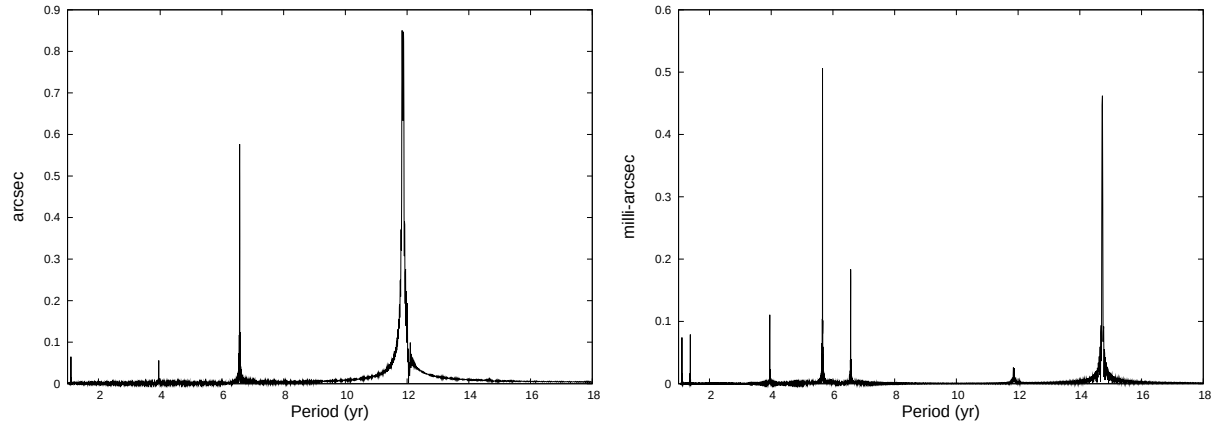

Figure 4.5: Fourier spectra of the residuals of the frequency analysis, for the longitudinal librations (left), and for the latitudinal librations (right) of Model 1. Here, only the contributions with periods between 1 and 18 years are plotted. The Fourier spectra for Model 2 have the same visual aspect.

l_o	l_V	l_E	l_J	l_S	ϖ_o	Period	σ_1	σ_2	K
1	-2	-	-	-	2	1.110 y	63 mas	0.57 mas	7.4×10^{-2} mas
1	-3	-	-	-	3	1.380 y	5 mas	0.88 mas	7.5×10^{-2} mas
-	-	-	3	-	-3	3.954 y	56 mas	0.98 mas	0.11 mas
2	-5	-	-	-	5	5.664 y	-	1.6×10^{-2} mas	0.51 mas
1	-	-4	-	-	4	6.575 y	578 mas	1.9 mas	0.18 mas
-	-	-	1	-	-1	11.862 y	0.7 as	5.9 mas	2.5×10^{-2} mas
-	-	-	-	2	-2	14.729 y	-	4.1 mas	0.47 mas

Table 4.12: Fourier spectra of the residuals of the solutions given by the 28 terms in the Model 1.

The Fourier spectra from Model 2 are given in Figure 4.6 and Table 4.13. For the range of periods 1-18 years, the Fourier spectra from Model 2 are very similar to Model 1 and we decide to plot them only on the range $18 - 90$ years, showing the periodic contributions that are neglected in the Model 1.

A lot of information can be found in these spectra. For instance, we can see two contributions that are close to $2l_J$ (5.931 years), i.e. $5l_S$ (5.891 years) and $4l_J - 5l_S$ (5.971 years). The proximity of these two contributions to $2l_J$ could explain the difference obtained between Models 1 and 2 for the nodal motion (σ_2, Table 4.10). We can also notice the anecdotal contribution of Mars in 1.881 year.

More interesting are the 84 and 42-year contributions. In the table they are labelled as due to Uranus, but we should not forget that the system Uranus-Neptune is close to a $2:1$ mean-motion resonance. These two contributions cannot be distinguished in our Fourier spectra.

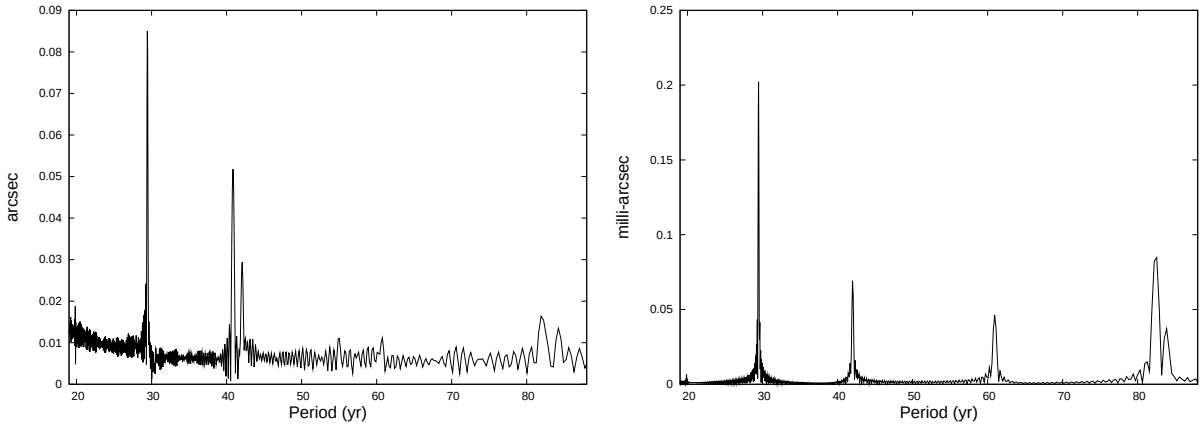

Figure 4.6: Fourier spectra of the residuals of the frequency analysis, for the longitudinal librations (left), and for the latitudinal librations, both in the Model 2 (i.e. 10000-term ephemerides). Here, only the contributions with periods between 18 and 90 years is plotted. The Fourier spectra for Models 1/1b do not give significant information in this range.

l_o	l_V	l_E	l_m	l_J	l_S	l_u	ϖ_o	Period	σ_1	σ_2	K
1	-2	-	-	-	-	-	2	1.110 y	59 mas	0.64 mas	7.2×10^{-2} mas
1	-3	-	-	-	-	-	3	1.380 y	12 mas	0.95 mas	8.6×10^{-2} mas
-	-	-	1	-	-	-	-1	1.881 y	-	6.7×10^{-3} mas	6.8×10^{-4} mas
-	-	-	-	4	-	-	-4	2.965 y	-	5.9×10^{-2} mas	6.4×10^{-3} mas
-	-	-	-	3	-	-	-3	3.954 y	60 mas	1.01 mas	0.11 mas
2	-5	-	-	-	-	-	5	5.664 y	-	1.46×10^{-2} mas	0.49 mas
-	-	-	-	-	5	-	-5	5.891 y	9.2 mas	8.4×10^{-2} mas	1.15×10^{-2} mas
-	-	-	-	2	-	-	-2	5.931 y	8.2 mas	0.15 mas	9.0×10^{-3} mas
-	-	-	-	4	-5	-	1	5.971 y	9.1 mas	8.9×10^{-2} mas	8.6×10^{-3} mas
1	-	-4	-	-	-	-	4	6.575 y	568 mas	1.8 mas	0.18 mas
-	-	-	-	-	4	-	-4	7.364 y	-	2.2×10^{-2} mas	2.5×10^{-3} mas
-	-	-	-	-	3	-	-3	9.819 y	136 mas	0.31 mas	3.6×10^{-2} mas
-	-	-	-	1	-	-	-1	11.862 y	380 mas	5.9 mas	2.75×10^{-2} mas
-	-	-	-	-	2	-	-2	14.729 y	-	4.2 mas	0.46 mas
-	-	-	-	1	-1	-	-	19.859 y	21 mas	5.3×10^{-2} mas	6.6×10^{-3} mas
-	-	-	-	-	1	-	-1	29.457 y	85 mas	0.30 mas	0.20 mas
-	-	-	-	2	-4	-	2	30.473 y	-	5.8×10^{-2} mas	-
-	-	-	-	-	-	2	-2	42.010 y	52 mas	0.63 mas	6.9×10^{-2} mas
-	-	-	-	1	-2	-	1	60.947 y	-	0.11 mas	4.6×10^{-2} mas
-	-	-	-	-	-	1	-1	84.020 y	16 mas	0.75 mas	8.3×10^{-2} mas

Table 4.13: Fourier spectra of the residuals of the solutions given by the complete VSOP orbital ephemerides (≈ 10000 terms).

4.3.4 Discussion on the results

Accuracy of the determined amplitudes

A good determination of the amplitudes of the periodic contributions is crucial to get information of the internal structure of Mercury. For instance, Margot et al. (2007) use the 88-day longitudinal libration to constrain the size of Mercury's core. Our study highlights some sources of error that might occur in the planetological interpretation of observed librations. We stress in particular two librations for which the interpretation might be altered:

- 87.97 days (the orbital period of Mercury)

  Because of its orbital eccentricity, longitudinal librations of the same period appear (Comstock & Bills, 2003). Unfortunately, there are several contributions with periods close to 88 days. Five of them ($l_o \pm 2l_J$ and $l_o \pm l_J$) are listed in Table 4.6, with periods of 84.5, 91.7, 86.2 and 89.8 days. The accumulated amplitude of these contributions is around 0.5 arcsec. Hence, in addition to the observational error, an other one of maximum 0.5 arcsec (when all the contributions are in phase) should be taken into account when inverting the observed amplitude.

- 5.93 years (half of the orbital period of Jupiter)

  Like the first two ones, this contribution is of high interest in the orbital and rotational dynamics of Mercury. The Fourier spectra related to the node and obliquity of Mercury show two contributions with periods very close to 5.93 years, i.e. $5l_S$ (5.89 years) and $4l_J - 5l_S$ (5.97 years) (see Table 4.13). These perturbations are respectively due to the orbital motion of Saturn, and to Jupiter-Saturn interactions. Their estimated amplitudes, relatively to the one associated with $2l_J$ (see Tables 4.7 & 4.8) are about 1%. These additional contributions should be taken into account when using the observed amplitude associated with 5.93 years.

In addition to these problems of contributions too close in the frequency space, the rotational dynamics of Mercury depends on several long-period contributions, especially in σ_2 and obliquity. As stated in the previous section, these perturbations induce a time-dependency on the amplitudes that can alter not only a numerical prediction (see Tables 4.9 to 4.11) but also an observation.

About the mean obliquity of Mercury

Recently, Margot et al. (2007) showed that their radar observations were compatible with Mercury occupying a Cassini equilibrium. In particular, the normal to its orbit, the spin orientation and the normal to its Laplace plane are coplanar. A mean obliquity with respect to the orbital plane of 2.11 ± 0.1 arcmin has been measured. The equilibrium value of the ecliptic obliquity $K^\star$ found in the previous chapter ($K^\star = 7.0201°$) does not match the equilibrium measured. The reason is that we consider a model with a spherical fluid core, valid on the short-term and $\bar{K}$ is the equilibrium of this model. Our study cannot be used to characterise the Cassini state and should be seen as complementary to the long-term ones of Peale (2006),

Yseboodt & Margot (2006), Bois & Rambaux (2007), Rambaux et al. (2007a) and D'Hoedt & Lemaitre (2008).

A potential resonance in latitude

In our model, the core is spherical and the resonant period T_2 is 615.69 years. As highlighted in the results, the oscillation in 883.2 years, resulting from the great inequality between Jupiter and Saturn, is the fourth largest contribution in the obliquity. The proximity between this forced period and the free period T_2 increases significantly the amplitude of the libration (inversely proportional to the difference between these two frequencies). Moreover the gravity coefficients of Mercury are not well known. The J_2 is known with an uncertainty of 33% and C_{22} presents an uncertainty of 50%. In this range of values, the free period T_2 could very well be 883 years or close to it. In this case, the rotational motion of Mercury could be strongly modified. D'Hoedt et al. (2010) studied this resonance more thoroughly.

Applying our perturbation method with different values of J_2 and C_{22} results in a change of the free period T_2. Figure 4.7 shows the variation of the obliquity around its equilibrium, with different values of T_2 obtained with the analytical method. The amplitude of the libration in 883.2 years can be very large (more than 20 arcsec for $T_2 = 883$ years). The evolution of the resonant angle σ_2 presents a similar behavior and is not represented here.

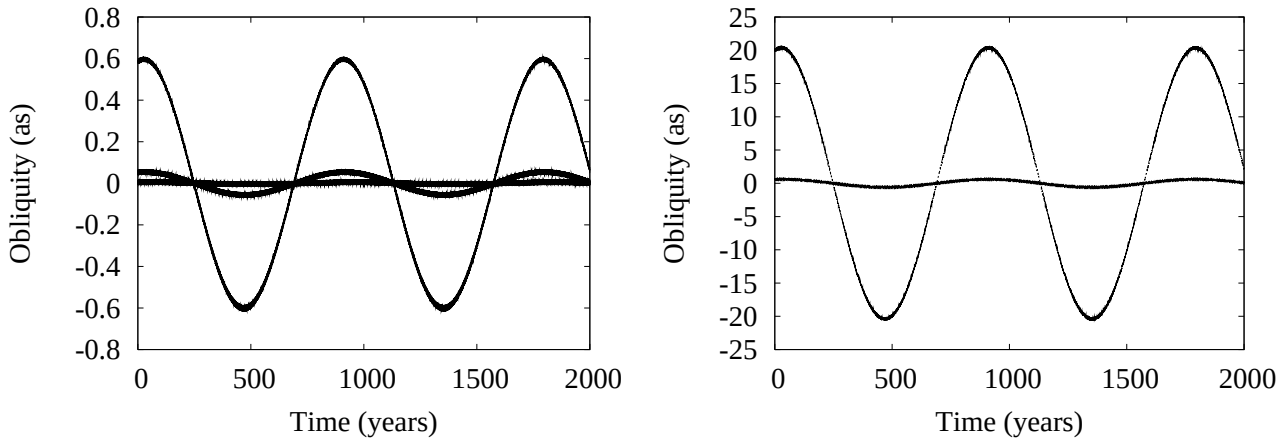

Figure 4.7: First panel: variation of the obliquity around its equilibrium for T_2=615, 853, and 880 years. Second panel: same evolution, with T_2=880 and 883 years.

Figure 4.8 shows the contribution of the great inequality on the ecliptic obliquity K in function of the free period T_2. Here again, we see that when T_2 comes close to 883.2 years, the amplitude of the libration due to the great inequality tends to be very large.

Even though the ratio $(B - A)/C_m$ was constrained by Margot et al. (2007) using radar measurements, there is still an error bar on this value as well as on the gravity coefficients J_2 and C_{22}. Another resonant forcing is then possible when T_2 is close to 883 years (within the range of uncertainty of J_2 and C_{22}), and could produce variations up to several tens of arcsec in the latitude.

Period of σ_2	Amplitude of the great inequality (as)
616.83	0.004730
777.41	0.014180
853.60	0.054674
880.09	0.597974
881.97	2.059613
883.04	58.05664
883.85	1.682152
885.46	0.616628
898.98	0.107959
1051.9	0.013287

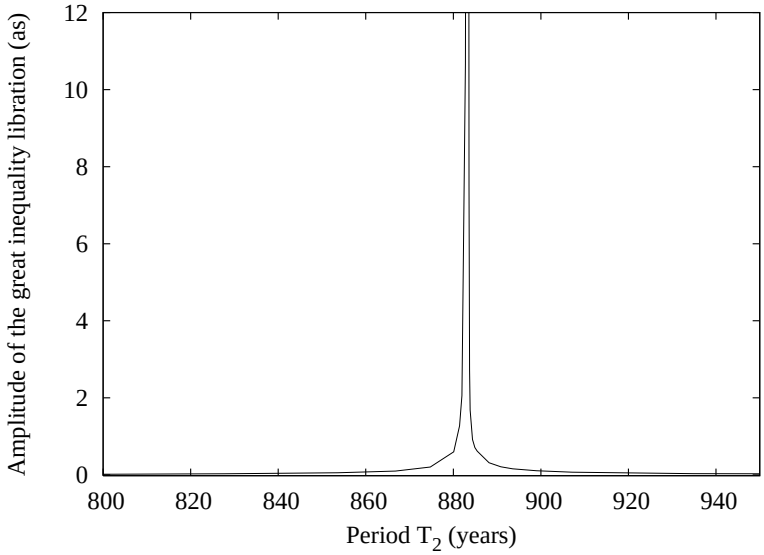

Figure 4.8: Importance of the great inequality contribution on the ecliptic obliquity K in function of the period of the free libration in latitude.

4.4 Planetary perturbations and the wobble motion

For the last degree of freedom similar analyses have been performed. We recall the amplitudes found without planetary perturbations (previous chapter) in Table 4.14.

Wobble angle J		
l_o	Period	Amplitude
1/2	175.93 d	106.12
3/2	58.646 d	49.368
5/2	35.187 d	7.1940
7/2	25.134 d	10.537
9/2	19.549 d	8.5522

Table 4.14: Variations of the wobble angle J in the case without planetary perturbations, obtained analytically using a second-order Lie transform. The amplitudes are expressed in milliseconds of arc.

While numerical investigations have been performed without finding any sign of planetary perturbations on this last degree of freedom, we managed to find planetary contributions using our analytical theory. As explained in the previous chapters, getting the series of the variables J thanks to the canonical variable $\Lambda_3 = \Lambda_1(1 - \cos J)$ is not an easy task. With planetary perturbations, the series Λ_3 does not have 13 terms anymore, but almost a thousand, making it impossible to use the method described in the previous chapter. As a result, we decided to look at the planetary terms added in Λ_3 , presented in Table 4.15.

We see that the first planetary contributions affect Λ_3 with an amplitude 200 times inferior

Λ_3 with planetary perturbations obtained analytically										
N	l_o	l_V	l_E	l_J	l_S	ϖ_o	Ω_o	Period	Amplitude	Ratio
1	1	-	-	-	-	-	-	87.970 d	0.26128d-12	1.00000
2	2	-	-	-	-	-	-	43.985 d	0.15486d-12	0.59271
3	3	-	-	-	-	-	-	29.323 d	0.63390d-13	0.24261
4	4	-	-	-	-	-	-	21.992 d	0.22271d-13	0.08524
5	5	-	-	-	-	-	-	17.594 d	0.75329d-14	0.02883
6	6	-	-	-	-	-	-	14.662 d	0.24702d-14	0.00945
7	1	-	-	-2	-	2	-	0.2510 y	0.13773d-14	0.00527
8	-	-	-	2	-	-2	-	5.9313 y	0.12087d-14	0.00462
9	2	-5	-	-	-	5	-	5.6632 y	0.44189d-15	0.00169

Table 4.15: Variations of Λ_3, canonical moment of the 3rd degree of freedom linked to J through $\Lambda_3 = \Lambda_1(1-\cos J)$. These largest amplitudes give rise to librations around 100 mas in the wobble angle J.

to the largest one. As a consequence, we may conclude that the planetary perturbations are very faint on the wobble angle J.

In this chapter we studied how indirect planetary perturbations affect the rotation of Mercury. After several comparisons (analytical-numerical, with Peale et al. (2007), with Peale et al. (2009)) ensuring the validity of our method, we highlighted a strong 11.86-year contribution of Jupiter (44 arcsec) in the libration in longitude, larger than the 88-day contribution due to the orbital motion of Mercury (36 arcsec). This Jovian perturbation is enhanced by a resonant forcing with the free period associated with the libration in longitude (T_1=12.057 years). Other planetary perturbations from Venus (3.6 arcsec), Saturn (1.6 arcsec) and the barycenter Earth-Moon (0.6 arcsec) were also found in the libration in longitude.

The librations in latitude are much below the arcsec level and should not be identified by the space missions. However, we emphasized the influence of the great inequality contribution, with an 883-year period. This period being quite close to the free period linked to the latitudinal motion (T_2=615.69 years), tends to raise the associated amplitude. We showed that in the range of uncertainty of the parameters of the problem (C_m/C, C_{22}, J_2), this amplitude could grow to several arcsec when T_2 approaches 883 years. On the wobble motion, these indirect planetary perturbations should be extremely small and no resonant forcing mechanism was found.

5
Core-mantle interactions

In the analyses of the previous chapters we always assumed that Mercury was a 2-layer body with an ellipsoidal mantle and a spherical liquid core without any interaction between the layers. The rotation studied was actually that of the mantle only. In this chapter, we put less emphasis on the planetary perturbations and concentrate on the core-mantle interactions, allowing the core to be non-spherical and to have its own motion.

Rambaux et al. (2007b) already explored the dynamics of the rotation of Mercury including core-mantle interactions using the SONYR model (Rambaux and Bois, 2004). We here propose an alternative study, starting from the Hamiltonian formulation of Touma and Wisdom (2001) and highlighting the dynamical implications of core-mantle interactions, by considering Mercury as composed of a rigid mantle and a triaxial ellipsoidal cavity filled with inviscid fluid of constant uniform density and vorticity. Henrard (2008) applied this Hamiltonian formulation to the rotational dynamics of Io, assuming that the core and the mantle were aligned and homothetic. Here we generalise the model of Henrard, allowing the core to be non-homothetic to the mantle.

In the first part, following Henrard (2008), we develop the kinetic energy of such a system. We then apply our perturbation theory and highlight the major differences between this case and the previous chapters. We take a particular care analysing the free periods and comparing them with those found using the same numerical method as in the previous chapter. These free periods are one of the early keys in understanding the dynamics of the problem. Finally we analyse the consequences on the observable rotation of Mercury.

These results will be published in Noyelles et al. (2010).

5.1 The rotational kinetic energy

The general Hamiltonian for this system is once again the sum of the 2-body problem Hamiltonian, the rotational kinetic energy of the system and the second-order gravitational potential due to the shape of Mercury:

$$H = H_{2B} + T + V_G. \tag{5.1}$$

The modification of the interior structure compared to our previous chapters does not affect the Keplerian term or the gravity potential of the problem, **only the kinetic energy will be modified**.

5.1.1 The physical model

The model used is that of a solid mantle and a triaxial ellipsoidal core filled with inviscid homogeneous fluid assumed to have uniform vorticity. The rotational motion of such a core is often referred to as the Poincaré motion. The differential equations ruling the motion of such a 2-layered body were derived by Hough (1895) and Poincaré (1910). More recently Touma and Wisdom (2001) gave a Hamiltonian formulation of the problem that we apply to our case.

With the hypotheses above, the core of the planet behaves as if it was rigid and the motions studied hereafter are related to pressure effects (non-spherical cavity) at the core-mantle boundary provoking transfers between the angular momenta of the whole planet and the core.

This model is obviously an approximation of a real ellipsoidal liquid core model but allows to use a Hamiltonian formalism and is a nice foundation for the study of core-mantle interactions.

To describe the motions of the mantle and the core, four references frames are being considered (Figure 5.1). We already introduced three of them in the previous chapters: the ecliptic frame at J2000 (X_0, Y_0, Z_0), the spin frame (X_2, Y_2, Z_2) (linked to the angular momentum of the mantle) and the figure frame (X_3, Y_3, Z_3) (linked to the principal axes of inertia) describe the motion of the mantle (top left side of Figure 5.1). The last one is the core spin frame (X_2^c, Y_2^c, Z_2^c) and is linked to the angular momentum of a *pseudo-core* that we shall define later. It will help describing the motion of the core (top right side of Figure 5.1).

In the figure frame, the matrix of inertia of Mercury reads:

$$I = \begin{pmatrix} A & 0 & 0 \\ 0 & B & 0 \\ 0 & 0 & C \end{pmatrix} \tag{5.2}$$

with $0 < A \leq B \leq C$, while we assume that the matrix of inertia of the core in the same reference frame is

$$I_c = \begin{pmatrix} A_c & 0 & 0 \\ 0 & B_c & 0 \\ 0 & 0 & C_c \end{pmatrix}, \tag{5.3}$$

implying that the mantle and the cavity have the same orientations. A misalignment of their principal axes would require to consider the mantle as elastic, and this is beyond the scope of this work. Similarly to the whole planet, we have $0 < A_c \leq B_c \leq C_c$ for the core. As a consequence of this alignment, the principal moments of inertia of the mantle are respectively $A_m = A - A_c$, $B_m = B - B_c$ and $C_m = C - C_c$. The principal elliptical radii of the cavity are written a, b, c, and we have

$$\begin{aligned} A_c &= \iiint_{\text{core}} (x_2^2 + x_3^2)\rho \, dx_1 \, dx_2 \, dx_3 = \tfrac{M_c}{5}(b^2 + c^2), \\ B_c &= \iiint_{\text{core}} (x_1^2 + x_3^2)\rho \, dx_1 \, dx_2 \, dx_3 = \tfrac{M_c}{5}(a^2 + c^2), \\ C_c &= \iiint_{\text{core}} (x_1^2 + x_2^2)\rho \, dx_1 \, dx_2 \, dx_3 = \tfrac{M_c}{5}(a^2 + b^2), \end{aligned}$$

where ρ is the density of mass of the fluid core, the integration being performed over the volume of the core.

5.1.2 Expression of the kinetic energy

In order to start our Hamiltonian analysis of the problem, the expression of the rotational kinetic energy is required. We consider each internal process (the core-mantle interactions in our case) as a part of the kinetic energy of Mercury.

In the figure frame, the components (v_1, v_2, v_3) of the velocity field at the location (x_1, x_2, x_3) inside the liquid core are assumed to be:

$$v_1 = \Big(\omega_2 + \frac{a}{c}\nu_2\Big)x_3 - \Big(\omega_3 + \frac{a}{b}\nu_3\Big)x_2, \tag{5.4}$$

$$v_2 = \Big(\omega_3 + \frac{b}{a}\nu_3\Big)x_1 - \Big(\omega_1 + \frac{b}{c}\nu_1\Big)x_3, \tag{5.5}$$

$$v_3 = \Big(\omega_1 + \frac{c}{b}\nu_1\Big)x_2 - \Big(\omega_2 + \frac{c}{a}\nu_2\Big)x_1, \tag{5.6}$$

where $(\omega_1, \omega_2, \omega_3)$ are the components of the angular velocity of the mantle with respect to an inertial frame, and the vector of coordinates (ν_1, ν_2, ν_3) specifies the velocity field of the core with respect to the moving mantle (relative velocity).

The angular momentum of the core $\vec{N}'_c$ expressed in the figure frame is obtained by:

$$\vec{N}'_c = \iiint_{\text{core}} (\vec{x} \times \vec{v})\rho \, dx_1 \, dx_2 \, dx_3 \tag{5.7}$$

and the result is:

$$\vec{N}'_c = \begin{pmatrix} \frac{M_c}{5}\Big(\big(\frac{c}{b}\nu_1 + \omega_1\big)b^2 + \big(\frac{b}{c}\nu_1 + \omega_1\big)c^2\Big) \\ \frac{M_c}{5}\Big(\big(\frac{c}{a}\nu_2 + \omega_2\big)a^2 + \big(\frac{a}{c}\nu_2 + \omega_2\big)c^2\Big) \\ \frac{M_c}{5}\Big(\big(\frac{b}{a}\nu_3 + \omega_3\big)a^2 + \big(\frac{a}{b}\nu_3 + \omega_3\big)b^2\Big) \end{pmatrix} \tag{5.8}$$

We now set the following quantities:

$$\begin{aligned} D_1 &= \tfrac{2M_c}{5}bc &&= \sqrt{\big(A_c - B_c + C_c\big)\big(A_c + B_c - C_c\big)} \\ D_2 &= \tfrac{2M_c}{5}ac &&= \sqrt{\big(-A_c + B_c + C_c\big)\big(A_c + B_c - C_c\big)} \\ D_3 &= \tfrac{2M_c}{5}ab &&= \sqrt{\big(-A_c + B_c + C_c\big)\big(A_c - B_c + C_c\big)} \end{aligned}$$

and we can write:

$$\vec{N}'_c = (A_c\omega_1 + D_1\nu_1, B_c\omega_2 + D_2\nu_2, C_c\omega_3 + D_3\nu_3), \tag{5.9}$$

while the angular momentum of the mantle is

$$\vec{N_m} = (A_m\omega_1, B_m\omega_2, C_m\omega_3), \tag{5.10}$$

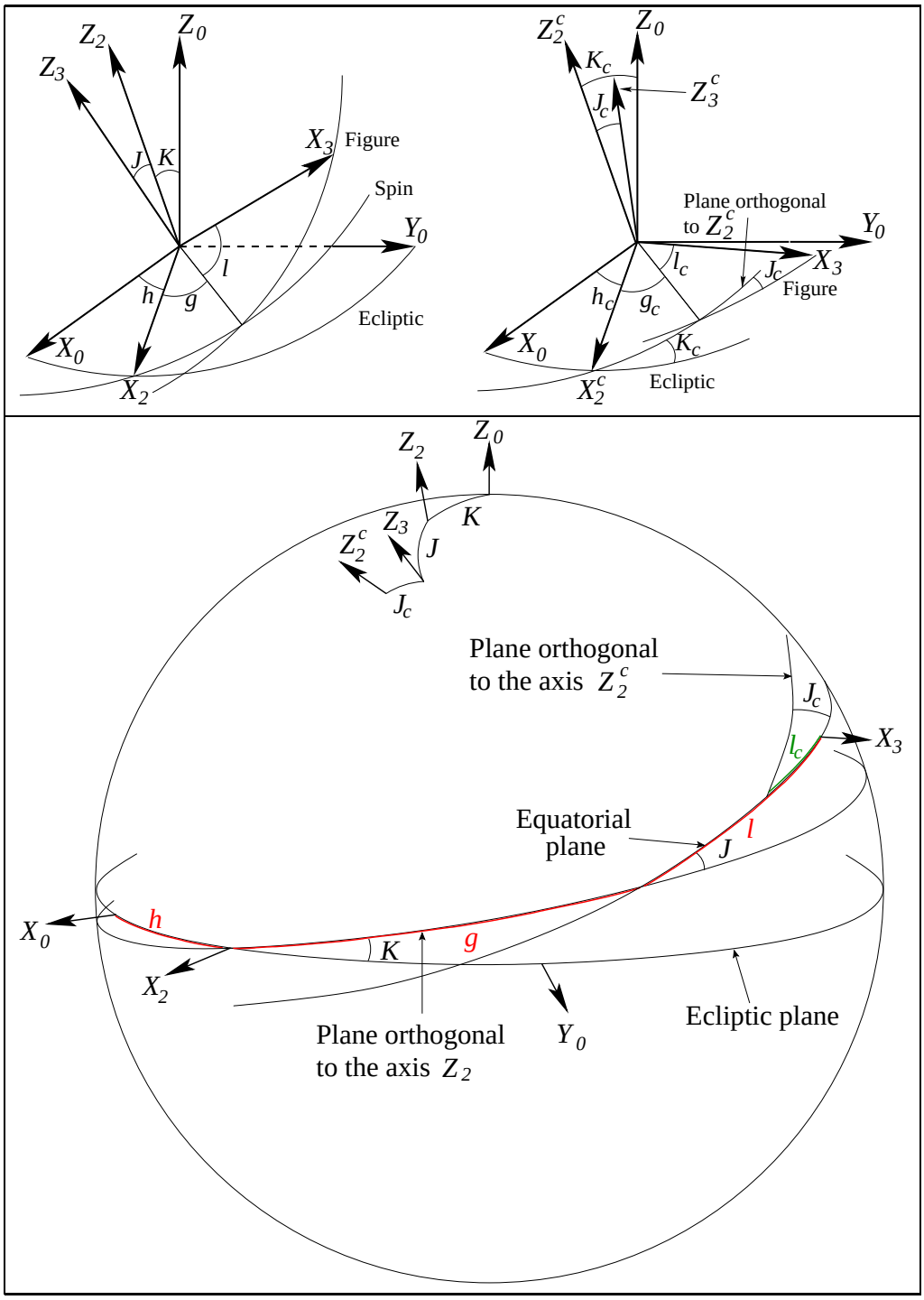

Figure 5.1: Top left side: the 3 reference frames needed for the rotation of the mantle: the ecliptic plane at J2000 (X_0, Y_0, Z_0), the spin frame (X_2, Y_2, Z_2) linked to the angular momentum $\vec{N}$, and the the figure frame (X_3, Y_3, Z_3) linked to the shape of the planet. The frames are located with two sets of Euler angles (h, K, g) and (g, J, l). Top right side: similar configuration but instead of the angular momentum of Mercury, we have a reference frame linked to the angular momentum of a pseudo-core (defined later). These frames are now located with the Euler angles (h_c, K_c, g_c) and (g_c, J_c, l_c). Note that due to the orientations of the planes, J_c is actually close to π, unlike J. Bottom: the four reference frames gathered in the same view.

and the total angular momentum of Mercury is

$$\vec{N} = (A\omega_1 + D_1\nu_1, B\omega_2 + D_2\nu_2, C\omega_3 + D_3\nu_3). \tag{5.11}$$

The kinetic energy of the core is

$$T_c = \frac{1}{2}\iiint_{core} \rho v^2 \, dx_1 \, dx_2 \, dx_3 \tag{5.12}$$

i.e.

$$T_c = \frac{1}{2}\Big(A_c(\omega_1^2 + \nu_1^2) + B_c(\omega_2^2 + \nu_2^2) + C_c(\omega_3^2 + \nu_3^2) + D_1\omega_1\nu_1 + D_2\omega_2\nu_2 + D_3\omega_3\nu_3\Big), \tag{5.13}$$

while the kinetic energy of the mantle T_m is

$$T_m = \frac{1}{2}\vec{N_m} \cdot \vec{\omega} = \frac{A_m\omega_1^2 + B_m\omega_2^2 + C_m\omega_3^2}{2}. \tag{5.14}$$

From $T = T_m + T_c$ we finally deduce the kinetic energy of Mercury:

$$T = \frac{1}{2}\big(A\omega_1^2 + B\omega_2^2 + C\omega_3^2 + A_c\nu_1^2 + B_c\nu_2^2 + C_c\nu_3^2 + 2D_1\omega_1\nu_1 + 2D_2\omega_2\nu_2 + 2D_3\omega_3\nu_3\big). \tag{5.15}$$

We can easily check the expressions of the partial derivatives, as

$$\frac{\partial T}{\partial \omega_i} = A\omega_i + D_i\nu_i = N_i \tag{5.16}$$

or

$$\frac{\partial T}{\partial \nu_i} = D_i\omega_i + A_c\nu_i = N_i^c, \tag{5.17}$$

where N_i are the components of the total angular momentum. N_i^c are not the components of the angular momentum of the core but are close to it for a cavity close to spherical. We have, for instance for the first component:

$$N_1^c - N_1'^c = (A_c - D_1)(\omega_1 - \nu_1) = \frac{M_c}{5}(c-b)^2(\omega_1 - \nu_1), \tag{5.18}$$

so the difference is of the second order in departure from the sphericity. From now on, we call *angular momentum of the pseudo-core* the vector $\vec{N^c} = (N_1^c, N_2^c, N_3^c)$ in the figure frame. This pseudo-core does not have any physical meaning and was introduced in order to have an easier mathematical formalism. The observable variables describing the physical motion of Mercury are computed in Section 5.3.

With these notations, the Poincaré-Hough's equations of motion, for the system mantle-core in the absence of external torque, are (Touma and Wisdom (2001)):

$$\frac{d\vec{N}}{dt} = \vec{N} \times \vec{\nabla}_{\vec{N}} T, \tag{5.19}$$

$$\frac{d\vec{N}_c}{dt} = -\vec{N}_c \times \vec{\nabla}_{\vec{N}_c} T \tag{5.20}$$

where T is expressed in terms of the components of the vectors $\vec{N}$ and $\vec{N}_c$, i.e.

$$\begin{aligned} T = \frac{1}{2\alpha}\big(A_c N_1^2 + A(N_1^c)^2 - 2D_1 N_1 N_1^c\big) + \frac{1}{2\beta}\big(B_c N_2^2 + B(N_2^c)^2 - 2D_2 N_2 N_2^c\big) \\ + \frac{1}{2\gamma}\big(C_c N_3^2 + C(N_3^c)^2 - 2D_3 N_3 N_3^c\big) \end{aligned} \tag{5.21}$$

with $\alpha = AA_c - D_1^2$, $\beta = BB_c - D_2^2$ and $\gamma = CC_c - D_3^2$.

Before trying to express this rotational kinetic energy in the variables chosen, we introduce four small parameters, assuming that Mercury and the cavity are almost spherical:

$$\epsilon_1 = \frac{2C - A - B}{2C} = \frac{J_2}{C}, \tag{5.22}$$

$$\epsilon_2 = \frac{B - A}{2C} = \frac{2C_{22}}{C}, \tag{5.23}$$

$$\epsilon_3 = \frac{2C_c - A_c - B_c}{2C_c} = \frac{J_2^c}{C_c}, \tag{5.24}$$

$$\epsilon_4 = \frac{B_c - A_c}{2C_c} = \frac{2C_{22}^c}{C_c}, \tag{5.25}$$

and also the parameter $\delta = C_c/C$, i.e. the ratio between the polar inertial momenta of the core and of Mercury. As already mentioned J_2 (and ϵ_1) represents the polar flattening of Mercury, while C_{22} (and ϵ_2) is its equatorial ellipticity. The parameters J_2^c (ϵ_3) and C_{22}^c (ϵ_4) have the same meaning for the cavity. If we assume the core of Mercury to be spherical, we have $\epsilon_3 = \epsilon_4 = J_2^c = C_{22}^c = 0$, while $\epsilon_4 = C_{22}^c = 0$ represents an axisymmetric cavity. Henrard (2008) considered that the ellipsoid of inertia of the core and the mantle were aligned and homothetic, which mathematical formulation is $\epsilon_1 = \epsilon_3$ ($J_2 = \delta J_2^c$) and $\epsilon_2 = \epsilon_4$ ($C_{22} = \delta C_{22}^c$). The values of the parameters are gathered in Table 5.1.

Table 5.1: The shape parameters of Mercury.

Parameter	Value	Reference
J_2	6×10^{-5}	Anderson et al. (1987)
C_{22}	10^{-5}	Anderson et al. (1987)
$C/(MR^2)$	0.34	Anderson et al. (1987)
$\delta = 1 - C_m/C$	0.421	Margot et al. (2007)

Coming back to the expression of the kinetic energy (5.21), we must express the angular momenta $\vec{N}$ and $\vec{N}^c$ in our canonical variables. To do so we introduce the two sets of Andoyer's

variables (Andoyer, 1926), (l, g, h, L, G, H) and $(l_c, g_c, h_c, L_c, G_c, H_c)$, related respectively to the whole Mercury and to its pseudo-core. The first one was already introduced previously and the other one is analogous: the Euler angles (h_c, K_c, g_c) and (g_c, J_c, l_c) position the pseudo-core spin frame with respect to the ecliptic frame, and the figure frame with respect to the pseudo-core spin frame. Figure 5.1 shows schematic views of all the reference frames and relevant angles.

The variables are (h, g, l) and (h_c, g_c, l_c) and the corresponding momenta ($H = G\cos K$, G the norm of the angular momentum, $L = G\cos J$) and ($H_c = G_c\cos K_c$, G_c the norm of the angular momentum of the pseudo-core, $L_c = G_c\cos J_c$). We must now express the components of $\vec{N}$ and $\vec{N^c}$ in the figure frame using Andoyer's variables. Using the fact that J_c is defined close to π, we have

$$\begin{aligned} N_1 &= \sqrt{G^2 - L^2}\sin l, & N_1^c &= -\sqrt{{G_c}^2 - {L_c}^2}\sin l_c,\\ N_2 &= \sqrt{G^2 - L^2}\cos l, & N_2^c &= -\sqrt{{G_c}^2 - {L_c}^2}\cos l_c,\\ N_3 &= L, & N_3^c &= -L_c. \end{aligned}$$

With these expressions, we can now perform changes of variables similar to those in Chapter 3 to express the angular momenta and consequently the kinetic energy T in our canonical variables. We start by the modified Andoyer's variables:

$$\begin{cases} \lambda_1 = l + g + h & \Lambda_1 = G,\\ \lambda_2 = -h & \Lambda_2 = G(1 - \cos K),\\ \lambda_3 = -l & \Lambda_3 = G(1 - \cos J). \end{cases}$$

For the pseudo-core, since J_c is close to π, it is slightly different:

$$\begin{cases} \lambda_1^c = -l_c + g_c + h_c & \Lambda_1^c = G_c,\\ \lambda_2^c = -h_c & \Lambda_2^c = G_c(1 - \cos K_c),\\ \lambda_3^c = l_c & \Lambda_3^c = G_c(1 + \cos J_c). \end{cases}$$

Using these changes of variables, the components of the angular momenta are

$$\begin{aligned} N_1 &= -\Lambda_1 \sin J \sin\lambda_3, & N_1^c &= -\Lambda_1^c \sin J_c \sin\lambda_3^c,\\ N_2 &= \Lambda_1 \sin J \cos\lambda_3, & N_2^c &= -\Lambda_1^c \sin J_c \cos\lambda_3^c,\\ N_3 &= \Lambda_1 - \lambda_3, & N_3^c &= \Lambda_1^c - \Lambda_3^c. \end{aligned}$$

One important thing to mention is that the components of the angular momentum of the pseudo-core (hence the kinetic energy) do not depend on λ_1^c or λ_2^c. Since they do not appear anywhere else in the Hamiltonian, the moments associated with these variables are constant and we have that $\Lambda_1^c = G_c$ and K_c are constants. As a consequence we only add one degree of freedom to the problem.

Let us also mention that, since the rotation now refers to the whole planet, the special value $\Lambda_1^\star$ is no longer $\Lambda_1^\star = \frac{3}{2}n_o C_m$, but is now $\Lambda_1^\star = \frac{3}{2}n_o C$. We also assume the constant $\Lambda_1^c = \frac{3}{2}n_o C_c = \delta\Lambda_1^\star$.

Similarly to the previous chapters, after a canonical change of variables to introduce the resonant angles, we perform a last canonical change of variables of multiplier $1/\Lambda_1^\star$ to cartesian coordinates:

$$\begin{aligned}&(l_o, \Lambda_o, \varpi_o, G'_o, \Omega_o, H''_o, \sigma_1, \Lambda_1, \sigma_2, \Lambda_2, \lambda_3, \Lambda_3, \lambda_3^c, \Lambda_3^c)\\ \rightarrow&(l_o, \Lambda'_o, \varpi_o, G''_o, \Omega_o, H'''_o, x_1, y_1, x_2, y_2, x_3, y_3, x_4, y_4)\end{aligned}$$

with

$$\left\{\begin{array}{lcl}\Lambda_o &=& \Lambda_1^\star \Lambda'_o\\ G'_o &=& \Lambda_1^\star G''_o\\ H''_o &=& \Lambda_1^\star H'''_o\\ \sigma_1 &=& x_1 \text{ (Taylor expansion around } \sigma_1 = 0)\\ \Lambda_1 &=& \Lambda_1^\star (1 + y_1)\\ x_2 &=& \sqrt{\frac{2\Lambda_2}{\Lambda_1^\star}} \sin\sigma_2\\ y_2 &=& \sqrt{\frac{2\Lambda_2}{\Lambda_1^\star}} \cos\sigma_2\\ x_3 &=& \sqrt{\frac{2\Lambda_3}{\Lambda_1^\star}} \sin\lambda_3\\ y_3 &=& \sqrt{\frac{2\Lambda_3}{\Lambda_1^\star}} \cos\lambda_3\\ x_4 &=& \sqrt{\frac{2\Lambda_3^c}{\Lambda_1^\star}} \sin\lambda_3^c\\ y_4 &=& \sqrt{\frac{2\Lambda_3^c}{\Lambda_1^\star}} \cos\lambda_3^c\end{array}\right. \tag{5.26}$$

and the kinetic energy reads:

$$T(y_1, x_3, y_3, x_4, y_4) = a_1 y_1^2 + a_2 x_3^2 + a_3 x_4^2 + a_4 x_3 x_4 + a_5 y_3^2 + a_6 y_4^2 + a_7 y_3 y_4, \tag{5.27}$$

with the coefficients depending on $\epsilon_1, \epsilon_2, \epsilon_3, \epsilon_4$.
The Hamiltonian for this problem is then

$$\begin{aligned}H = n_o \Lambda'_o + T(y_1, x_3, y_3, x_4, y_4) + \dot{\varpi}_o (G''_o - y_1) + \dot{\Omega}_o \left(H'''_o + \frac{x_2^2 + y_2^2}{2} \right)\\ + \frac{1}{\Lambda_1^\star} V_G(l_o, x_1, y_1, x_2, y_2, x_3, y_3)\end{aligned} \tag{5.28}$$

The four (main) degrees of freedom of this Hamiltonian are

1. the libration in longitude (x_1, y_1),
2. the libration in latitude (x_2, y_2),
3. the wobble of the whole body (x_3, y_3),
4. the wobble of the pseudo-core (x_4, y_4).

5.2 Comparison between analytical and numerical methods

To study this problem, we use both analytical and numerical methods that allow us to compare their efficiencies and check the reliability of the results. The numerical technique used in this chapter was described in the previous one, with the same integrator (but this time with a 13000-year integration time) and frequency analysis. The analytical method is also the one described in the previous chapters. As a reminder, here are the 5 steps:

① Choice of the transformation and of the parts H_i^0

② Computation of the transformed Hamiltonian and of the generators of the transformation through the algorithm of the Lie triangle

③ Correction to the frequencies

④ Expression of the transformed variables $\bar{q}$ and $\bar{p}$

⑤ Use of the generators and the expression of $\bar{q}$ and $\bar{p}$ to compute the evolution of the variables.

We will see that the steps are very similar to what was done previously and we will not go into each of them once more. However we will emphasize the changes occurring during the process. The main changes will be:

- the addition of one free period due to the extra degree of freedom.
- a large modification of one of the free periods in step ③

5.2.1 The additional degree of freedom

The transformation is an averaging transformation over the fast angular variable l_o. We choose as H_0^0 the first line of equation (5.28), containing terms of order 2 at most in the variables:

$$H_0^0 = n_o\Lambda_o' + T(y_1, x_3, y_3, x_4, y_4) + \dot{\varpi}_o\,(G_o'' - y_1) + \dot{\Omega}_o\left(H_o''' + \frac{x_2^2 + y_2^2}{2}\right) \tag{5.29}$$

and as H_1^0 the gravitational potential:

$$H_1^0 = \frac{1}{\Lambda_1^\star} V_G(l_o, x_1, y_1, x_2, y_2, x_3, y_3), \tag{5.30}$$

with $H_i^0 = 0 \quad \forall i \geq 2$.

To get the free periods of the system we first perform a translation to the equilibria of all the variables in order to vanish the linear terms. Assuming that Mercury lies at a Cassini equilibrium and that the wobbles of the whole planet and the pseudo-core are zero at the equilibrium, we compute the equilibria in a similar way as in Chapter 3. We find:

$$y_1^\star = 1.5 - 6.117 \times 10^{-7} \quad \text{and} \quad y_2^\star = 0.1502, \tag{5.31}$$

resulting in an ecliptic obliquity of

$$K^\star = 7^\circ 1.873 \text{ arcmin}. \tag{5.32}$$

After a translation to these equilibria, H_0^0 has only quadratic terms:

$$H_0^0 = b_1 x_1^2 + b_2 x_1 x_2 + b_3 x_2^2 + b_4 y_1 + b_5 y_1 y_2 + b_6 y_2^2 + b_7 x_3^2 + b_8 x_3 x_4 + b_9 x_4^2 + b_{10} y_3^2 + b_{11} y_3 y_4 + b_{12} y_4^2. \tag{5.33}$$

We notice that the degrees of freedom related to the librations in longitude (x_1, y_1) and latitude (x_2, y_2), and those related to the wobbles of the planet (x_3, y_3) and the pseudo-core (x_4, y_4) are coupled two by two, the coupling being much weaker in the first case than in the second one.
We must now disentangle the coupled degrees of freedom. To do this we use an untangling transformation (Henrard & Lemaitre, 2005) twice, and after changes of variables to action-angle variables:

$$\begin{cases} x_1 = \sqrt{2U}\sin u, & y_1 = \sqrt{2U}\cos u, \\ x_2 = \sqrt{2V}\sin v, & y_2 = \sqrt{2V}\cos v, \\ x_3 = \sqrt{2W}\sin w, & y_3 = \sqrt{2W}\cos w, \\ x_4 = \sqrt{2Z}\sin z, & y_4 = \sqrt{2Z}\cos z, \end{cases} \tag{5.34}$$

we have the following Hamiltonian:

$$H_0^0 = n_1 U + n_2 V + n_3 W + n_4 Z, \tag{5.35}$$

with n_1, n_2, n_3, n_4 the free frequencies corresponding respectively to the libration in longitude, the libration in latitude, the wobble of the planet and the wobble of the pseudo-core.
These frequencies (especially n_2) actually depend on the shape of the core. For the parameters given in Table 5.1 and $\epsilon_3 = \epsilon_1$ and $\epsilon_4 = \epsilon_2$, the corresponding fundamental periods are

$$T_1 = 12.0601 \text{ years}, \qquad T_2 = 1065.99 \text{ years}, \tag{5.36}$$
$$T_3 = 337.726 \text{ years}, \qquad T_4 = 58.6219 \text{ days}. \tag{5.37}$$

The step ② of our perturbation process does not bring any noticeable change beyond the fact that we have an extra degree of freedom.

5.2.2 The correction on the frequencies

The step ③ however brings significant changes. Going to orders higher than 2 in the Lie triangle brings changes to the linear terms in U, V, W and Z, yielding corrections to the free frequencies. In our 2- and 3-degree of freedom models, the corrections were barely noticeable.

On the other hand, these higher-order corrections play a major role here. Here are the corrected fundamental periods (with the values without corrections in brackets):

$$T_1 = 12.0568 \text{ years} \quad (12.0601), \qquad T_2 = 1626.51 \text{ years} \quad (1065.99) \tag{5.38}$$
$$T_3 = 337.853 \text{ years} \quad (337.726), \qquad T_4 = 58.6189 \text{ days} \quad (58.6219). \tag{5.39}$$

We notice the very large change in T_2, the period related to the libration in latitude.
The period of rotation of Mercury is 58.646 days. The fundamental period linked to the wobble of the pseudo-core of Mercury is really close to this fundamental period and this particular combination of angles is present in the series related to the 2nd degree of freedom (linked to the libration in latitude). We are in fact close to a resonance that alters the efficiency of the algorithm.
As a consequence, the numerical convergence of the algorithm is really slow when we take values of ϵ_3 close to ϵ_1 or smaller. For $\epsilon_3 = \epsilon_1$, we used a 13th order Lie triangle to barely converge to the free period T_2. During this process, we multiplied series of millions of terms, which took several days of computation. The process is divergent whenever $\epsilon_3 \leq 0.9\ \epsilon_1$ because of the closeness of Mercury's rotational period and the period T_4. A way to bypass this convergence issue would have been to introduce another resonant angle describing this resonance and preventing small divisors in different steps of the Lie triangle procedure.

The numerical method and the frequency analysis do not have convergence issues however and we can make a pertinent comparison of the free periods using both method.

Table 5.2 gives our analytical and numerical results for 5 different sets of values for ϵ_3 (related to J_2^c) and ϵ_4 (related to C_{22}^c), ϵ_1, ϵ_2 being fixed with the usual values of J_2, C_{22} and $\delta = 1 - C_m/C$. These 5 different sets are:

- Case 1 : $\epsilon_3 = \epsilon_4 = 0$. This is a singular case, because the core-mantle interactions should not exist when the core is spherical (no viscous interactions). Moreover, we are at the **exact resonance** between the proper mode n_4 related to the wobble of the pseudo-core and the spin frequency of Mercury ω. We computed this case to look for an agreement with our previous study (Dufey et al., 2009), in which the spherical core was just removed.

- Case 2 : $\epsilon_3/\epsilon_1 = 0.1$, $\epsilon_4 = 0$. We are close to the resonance, we here aim at detecting any discontinuity in the behaviour of the system close to the exact resonance.

- Case 3 : $\epsilon_3/\epsilon_1 = \epsilon_4/\epsilon_2 = 1$. The cavity is homothetical to Mercury, this was the configuration studied by Henrard (2008) for Io.

- Case 4 : $\epsilon_3/\epsilon_1 = 3$, $\epsilon_4 = 0$. We here take some distance with the resonance.

- Case 5 : $\epsilon_3/\epsilon_1 = \epsilon_4/\epsilon_2 = 3$. By comparing this configuration with the previous one, we study the influence of the parameter ϵ_4, i.e. the equatorial ellipticity of the core.

We made tests for a wider range of the parameters, but retained only these 5 cases for the sake of conciseness.

The analysis of the free periods is very important because it gives the first results on the influence of the shape of the core on the behaviour of the system. They act like a "barometer" for the changes in the dynamics and were always one of our first concerns as well as one of the first indicators to know whether or not our method was correct. We can notice that the two periods T_1 and T_3 stay relatively constant. This is especially interesting for T_1. Indeed, this degree of freedom linked with the longitudinal motion is very weakly coupled with the variations of the obliquity (very small values of the mixed term in the untangling transformation), and even

Fundamental periods for the 5 cases								
ϵ_3/ϵ_1	0	0.1	1		3		3	
ϵ_4/ϵ_2	0	0	1		3		0	
	Num.	Num.	An.	Num.	An.	Num.	An.	Num.
T_1 (y)	12.0580	12.0577	12.0568	12.0577	12.0568	12.0578	12.0568	12.0577
T_2 (y)	615.77	(large)	1626.51	1636.43	1216.46	1214.91	1216.41	1216.09
T_3 (y)	337.82	337.82	337.85	337.87	338.03	338.14	338.03	338.20
T_4 (d)	–	58.630	58.619	58.619	58.585	58.585	58.585	58.585
$T_{4-\omega}$ (y)	–	574.06	344.88	343.45	154.08	154.04	154.05	154.01

Table 5.2: Proper periods of the system, numerically and analytically determined with a good agreement. Analytical values are missing when ϵ_3/ϵ_1 is small, because of singularities met by our algorithm of Lie transforms. ω is the spin frequency of Mercury, the last line represents the distance of the system with the resonance between ω and n_4. We do not give any numerical value of T_4 for the exact resonance ($\epsilon_3 = \epsilon_4 = 0$) because we actually cannot numerically distinguish the free librations of the core from forced contributions at 58.646 days.

less with the two other ones. This should mean that this longitudinal motion is basically not influenced by the shape of the core, and the amplitude of longitudinal librations should depend only on C_m/C, even with very accurate observations.

The variations of the periods T_2 are worth noticing, because they present a discontinuous behaviour. From $\epsilon_3/\epsilon_1 = 3$ to 0.1 this period is getting larger and larger. The value $\epsilon_3/\epsilon_1 = 0.33$ gives $T_2 = 3335.16$ years, while this period is too long to be numerically determined for $\epsilon_3/\epsilon_1 = 0.1$. However, we have $T_2 \approx 616$ years at the exact resonance, which is consistent with the results obtained by simply removing the spherical core from the system. We think that this discontinuity emphasizes the change of behaviour when the system is trapped into the resonance.

As can be seen in Table 5.3 and Figure 5.2, out of the resonance, the period is decreasing, tending to reach the rigid value of 1065 years. A least-square fit of T_2 gives $T_2 \approx A(\epsilon_3/\epsilon_1)^B + C$, with $A = 564.488 \pm 4.146$ y, $B = -1.25224 \pm 6.003 \times 10^{-3}$ and $C = 1074.3 \pm 3.233$ y. By including ϵ_1 in the constant and considering that 1074 is close to the rigid value of 1065 years (D'Hoedt & Lemaitre, 2004; Rambaux and Bois, 2004), we can guess for T_2 an evolution such as

$$T_2 \approx A\epsilon_3^{-5/4} + T_{2r}, \tag{5.40}$$

where A is a constant and T_{2r} is the rigid value of T_2. The influence of ϵ_4 is very small. We could not find any reason for this rational value of the exponent, but the proximity to this exact value is quite surprising and we thought it was worth mentioning it. This behaviour illustrates what Kelvin and Poincaré (1910) called the *gyrostatic rigidity*: when the cavity is far from a sphere (large ϵ_3), the body tends to behave as if it was rigid, while a cavity close to a sphere (but not a sphere) underlines a resonant behaviour.

Similarly to T_2, T_4 is decreasing when ϵ_3 is growing, but not as drastically. It confirms that the resonance between the proper rotation of the core and the period of the spin is reached for

ϵ_3/ϵ_1	T_2 (y)	T_4 (d)	$T_{4-\omega}$ (y)
0.33	3335.16	58.628	511.17
0.7	1966.31	58.623	409.08
0.8	1823.63	58.622	385.35
0.9	1718.34	58.620	363.50
1.0	1636.35	58.619	343.46
1.1	1570.86	58.617	325.10
1.2	1519.36	58.616	308.30
1.5	1408.10	58.611	266.01
2	1313.11	58.602	214.85
2.5	1250.26	58.594	179.64
3	1216.09	58.585	154.01
3.5	1198.68	58.576	134.72
5	1149.35	58.550	97.69
10	1107.62	58.462	50.83

Table 5.3: Evolution of the periods T_2 and T_4 with respect to ϵ_3/ϵ_1, with $\epsilon_4 = 0$. These periods have been numerically determined, and confirmed analytically with a very good agreement when $\epsilon_3/\epsilon_1 > 1$.

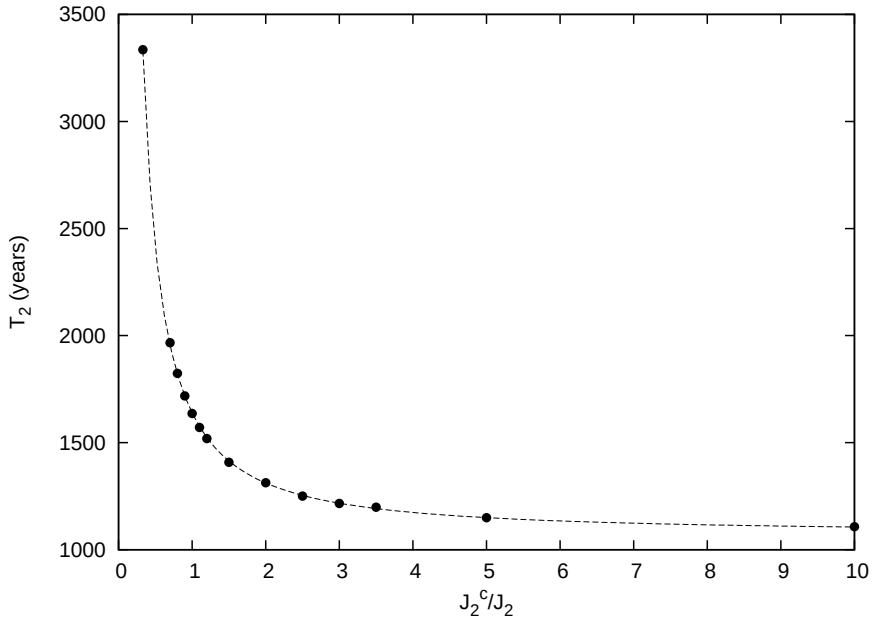

Figure 5.2: Graphical representation of the free period T_2, associated with the latitudinal motion. This curve can be fitted by $f(\epsilon_3) \approx T_{2r} + A\epsilon_3^{-5/4}$, where A is a constant and T_{2r} is the value of T_2 when Mercury is considered as rigid. The circles are the outputs of the frequency analysis after numerical integration, while the solid line is $f(\epsilon_3/\epsilon_1) = A(\epsilon_3/\epsilon_1)^B + C$ with $A = 564.488$ y, $B = -1.25224$ and $C = 1074.3$ y.

$\epsilon_3 = 0$. The third column of Table 5.3 is more significant because it represents the distance of this frequency ω_4 from the exact resonance.

We would like to emphasize that the period of the great inequality between Jupiter and Saturn (883 years) does not belong to the interval of the possible periods for T_2. According to Table 5.3, with a triaxial core almost spherical, the period T_2 tends to be very large while a core with a large ratio ϵ_3/ϵ_1 should bring this period close to a rigid Mercury case (1065 years). As a consequence, unlike the previous chapter, there should not be any resonant forcing due to the great inequality in the ecliptic obliquity K and the angle σ_2.

5.3 Consequences on the observable rotation

Our canonical variables are very convenient to describe the dynamics of the system, unfortunately they are not observable variables. Observations of the rotation of Mercury are in fact observations of its surface, i.e. the rigid mantle in our model. Consequently we have to express the components of the angular momentum of the mantle in the figure frame (with unit vectors $\vec{f_1}$, $\vec{f_2}$, $\vec{f_3}$ in the direction of X_3,Y_3,Z_3):

$$\vec{N_m} = A_m\omega_1\vec{f_1} + B_m\omega_2\vec{f_2} + C_m\omega_3\vec{f_3}. \tag{5.41}$$

5.3.1 The observable variables

We deduce from the equations (5.16) and (5.17):

$$\omega_1 = \frac{D_1N_1^c - A_cN_1}{D_1^2 - AA_c} \quad \omega_2 = \frac{D_2N_2^c - B_cN_2}{D_2^2 - BB_c} \quad \omega_1 = \frac{D_3N_3^c - C_cN_3}{D_3^2 - CC_c} \tag{5.42}$$

Replacing these in equation (5.41), we have the expression of the angular momentum of the mantle with respect to the components of $\vec{N}$ and $\vec{N^c}$:

$$\vec{N_m} = A_m\frac{D_1N_1^c - A_cN_1}{D_1^2 - AA_c}\vec{f_1} + B_m\frac{D_2N_2^c - B_cN_2}{D_2^2 - BB_c}\vec{f_2} + C_m\frac{D_3N_3^c - C_cN_3}{D_3^2 - CC_c}\vec{f_3}. \tag{5.43}$$

We can define a wobble J_m and a precession angle l_m of the mantle of Mercury in this way:

$$\vec{N_m} = G_m \sin J_m \sin l_m\vec{f_1} + G_m \sin J_m \cos l_m\vec{f_2} + G_m \cos J_m\vec{f_3}, \tag{5.44}$$

where G_m is the norm of $\vec{N_m}$. Because of the $3:2$ spin-orbit resonance, G_m is expected to be close to $3n_oC_m/2$. We get the expressions of G_m, J_m and l_m by comparing the equations (5.43) and (5.44).

We now need to express the obliquity K_m and the node h_m of the mantle relatively to the inertial frame (X_0, Y_0, Z_0). Naming M_1, M_2 and M_3 the coordinates of $\vec{N_m}$ in the inertial frame, we have:

$$\begin{pmatrix} M_1 \\ M_2 \\ M_3 \end{pmatrix} = R_3(h_m)R_1(K_m)R_3(g_m) \begin{pmatrix} 0 \\ 0 \\ G_m \end{pmatrix}, \tag{5.45}$$

with $(0, 0, G_m)^T$ the coordinates of $\vec{N_m}$ in a reference frame linked to the spin of the mantle. We then have:

$$M_1 = G_m \sin(K_m) \sin(h_m), \tag{5.46}$$
$$M_2 = -G_m \sin(K_m) \cos(h_m), \tag{5.47}$$
$$M_3 = G_m \cos(K_m). \tag{5.48}$$

Naming $M_1'^c$, $M_2'^c$ and $M_3'^c$ the coordinates of the angular momentum of the core $\vec{N'^c}$ in the inertial frame (X_0, Y_0, Z_0), we have:

$$\begin{pmatrix} M_1'^c \\ M_2'^c \\ M_3'^c \end{pmatrix} = R_3(h)R_1(K)R_3(g)R_1(J)R_3(l) \begin{pmatrix} N_1'^c \\ N_2'^c \\ N_3'^c \end{pmatrix}, \tag{5.49}$$

with $(N_1'^c, N_2'^c, N_3'^c)$ the components of the core in the figure frame. Using the fact that the core and the mantle are aligned, we now get:

$$G_m \sin(K_m) \sin(h_m) = G \sin(K) \sin(h) - M_1'^c, \tag{5.50}$$
$$-G_m \sin(K_m) \cos(h_m) = -G \sin(K) \cos(h) - M_2'^c, \tag{5.51}$$
$$G_m \cos(K_m) = G \cos(K) - M_3'^c, \tag{5.52}$$

and finally

$$K_m = \arccos\Big(\frac{G\cos(K) - M_3'^c}{G_m}\Big), \tag{5.53}$$
$$h_m = \arctan\Big(\frac{G\sin(K)\sin(h) - M_1'^c}{G\sin(K)\cos(h) + M_2'^c}\Big). \tag{5.54}$$

Equaling products of rotation matrices and using considerations similar to the computations above, it is also possible to compute the angle g_m. It is now straightforward to derive an angle p_m, analogous to p, with

$$p_m = l_m + g_m + h_m. \tag{5.55}$$

The wobble J_c' and the precession angle l_c' of the core are directly derived from (5.9), using the values ω_i (5.42) as we did for J_m and l_m. They are not observable variables, but can be of planetological interest.

5.3.2 Results

The outputs given are chosen for their physical relevance. We express

- the longitudinal motion of Mercury,

- the obliquity of the mantle with respect to its orbital motion,
- the polar motion of the mantle,
- the wobble of the core.

The first three variables can be observed, while the last one has indirect implications on Mercury's magnetic field for example.

Due to the complexity of the formulas of the previous section, we do not try to express the outputs as Poisson series. The results are given using numerical methods only.

Longitudinal motion

In the previous chapter we saw two main contributions for the libration in longitude: a 88-day one of around 36 arcsec, due to the orbital motion of Mercury, and a 11.86-year one of approximately 42 arcsec, due to the Jovian perturbation on Mercury's orbit. Its amplitude is highly sensitive to the size of the core, because of the proximity of a secondary resonance between the period $T_1 = 12.06$ years and the orbital period of Jupiter, 11.86 years.

We have determined the longitudinal librations thanks to a frequency analysis of the angle p_m (5.55), after removal of a slope, i.e. the spin frequency of 39.1318408 rad/y. In all our numerical simulations, we get an amplitude between 35.829 and 35.830 arcsec for the 88-day contribution, and between 41.316 and 41.321 arcsec for the 11.86-year one. These results are in good agreement with the previous studies considering a spherical core, and do not show any significant variations. Rambaux et al. (2007b) had the same conclusion in a similar study, this means that the shape of the liquid (or molten) core cannot be derived from observations of the longitudinal motion. This result was expected from the negligible variations of the free period T_1 associated with the longitudinal motion (Table 5.2).

The obliquity of the mantle

There are many ways to define the obliquity of the mantle. K_m (5.53) is the obliquity with respect to the inertial reference plane, i.e. the ecliptic at J2000. θ is the orbital obliquity, defined as the angle between the normal to the orbit and the spin axis. Even though we showed in Chapter 3 that the variations of both obliquities are extremely close, we here choose to use the orbital obliquity θ for its greater physical relevance. It is derived from the scalar product between $\vec{N}_m$ and the normal to the orbit, given by the cross product of the position and velocity vectors of Mercury. We show its variations in Figure 5.3 in 4 different cases.

This quantity shows essentially a secular behaviour, as expected (see e.g. Peale (2006); Yseboodt & Margot (2006); D'Hoedt & Lemaitre (2008); Dufey et al. (2009)). Moreover, we can see from the plots that the obliquity is always close to 1.66 arcmin, except in the strict resonant case ($\epsilon_3 = \epsilon_4 = 0$), where the obliquity is close to 1 arcmin, joining up with our previous computations of spherical core. Note that there are no reason why this core should be perfectly spherical and the resonant case is very improbable.

Looking at the non-resonant case of Figure 5.3, we see very few differences when the shape parameters ϵ_3/ϵ_1 and ϵ_4/ϵ_2 vary. Hence we can say that the shape of the core could probably not be derived from observations.

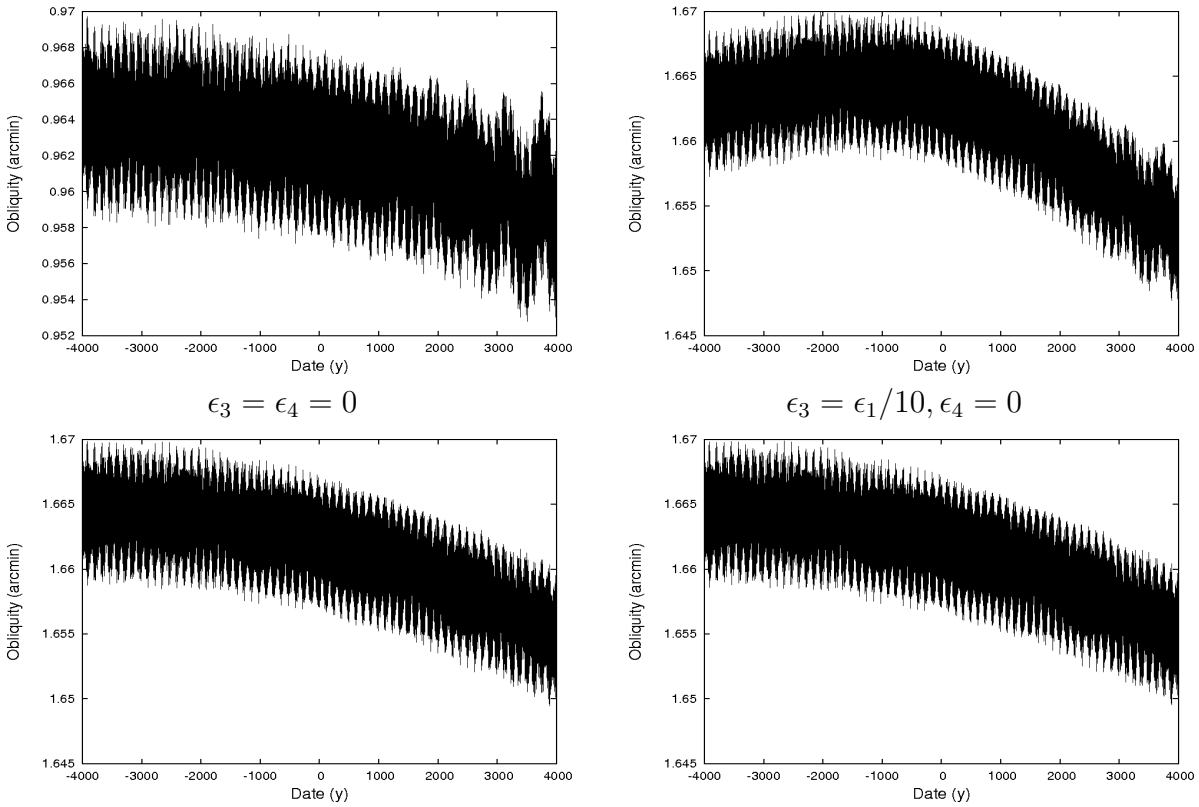

$\epsilon_3 = \epsilon_4 = 0$ $\epsilon_3 = \epsilon_1/10, \epsilon_4 = 0$

$\epsilon_3/\epsilon_1 = \epsilon_4/\epsilon_2 = 1$ $\epsilon_3 = 3\epsilon_1, \epsilon_4 = 0$

Figure 5.3: Variations of the orbital obliquity ϵ of the mantle of Mercury for different shapes of the core. The time origin is J2000.

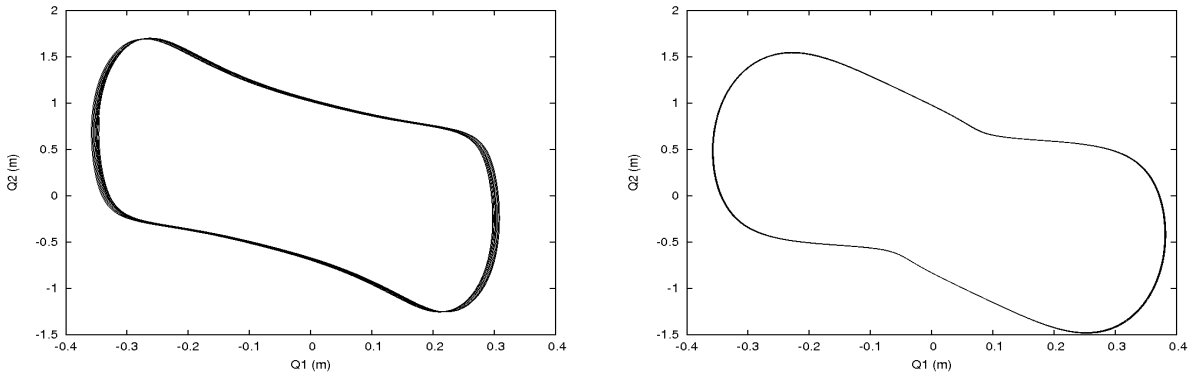

$\epsilon_3/\epsilon_1 = \epsilon_4/\epsilon_2 = 1$ $\epsilon_3 = 3\epsilon_1, \epsilon_4 = 0$

Figure 5.4: Polar motion of the mantle, plotted over 5 years from J2000.

Polar motion of the mantle

As in the previous chapters, we give here the polar motion of the rotation axis of the mantle about the geometrical North Pole. Following Henrard (2005a), we define the first two components Q_1 and Q_2 of the unit vector in the direction of the instantaneous axis of rotation by $Q_1 \approx \sin J_m \sin l_m[1 + (C_m - A_m)/C_m]$ and $Q_2 \approx \sin J_m \cos l_m[1 + (C_m - B_m)/C_m]$, and multiply them by the polar radius of Mercury, i.e. 2439.7 km (Seidelmann et al., 2007).

In Figure 5.4, we show the polar motion of the mantle over 5 years, starting from J2000, for two different shapes of the core. In both cases and like in the previous chapters, we see that this motion has a very small amplitude (smaller than 2 meters), and so should not be detected by the spacecrafts. They present similar aspects, the differences between the two representations being emphasized in Table 5.4.

This table gives quasiperiodic representations of the polar motion of the mantle, defined by the quantity $Q_1 + \sqrt{-1}Q_2$, in the same cases as in Figure 5.4. The frequencies and the amplitudes associated have been numerically obtained using frequency analysis. The basic frequency of this motion, here named τ, is the frequency of the sidereal Hermean day. Its period is twice the orbital period of Mercury and thrice its rotational one. We can consider it as the frequency of precession of the rotation axis of the mantle around the geometrical pole. The other frequencies are odd harmonics of τ. This table confirms that the amplitude of this motion is small. We can in particular notice that we cannot detect any resonant excitation of the 3τ contribution, while it is close to the free frequency ω_z.

Polar motion of the core

Even if the core cannot be observed, its rotation should still be described. It could indeed have some planetological implications, for instance in the origin of Mercury's magnetic field (see e.g. Christensen (2006)). Figure 5.5 gives the evolution of its wobble J_c for different values of the shape parameters of the core ϵ_3 and ϵ_4. Table 5.5 is a synthetic description of the quantity $J_c \exp(\sqrt{-1}l_c)$, representing the precessional motion of the core.

The wobble J_c is quite large when the system is close to the resonance, and its amplitude

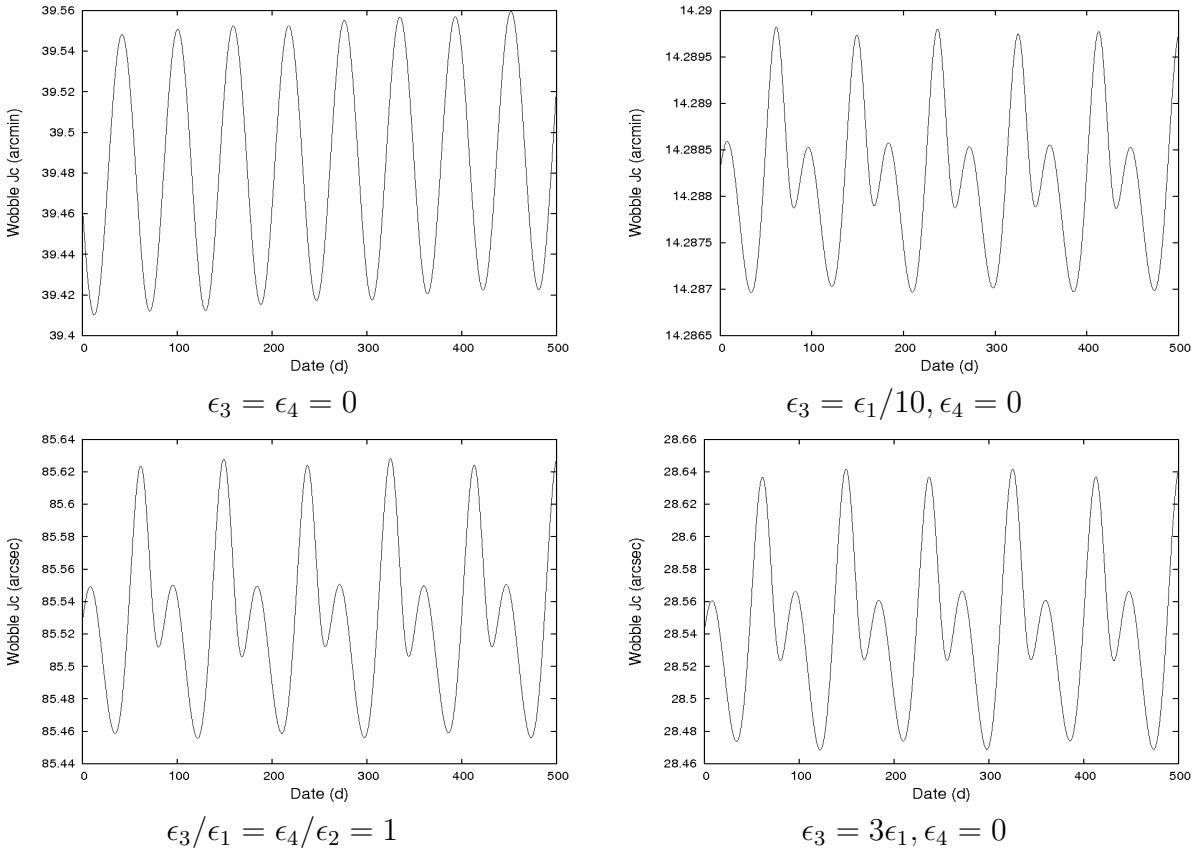

Figure 5.5: Wobble of the core J_c, obtained from numerical simulations after removal of the free librations. We can see that for a spherical core ($\epsilon_3 = \epsilon_4 = 0$) the visual aspect is very different from the other cases. Moreover, a long-term visualisation of J_c shows a slope, i.e. a secular increase of the wobble of the core, while the other cases (out of the resonance) do not show it.

Table 5.4: Synthetic representation of the polar motion of the mantle $Q_1 + \sqrt{-1}Q_2$. This motion can be expressed with a high accuracy (see the amplitudes) just with harmonics of the sidereal Hermean frequency τ. The two columns "Amplitude" are related to the two cases shown in Figure 5.4. We can see that the differences between the two cases are quite small.

τ	Amplitude (m) $\epsilon_3/\epsilon_1 = \epsilon_4/\epsilon_2 = 1$	Amplitude (m) $\epsilon_3 = 3\epsilon_1, \epsilon_4 = 0$	Period (d)
1	0.73344	0.73118	175.9
−1	0.44199	0.44064	−175.9
3	0.20077	0.24330	58.6
−3	0.17937	0.17844	−58.6
5	0.06283	0.06264	35.2
−5	0.06246	0.06231	−35.2
7	0.01765	0.01760	25.1
−7	0.01490	0.01486	−25.1
9	0.00507	0.00505	19.5
−9	0.00146	0.00377	−19.5

decreases when ϵ_3 (the polar flattening of the core) increases, i.e. when the system takes distance from the exact resonance. In fact, for $\epsilon_3 = 0$, the mean value of J_c is linearly growing, and the value of 40 arcmin that can be read on Figure 5.5 is not reliable. However, we are confident in the behaviour of the system out of the resonance, and we can see on the other three plots a quite similar visual aspect, except for the mean value. This aspect can be better understood thanks to Table 5.5.

We see on this table the overwhelming predominance of the 58.6-d contribution, i.e. the rotational period. As expected, it is excited by the proximity of the $1:1$ secondary resonance with the free frequency ω_z. We can see that the amplitude associated is roughly the mean value of J_c as can be read from Figure 5.5 (858.344 arcsec = 14.306 arcmin). We also note some similarities with the precession of the rotation axis of the mantle (Table 5.4), the frequencies

Table 5.5: Synthetic representation of the precession of the rotation axis of the core about its geometrical pole axis. The quantity here analysed is $J_c \exp(\sqrt{-1}l_c)$. Contrary to the polar motion of the mantle, we see a high 58.6-day contribution. The amplitude associated is raised by the proximity of the resonance with the free frequency of the core.

τ	Amplitude (arcsec) $\epsilon_3 = \epsilon_1/10, \epsilon_4 = 0$	Amplitude (arcsec) $\epsilon_3/\epsilon_1 = \epsilon_4/\epsilon_2 = 1$	Amplitude (arcsec) $\epsilon_3 = 3\epsilon_1, \epsilon_4 = 0$	Period (d)
3	858.344	85.532	28.546	58.6
−3	-	0.046	0.010	−58.6
1	-	0.049	0.053	175.9
−1	0.045	0.011	0.046	−175.9
5	0.067	-	0.005	35.2
−5	-	-	0.002	35.2

involved being the same ones.

With this last part, we finish our investigations of the 4-degree of freedom behaviour of a rotating Mercury composed of a rigid mantle and a fluid ellipsoidal core. We found very good agreements between analytical and numerical methods. We emphasized the influence of the proximity of a resonance with the spin of Mercury, that can raise the velocity field of the fluid constituting the core. Because of this resonance and the complexity of the formulas, a numerical method is a lot more convenient here, but the analytic method is still useful in order to have several confirmations.

We were able to rule out the possibility of a resonant forcing in the latitudinal motion that appeared in the case of a spherical liquid core because of the Jupiter-Saturn great inequality.

We showed that neither the observations of the longitudinal motion of Mercury, nor of its polar one, could be inverted to get the shape of the core. However, as shown in the previous chapters, they will give information on its size (i.e. the parameter δ).

6

Additions to the theory of rotation

This chapter deals with a few auxiliary questions on Mercury's rotation that arose during this thesis. Among many of these, two in particular retain our interest.

The first one is an in-depth study of the near resonance between the orbital period of Jupiter and the fundamental period associated with the libration in longitude that we referred to as T_1. We use a 1-degree of freedom model with the *indirect* perturbation of Jupiter. After a few transformations, the Hamiltonian is reduced to a second fundamental model of resonance (Henrard & Lemaitre, 1983). We then analyse whether this new resonance could play a role in the rotational dynamics of the planet using two values of the moment ratio $(B - A)/C_m$, the one used in the previous chapters, quite far from the resonance, and the other one almost exactly at the resonance.

The second question is that of the *direct* planetary perturbations on the rotation. Unlike the indirect perturbations, the direct ones are expected to have an insignificant effect on the rotation, but we would like to prove it once and for all. To do so, we introduce the gravity potential due to the other planets, taking into account the shape of Mercury (in a similar way than what was done for the gravity potential of the Sun). Since we are looking for the order of magnitude of these effects rather than extra accurate amplitudes, we make the simplifying hypotheses of a planar problem and circular orbits for the other planets. This study allows to make a ranking of the direct effects of the planets and to show that they are indeed insignificant compared to the indirect planetary perturbations.

6.1 Study of the resonance with the orbital period of Jupiter

In Chapter 4, we showed that the indirect planetary perturbations have a strong influence in the rotation of Mercury. Especially on the libration in longitude, for a value of $C_m/C = 0.579$ the 11.86-year contribution from Jupiter is larger than the 88-day contribution coming from the orbital motion of Mercury. This large 11.86-year effect is triggered by a resonant forcing between this orbital period of Jupiter and the free period associated with the libration in longitude (around 12 years).

In this study we formally describe this resonance and study it for different values of the moment ratio $(B - A)/C_m$. To describe the dynamics of this problem, we use a 1-degree of freedom Hamiltonian with the inclination of Mercury set to zero. The only indirect planetary

perturbation that we include is the 11.86-year period one and we use a similar method as in Chapter 4 to include Jupiter's effect.

Since the Hamiltonian will turn out as a second fundamental model for resonance we first briefly recall the model and the theory associated. Then we show how to get to this model and finally analyse it for a value of the moment ratio bringing the model close to the exact resonance.

6.1.1 The second fundamental model for resonance

The pendulum has often been taken as the basic model for resonance, it is the "first fundamental model for resonance". Its dynamics, phase space and particularities are extremely well known and the pendulum is mentioned implicitly or explicitly in almost any reference about resonances. The Hamiltonian of the pendulum is

$$H = \frac{a}{2}I^2 - b\cos\phi. \tag{6.1}$$

A resonance problem is often reduced to the pendulum using the following steps:

1. Action-angle variables are introduced such that the Hamiltonian K of the problem is separated in two parts:
$$K = K_0(S) + \epsilon K_1(S, s), \tag{6.2}$$
with K_0 independent of the resonant angle s and K_1 2π-periodic in this angle. Usually, $\partial K_0/\partial S$ is small for S close to a value $S^\star$.

2. K_0 and K_1 are expanded in series around $S^\star$ and only the most significant terms are kept.

3. If the term of $K_1(0, s)$ is a non-constant function of s, we have this kind of truncated Hamiltonian
$$K' = \alpha S + \beta S^2 + \epsilon\cos s \tag{6.3}$$
which leads to the pendulum (6.1) after a simple translation $S = I - \alpha/2\beta$.

However, in many instances in celestial mechanics, the function K_1 possesses the d'Alembert characteristic, meaning that the terms of K_1 are of the type $(\sqrt{S})^m\cos(ns)$ (or sine), with m and n having the same parity and $m \geq n$. In this case $K_1(0, s)$ is a constant and the analogous simplest truncated Hamiltonian is

$$K'' = \alpha S + \beta S^2 + \epsilon\sqrt{2S}\cos s. \tag{6.4}$$

This Hamiltonian is the **second fundamental model of resonance**. It was introduced in a paper by Henrard & Lemaitre (1983) in order to provide another well-documented model for resonances of the type (6.4).

This model can be described using only one parameter instead of three:

$$\delta = -\text{sign}(\alpha\beta) \times \left|\frac{4}{27}\frac{\alpha^3}{\beta\epsilon^2}\right|^{1/3} - 1. \tag{6.5}$$

$\delta = -1$ indicates an exact resonance, values of $|\delta| > 5$ indicate that we are already too far from the resonance for any approximation to be useful.

In the next section, we show how our simplified Hamiltonian after introduction of a new resonant angle emerges as a second fundamental model of resonance and for which values of the moment-ratio $(B - A)/C_m$ this model makes sense.

6.1.2 Getting to the 2nd fundamental model of resonance

The 1-degree of freedom Hamiltonian without inclination and before the introduction of the resonant angle and the planetary perturbations is the following:

$$H = H_{2B}(L_o) + T(\Lambda_1) + V_G(l_o, L_o, \varpi_o, \lambda_1), \tag{6.6}$$

Since we assume that the problem is planar, the planetary perturbations affect 4 orbital elements:

$$\begin{aligned} a &= a^\star + a_1 \cos(l_J) + a_2 \sin(l_j) \\ l_M &= l_M^\star + b_1 \cos(l_J) + b_2 \sin(l_j) \\ e &= e^\star + c_1 \cos(l_J) + c_2 \sin(l_j) \\ \varpi_o &= \varpi_o^\star + d_1 \cos(l_J) + d_2 \sin(l_j), \end{aligned}$$

with $a_1, a_2, b_1, b_2, c_1, c_2, d_1, d_2$ constants, l_J the longitude of Jupiter and l_M the longitude of the Sun (in the hermeocentric frame) with the relation $l_M = l_o + \varpi_o$.
As in Chapter 4, we introduce these series in the gravitational potential $V_G(e, \varpi_o, l_o, L_o(a), \lambda_1)$. After the introduction of the resonant angle σ_1 and similar considerations as in Chapter 3 allowing to replace the coefficient of the gravitational potential by a constant, the Hamiltonian obtained is similar to (3.35):

$$\begin{aligned} H =& n_o(\Lambda_o - 3\Lambda_1/2) + n_J\Lambda_J + \frac{\Lambda_1^2}{2C_m} - m_1\cos(2\sigma_1) - m_2\cos(2\sigma_1 + l_J) && (6.7)\\ &+ m_2\cos(2\sigma_1 - l_J) + m_3\sin(2\sigma_1 + l_J) + m_3\sin(2\sigma_1 - l_J) + P(l_o, l_J, \sigma_1) && (6.8)\\ =& n_o(\Lambda_o - 3\Lambda_1/2) + n_J\Lambda_J + \frac{\Lambda_1^2}{2C_m} - m_1\cos(2\sigma_1) + 2m_2\sin(2\sigma_1)\sin(l_J) && (6.9)\\ &+ 2m_3\sin(2\sigma_1)\cos(l_J) + P(l_o, l_J, \sigma_1) && (6.10) \end{aligned}$$

where n_J is the orbital frequency of Jupiter and Λ_J is the moment associated with l_J. $P(l_o, l_J, \sigma_1)$ is the part of the Hamiltonian containing only periodic terms in l_o, hence the fast terms (88-day period compared to the 11.862 years of the orbital period of Jupiter). We have the relation $m_i = C_{22}m_{iB}$, with

$$\begin{aligned} m_{1B} &= 0.1335861699455342 \times 10^4 \\ m_{2B} &= 0.6332983771096271 \times 10^{-2} \\ m_{3B} &= 0.6569252080048005 \times 10^{-2}, \end{aligned}$$

coming from the expansions of r/a and f in eccentricity. The coefficients m_i are then easily modifiable with any change of the parameter C_{22}.

We average the Hamiltonian with respect to the short-period variable, i.e. the mean longitude l_o and also perform the canonical change of variables of multiplier $1/\Lambda_1^\star$

$$(l_o, \Lambda_o, \sigma_1, \Lambda_1, l_J, \Lambda_J) \rightarrow (l_o, \Lambda'_o, \sigma_1, y_1, l_J, \Lambda'_J),$$

with $\Lambda_o = \Lambda_1^\star \Lambda'_o$, $\Lambda_1 = \Lambda_1^\star(1+y_1)$, $\Lambda_J = \Lambda_1^\star \Lambda'_J$ and where σ_1 is expanded in Taylor series. Since we do not expect σ_1 to be larger than $10^{-3} (\approx 200$ arcsec), the expansions are $\cos 2\sigma_1 = 1 - 2\sigma_1^2 + 2\sigma_1^4/3$ and $\sin 2\sigma_1 = 2\sigma_1$ (the cosine is expanded until the fourth order because it is multiplied by a coefficient much larger than the sine). The Hamiltonian is then (taking into account the multiplier $1/\Lambda_1^\star$):

$$\begin{aligned} H &= \frac{1}{\Lambda_1^\star}\left(n_o \Lambda_1^\star \Lambda'_o + n_J \Lambda_1^\star \Lambda'_J + \frac{\Lambda_1^{\star 2} y_1^2}{2C_m} + 2m_1\sigma_1^2 - \frac{2}{3} m_1 \sigma_1^4 + 4m_2 \sigma_1 \sin(l_J) + 4m_3 \sigma_1 \cos(l_J) \right) \\ &= n_o \Lambda'_o + n_J \Lambda'_J + \frac{\Lambda_1^\star y_1^2}{2C_m} + 2\frac{m_1}{\Lambda_1^\star}\sigma_1^2 - \frac{2}{3}\frac{m_1}{\Lambda_1^\star}\sigma_1^4 + 4\frac{m_2}{\Lambda_1^\star}\sigma_1 \sin(l_J) + 4\frac{m_3}{\Lambda_1^\star}\sigma_1 \cos(l_J) \end{aligned}$$

where the linear term in y_1 of the Keplerian contribution and the kinetic energy cancel each other, as was shown in Chapter 3. After the averaging, the Hamiltonian is obviously independent of the mean anomaly l_o and the associated moment Λ'_o is a constant. As a consequence, we drop it from the Hamiltonian. In order to have the same coefficient for the quadratic terms in σ_1 and y_1, we perform the canonical change of variables $\sigma_1 = \sqrt[4]{\frac{\Lambda_1^{\star 2}}{4m_1 C_m}} x_1 = s_1 x_1$ and $y'_1 = \sqrt[4]{\frac{4m_1 C_m}{\Lambda_1^{\star 2}}} y_1 = y'_1/s_1$ to get

$$H = n_J \Lambda'_J + \sqrt{\frac{m_1}{C_m}}(x_1^2 + {y'_1}^2) - \frac{2}{3} m'_1 x_1^4 + 4m'_2 x_1 \sin(l_J) + 4m'_3 x_1 \cos(l_J), \tag{6.11}$$

with $m'_1 = s_1^4 m_1/\Lambda_1^\star$, $m'_2 = s_1 m_2/\Lambda_1^\star$ and $m'_3 = s_1 m_3/\Lambda_1^\star$.

Then using another canonical change of variables to polar coordinates $x_1 = \sqrt{2U}\sin u$, $y'_1 = \sqrt{2U}\cos u$, the Hamiltonian becomes

$$H = n_J \Lambda'_J + 2\sqrt{\frac{m_1}{C_m}} U - \frac{8}{3} m'_1 U^2 \sin^4 u + 4m'_2 \sqrt{2U}\sin(u)\sin(l_J) + 4m'_3\sqrt{2U}\sin(u)\cos(l_J). \tag{6.12}$$

Finally, recombining the products of sines and cosines, we have

$$\begin{aligned} H =& n_J \Lambda'_J + 2\sqrt{\frac{m_1}{C_m}} U - \frac{8}{3} m'_1 U^2 \left(\frac{3}{8} - \frac{1}{2}\cos(2u) + \frac{1}{8}\cos(4u) \right) \\ & - 2m'_2\sqrt{2U}\big(\cos(u + l_J) - \cos(u - l_J)\big) + 2m'_3\sqrt{2U}\big(\sin(u + l_J) + \sin(u - l_J)\big). \end{aligned}$$

We now introduce another resonant angle, expressing the proximity of the orbital period of Jupiter and the first free period: $\rho = u - l_J$. Assuming that we keep U as the moment associated

with ρ, the moment associated with l_J changes to keep a canonical set of variable: $\Lambda''_J = \Lambda'_J + U$ and the Hamiltonian is

$$\begin{aligned} H =& n_J\Lambda''_J + \left(2\sqrt{\frac{m_1}{C_m}} - n_J\right) U - \frac{8}{3}m'_1U^2\left(\frac{3}{8} - \frac{1}{2}\cos(2(\rho+l_J)) + \frac{1}{8}\cos(4(\rho+l_J))\right) \\ & - 2m'_2\sqrt{2U}\big(\cos(\rho+2l_J) - \cos(\rho)\big) + 2m'_3\sqrt{2U}\big(\sin(\rho+2l_J) + \sin(\rho)\big). \end{aligned}$$

Once again, we have a situation with a fast angle (l_J) compared to the slow resonant angle (ρ). We average this last Hamiltonian over l_J and have (dropping the term in Λ''_J now constant with the disappearance of the angle l_J in the Hamiltonian):

$$\begin{aligned} H &= \left(2\sqrt{\frac{m_1}{C_m}} - n_J\right) U - m'_1U^2 + \epsilon\sqrt{2U}\cos(\underbrace{\rho - \rho_0}_{\rho'}) && (6.13) \\ &= \alpha U + \beta U^2 + \epsilon\sqrt{2U}\cos(\rho'), && (6.14) \end{aligned}$$

and we finally arrive to a second fundamental model of resonance. The values of the parameters β and ρ_0 are constant while α and ϵ are functions of the ratio C_{22}/C_m, or equivalently $(B-A)/C_m$:

$$\begin{aligned} \alpha &= 2\sqrt{m_{1B}}\sqrt{\frac{C_{22}}{C_m}} - n_J = \sqrt{m_{1B}}\sqrt{\frac{B-A}{C_m}} - n_J && (6.15) \\ \beta &= -\frac{3}{8}n_o = -9.783 && (6.16) \\ \epsilon &= 2\sqrt[4]{\frac{1}{9n_o^2m_{1B}}}\left(\frac{C_{22}}{C_m}\right)^{3/4}\sqrt{m_{2B}^2 + m_{3B}^2} && (6.17) \\ &= \sqrt[4]{\frac{1}{36n_o^2m_{1B}}}\left(\frac{B-A}{C_m}\right)^{3/4}\sqrt{m_{2B}^2 + m_{3B}^2} && (6.18) \\ \rho_0 &= \arctan\frac{m_{3B}}{m_{2B}} = 46.049^\circ && (6.19) \end{aligned}$$

As mentioned earlier, the second fundamental model of resonance is characterised by the parameter δ, defined as follows:

$$\delta = -\text{sign}(\alpha\beta) \times \left|\frac{4}{27}\frac{\alpha^3}{\beta\epsilon^2}\right|^{1/3} - 1. \qquad (6.20)$$

This parameter represents the proximity to the resonance. Large values of δ ($|\delta| > 5$) physically correspond to systems not very close to a resonance or with a weak restoring force. Indeed a large value of α means that we move away from the resonance (6.15) while a small value of ϵ means that the coefficients m_2 and m_3 of the perturbation are small. For the values of the parameters $C_{22} = 10^{-5}$ and $C_m = 0.19686$ used throughout the previous chapters, we have

$$\alpha = -0.0087 \qquad \epsilon = 2.0531 \times 10^{-7} \qquad \delta = -62.8262, \qquad (6.21)$$

meaning that this system is quite far from the resonance, and also has a very weak restoring force (perturbation). As a consequence, this resonance forcing should not have particular effects other than the enhancement of the 11.86-year period amplitude in the libration in longitude.

However, if we analyse the expression of δ in function of $(B-A)/C_m$, we have

$$\delta = \frac{4\left(\sqrt{m_{1B}}\sqrt{\frac{B-A}{C_m}} - n_J\right)}{3\left(\frac{(m_{2B}^2+m_{3B}^2)}{\sqrt{m_{1B}}}\right)^{1/3}\sqrt{\frac{B-A}{C_m}}} - 1. \tag{6.22}$$

Figure 6.1 shows that, for values of the coefficient $(B-A)/C_m$ in the interval $(2.03 \pm 0.12) \times 10^{-4}$ found by Margot et al. (2007), it is possible to find values small values for δ. In particular for $(B-A)/C_m$ in the interval $[2.096 \times 10^{-4}\ ,\ 2.107 \times 10^{-4}]$, δ is situated in the interval $[-5\ ,\ 5]$.

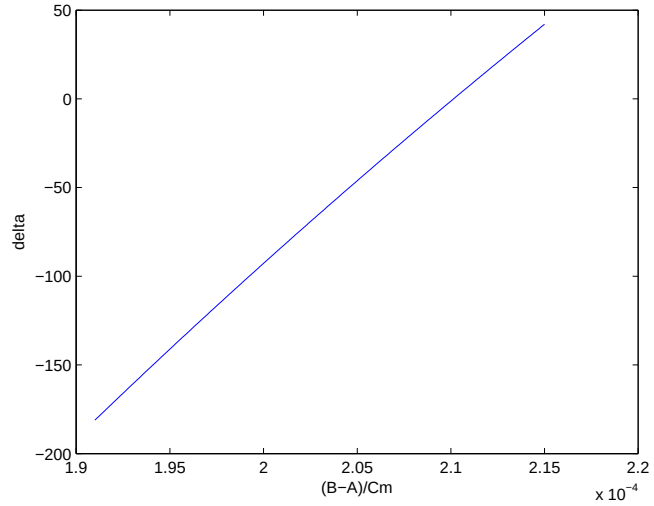

Figure 6.1: Plot of the parameter δ in function of the moment ratio $(B-A)/C_m$.

In the next section, we analyse a particular case of δ close to -1 (almost the exact resonance) by computing the equilibria and period associated with the resonance.

6.1.3 Equilibria and period of the new resonance

In this part, we position our system almost at the exact resonance. For that, we use the value of $C_m = 0.1904496$ and $C_{22} = 10^{-5}$. The values of the parameters are then

$$\alpha = -7.5685 \times 10^{-7} \qquad \epsilon = 2.1047 \times 10^{-7} \qquad \delta = -1.0053. \tag{6.23}$$

The first thing to do is to find the equilibria of the problem. The polar coordinates in (6.14) make the Hamiltonian non differentiable at $U = 0$. Let us then go to cartesian coordinates: $x = \sqrt{2U}\sin(\rho')$ and $y = \sqrt{2U}\cos(\rho')$:

$$H = \frac{\alpha}{2}(x^2+y^2) + \frac{\beta}{4}(x^2+y^2)^2 + \epsilon y. \tag{6.24}$$

Using Hamilton's equations to find the equilibria, we have

$$\dot{x} = \frac{\partial H}{\partial y} = \alpha y + \beta(x^2+y^2)y + \epsilon = 0 \tag{6.25}$$

$$\dot{y} = -\frac{\partial H}{\partial x} = -\alpha x - \beta(x^2+y^2)x = 0 \tag{6.26}$$

From the second equation, we either have $x^\star = 0$ or $x^{\star 2} = \frac{-\alpha-\beta y^2}{\beta}$, but since α and β are negative, x would be complex and we are not interested in complex solutions. Let us thus take $x^\star = 0$ as equilibrium value (implying that $\rho^\star = \rho_0$ is the equilibrium if $U^\star \neq 0$). Putting $x = 0$ in equation (6.26), we obtain $\beta y^3 + \alpha y + \epsilon = 0$, equation that we can solve with Cardan's method. Let us normalize it first: $y^3 + py + q = 0$, with $p = \alpha/\beta$ and $q = \epsilon/\beta$. The discriminant is

$$\Delta = q^2 + \frac{4}{27}p^3 = 4.6287 \times 10^{-16}. \tag{6.27}$$

Since it is positive, we have one real solution and two complex ones. The real solution is computed by the following formula:

$$y^\star = \sqrt[3]{\frac{-q+\sqrt{\Delta}}{2}} + \sqrt[3]{\frac{-q-\sqrt{\Delta}}{2}} = 2.7720 \times 10^{-3}. \tag{6.28}$$

Let us now compute the fundamental period. For that, we will expand the Hamiltonian around the equilibrium $(x^\star, y^\star)$ with the following change of variables: $Y = y - y^\star$. We have

$$\begin{aligned} H &= \frac{\alpha}{2}\left(x^2 + (Y+y^\star)^2\right) + \frac{\beta}{4}\left(x^2 + (Y+y^\star)^2\right)^2 + \epsilon(Y+y^\star) \\ &= \frac{\alpha}{2}(x^2 + Y^2 + y^{\star 2} + 2Yy^\star) + \epsilon Y + \epsilon y^\star \\ &+ \frac{\beta}{4}\left(x^4 + Y^4 + y^{\star 4} + 4Y^2y^{\star 2} + 2y^{\star 2}Y^2 + 4y^\star Y^3 + 2Y^2x^2 + 4y^{\star 3}Y + 2y^{\star 2}x^2 + 4y^\star Y x^2\right). \end{aligned}$$

Dropping the constant terms, we get

$$\begin{aligned} H =& x^2\left(\frac{\alpha}{2} + \frac{\beta}{4}y^{\star 2}\right) + Y^2\left(\frac{\alpha}{2} + \frac{3}{2}\beta y^{\star 2}\right) + Y\underbrace{\left(\beta y^{\star 3} + \alpha y^\star + \epsilon\right)}_{0} \\ &+ \frac{\beta}{4}\left(Y^4 + x^4 + 2Y^2x^2 + 4y^\star Y^3 + 3y^\star Y x^2\right). \end{aligned}$$

If we suppose that we stand very close to the equilibrium ($x \approx 0$,$Y \approx 0$), the terms of order 3 and 4 vanish and we have

$$H = Ax^2 + BY^2, \tag{6.29}$$

with $A = \left(\frac{\alpha}{2} + \frac{\beta}{4}y^{\star 2}\right)$ and $B = \left(\frac{\alpha}{2} + \frac{3}{2}\beta y^{\star 2}\right)$. We perform the following canonical change of variables: $x' = \sqrt[4]{\frac{A}{B}}x$ and $Y' = \sqrt[4]{\frac{B}{A}}Y$ to have

$$H \approx \sqrt{AB}\left(x'^2 + Y'^2\right), \tag{6.30}$$

and finally going back to polar coordinates, $X' = \sqrt{2P}\sin\psi$, $Y' = \sqrt{2P}\cos\psi$ the Hamiltonian becomes

$$H \approx 2\sqrt{AB}P. \tag{6.31}$$

With this Hamiltonian, we have a corresponding period of 134 913 years. Should the parameter $(B-A)/C_m$ be such that the system is almost at the exact resonance, the period would be so long that the amplitude should be damped over the years due to dissipations (Peale, 2005).

Moving away from the resonance, this period decreases, but not fast enough to keep the parameter δ sufficiently close to 0. As an example, taking $C_m = 0.19686$, the period is 1444 years.

After analysing in more details this resonance, we can conclude that its only effect should be the resonant forcing applied to the 11.86-year amplitude in the longitudinal librations, already mentioned in the previous chapters. In a configuration close to the exact resonance, the amplitude of this resonant term has such a long period that it should be dissipated over the years.

6.2 The direct planetary perturbations

In Chapter 4, we introduced the planetary perturbations in the rotation of Mercury in an indirect way: we considered that the rotation was affected by the changes in the orbital elements, caused themselves by planetary perturbations.

However the gravitational pulls of the planets also affect the rotation directly due to the non-spherical shape of the planet. We expect these perturbations to be really small since the planets are further away from Mercury and not as massive as the Sun. This section aims at gauging these effects.

Let us recall how we use the gravitational pull of the Sun. Since Mercury is not a perfect sphere or a point mass, the potential of the Sun affects the rotation. The potential is expanded in spherical harmonics. Only a second-order expansion is used because Mercury's shape is not well known (we recall that only J_2 and C_{22} are known with large error bars). The gravitational potential is the following:

$$V_S = -\frac{GMm}{r} - \frac{GMmR_e^2}{r^3}\left(-\frac{J_2}{2}\Big(2-3(x^2+y^2)\Big) + 3C_{22}(x^2-y^2)\right), \tag{6.32}$$

with M the mass of the Sun, m that of Mercury, r the distance Sun-Mercury, R_e the equatorial radius of Mercury and (x, y, z) the coordinates of the unit vector pointing to the Sun.
The first term of V_S is included in the Keplerian contribution H_{2B} of the Hamiltonian and only affects the orbit. Indeed, this term is the potential as if Mercury was a perfect sphere and the resulting torque of the gravity pull of the Sun on each element of a sphere is zero, thus does not affect the rotation. The second term was referred to as the (second-order) gravitational potential V_G in the previous chapters and was the cause of the rotational librations.

Let us now analyse the potential due to Venus, the closest planet. The same expansion as the Sun can be made for this potential:

$$V_V = -\frac{GM_Vm}{r_{MV}} - \frac{GM_VmR_e^2}{r_{MV}^3}\left(-\frac{J_2}{2}\Big(2-3(x_V^2+y_V^2)\Big) + 3C_{22}(x_V^2-y_V^2)\right), \tag{6.33}$$

Body	Ratio M/r^3
Sun	$4.50427764306960802\times10^{-7}$
Venus	$1.68976532470965179\times10^{-13}$
Mars	$2.39910128463365264\times10^{-15}$
Earth	$7.84795713725909887\times10^{-14}$
Jupiter	$1.77326739861737466\times10^{-13}$
Saturn	$8.50579479681784992\times10^{-15}$
Uranus	$1.60599491474021883\times10^{-16}$
Neptune	$4.94909118178259562\times10^{-17}$

Table 6.1: Ratio M/r^3 of the Sun and each planet where M is the mass of each body and r is the distance body-Mercury (planet-Sun as first approximation for the 7 other planets).

with, this time, M_V the mass of Venus, r_{MV} the distance Mercury-Venus and (x_V, y_V, z_V) the unit vector pointing to Venus.
As for the Sun, the first term actually affects the orbit of Mercury around the Sun. This change of the orbital elements will affect the rotation through the 3:2 spin-orbit resonance. In other words it produces the indirect planetary perturbations on the rotation. Since we already studied them in Chapter 4, we will not consider this first term in this problem and we simply drop it.

The second term however will be linked directly to the rotation of Mercury. This term is indeed the expression of the non-zero torque applied by a mass on a non-spherical planet.

Taking a look at equation (6.33), we notice that the important ratio is actually the mass of the planet over the cube of the distance Mercury-planet. Table 6.1 gives this ratio for the Sun and each of the 7 other planets, with the distance Mercury-planet actually being the distance Sun-planet as a first approximation. The main planetary effects should come from Venus and Jupiter with approximately the same order of magnitude, then should come the Earth and Saturn. We also notice that the effect of the Sun is at least 10^6 times larger than the effect of any planet. As a matter of fact, this table alone is enough to explain why the direct planetary perturbations are negligible in the rotation of Mercury.

However, the introduction of these changes into our method is almost straightforward and we decide to analyse this situation in more details. We expect these direct perturbations to be small and are not looking for extra accurate results but rather for the order of magnitude of the corrections on the rotation. As a consequence, we make the following simplifying assumptions:

- all the orbital motions take place in the ecliptic plane,
- we use the 1-degree of freedom Hamiltonian developed in Chapter 3,
- we consider the orbits of the other planets around the Sun as circular.

To use the gravitational potential of the Sun, we expanded the normalized distance r/a in function of the eccentricity and the true anomaly, as well as $\cos f$ and $\sin f$, f being the true anomaly.
However, since Mercury does not orbit Venus, we cannot use the same form for the potential V_V, at least not as straightforwardly. Figure 6.2 pictures the situation. To compute the distance

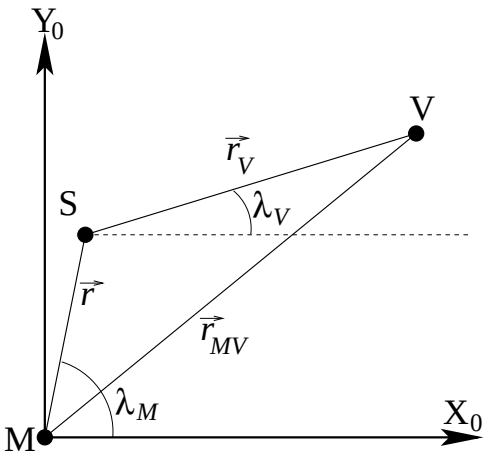

Figure 6.2: Mercury, the Sun and Venus in a hermeocentric ecliptic frame. The vector Mercury-Venus is the sum of the vectors Mercury-Sun and Sun-Venus: $\overrightarrow{r_{MV}} = \vec{r} + \overrightarrow{r_V}$. The angles λ_M and λ_V are the longitudes of Mercury and Venus respectively.

$r_{MV} = \|\overrightarrow{r_{MV}}\|$ and be able to use expansions in eccentricity and mean anomaly, we must go through $\overrightarrow{r_{MV}} = \vec{r} + \overrightarrow{r_V}$. Taking a look at figure 6.2, we see that

$$\overrightarrow{r_{MV}} = \begin{pmatrix} r\cos\lambda_M + r_V\cos\lambda_V \\ r\sin\lambda_M + r_V\sin\lambda_V \end{pmatrix}, \tag{6.34}$$

with $r = \|\vec{r}\|$ that we will expand in eccentricity and semi-major axis and $r_V = \|\overrightarrow{r_V}\|$, which is a constant since we assume that the eccentricity of Venus is 0. The distance $r_{MV} = \|\overrightarrow{r_{MV}}\|$ is then

$$\begin{aligned} r_{MV} &= \Big(r_M^2\cos^2\lambda_M + r_V^2\cos^2\lambda_V + 2r_M r_V\cos\lambda_M\cos\lambda_V && (6.35)\\ &\quad + r_V^2\sin^2\lambda_M + r_V^2\sin^2\lambda_V + 2r_M r_V\sin\lambda_M\sin\lambda_V\Big)^{1/2} && (6.36)\\ &= \Big(r_M^2 + r_V^2 + 2r_M r_V\cos(\lambda_M - \lambda_J)\Big)^{1/2} && (6.37)\\ &= r_V\left(1 + \frac{{r_M}^2}{r_V} + 2\frac{r_M}{r_V}\cos(\lambda_M - \lambda_J)\right)^{1/2} && (6.38) \end{aligned}$$

and

$$\frac{1}{{r_{MV}}^3} = \frac{1}{r_V^3}\left(1 + \frac{{r_M}^2}{r_V} + 2\frac{r_M}{r_V}\cos(\lambda_M - \lambda_J)\right)^{-3/2}. \tag{6.39}$$

Let us recall that all the expressions that we are considering are Poisson series. Since it is not possible to compute the square root of Poisson series, we must go through expansions. For the equation above, we use an expansion to order 10 of the function $(1+x)^{-3/2}$ around $x = 0$ since r_M is around one half or r_V.
We still need to compute the components x_V and y_V of the unit vector pointing towards Venus. The expression of these components is quite simply

$$\begin{pmatrix} x_V \\ y_V \end{pmatrix} = \frac{1}{r_{MV}}\overrightarrow{r_{MV}} = \frac{1}{r_{MV}}\begin{pmatrix} r\cos\lambda_M + r_V\cos\lambda_V \\ r\sin\lambda_M + r_V\sin\lambda_V \end{pmatrix}, \tag{6.40}$$

Direct influence of Venus on the rotation					
l_o	l_v	ϖ_o	Period	Amplitude	Ratio
2	-5	5	5.6632 y	0.12362×10^{-4} as	0.34498×10^{-6}
1	-2	2	1.1098 y	0.34843×10^{-5} as	0.97235×10^{-7}
2	-1	1	0.1497 y	0.32106×10^{-5} as	0.89596×10^{-7}
1	-1	1	0.3958 y	0.25793×10^{-5} as	0.71978×10^{-7}
1	-3	3	1.3803 y	0.24492×10^{-5} as	0.68347×10^{-7}
3	-2	2	0.1086 y	0.20829×10^{-5} as	0.58126×10^{-7}
2	-2	2	0.1979 y	0.90140×10^{-6} as	0.25155×10^{-7}
0	2	-2	0.3076 y	0.74622×10^{-6} as	0.20824×10^{-7}

Table 6.2: Direct planetary perturbations on the longitudinal libration angle caused by Venus. The amplitudes are expressed in arcsec and the ratio is computed with respect to the amplitude of the 88-day contribution which is 35.849 arcsec.

Direct influence of Jupiter on the rotation					
l_o	l_J	ϖ_o	Period	Amplitude	Ratio
0	1	-1	11.863 y	0.15661×10^{-2}	0.43705×10^{-4}
3	-1	1	0.0813 y	0.27795×10^{-5}	0.77566×10^{-7}
1	-1	1	0.2458 y	0.74933×10^{-6}	0.20911×10^{-7}
1	1	-1	0.2360 y	0.56247×10^{-6}	0.15696×10^{-7}
2	-1	1	0.1216 y	0.34951×10^{-6}	0.97537×10^{-8}
4	-3	3	0.0611 y	0.14238×10^{-6}	0.39733×10^{-8}
0	2	-2	5.9313 y	0.75015×10^{-7}	0.20934×10^{-8}

Table 6.3: Direct planetary perturbations of Jupiter on the longitudinal libration angle. The amplitudes are expressed in arcsec and the ratio is computed with respect to the amplitude of the 88-day contribution which is 35.849 arcsec.

with the longitude of Mercury $\lambda_M = f + \varpi_o$.

The gravitational potential due to Venus now depends on r the distance Mercury-Sun and on $\cos f$ and $\sin f$. Similarly to the planar case of Chapter 3, we expand these quantities in function of the eccentricity of Mercury e and of its mean longitude l_o. We then perform a rotation of angle λ_1 to move to the figure frame of Mercury and use the similar perturbation theory to compute the libration in longitude angle. Table 6.2 gives the direct planetary perturbations of Venus on the resonant angle σ_1. We note that, as expected, these amplitudes are very small, around 10^{-5} arcsec. The column "ratio" gives the amplitudes with respect to the 88-day contribution amplitude of 35.849 arcsec. Compared to this amplitude, the direct planetary perturbations from Venus are at least 10^6 times smaller.

The procedure described above is actually valid for any planet (or any body), the only parameters to change are the distance Sun-planet, the mass of the planet and the longitude. We chose Venus because it is the closest planet to Mercury, however it is not massive. Jupiter is the most massive but a lot further away from Mercury than Venus.

Tables 6.3, 6.4, 6.5 show the direct planetary perturbations on the libration in longitude

Direct influence of the Earth on the rotation					
l_o	l_E	ϖ_o	Period	Amplitude	Ratio
3	-2	2	0.0956 y	0.10851×10^{-5} as	0.30283×10^{-7}
2	-1	1	0.1369 y	0.94635×10^{-6} as	0.26409×10^{-7}
0	1	-1	1.0000 y	0.76314×10^{-6} as	0.21297×10^{-7}
1	-1	1	0.3172 y	0.60353×10^{-6} as	0.16842×10^{-7}
2	-2	2	0.1586 y	0.28195×10^{-6} as	0.78683×10^{-8}

Table 6.4: Direct planetary perturbations of the Earth on the longitudinal libration angle. The amplitudes are expressed in arcsec and the ratio is computed with respect to the amplitude of the 88-day contribution which is 35.849 arcsec.

Direct influence of Saturn on the rotation					
l_o	l_S	ϖ_o	Period	Amplitude	Ratio
3	-2	2	0.0807 y	0.13271×10^{-6} as	0.37035×10^{-8}
0	2	-2	14.730 y	0.11062×10^{-7} as	0.30869×10^{-9}
2	-1	1	0.1209 y	0.88825×10^{-8} as	0.24788×10^{-9}
4	-3	3	0.0606 y	0.36937×10^{-8} as	0.10308×10^{-9}
1	-1	1	0.2428 y	0.36449×10^{-8} as	0.10171×10^{-9}

Table 6.5: Direct planetary perturbations of Saturn on the longitudinal libration angle. The amplitudes are expressed in arcsec and the ratio is computed with respect to the amplitude of the 88-day contribution which is 35.849 arcsec.

caused by Jupiter, the Earth and Saturn respectively.

Most of the direct perturbations of Jupiter are of the same order than those of Venus, as expected by the ratios of table 6.1, except for one. The 11.863 year-period contribution is in this case again a lot larger than all the others. This can be explained by the same reason than for the indirect perturbations: this contribution benefits from a resonant forcing between Jupiter's orbital period and the free period of the libration in longitude.

The contributions due to the Earth and Saturn are much smaller than the other ones. We notice that the angle combination present in the indirect perturbations ($l_o - 4l_E$) does not appear here.

With this short study, we gave an order of magnitude of the importance of the direct planetary perturbations on the rotation of Mercury. As expected, these amplitudes are negligible (1.5 milli arcsec at most), especially when we compare them to the indirect planetary perturbations (dozens of arcsec).

Conclusions and perspectives

In this work, we were able to study the short-period contributions on a very elaborate model of the rotation of Mercury. Using a Hamiltonian formalism and a perturbation theory based on canonical Lie transforms, we could emphasize the importance of the main planetary perturbations on the rotational motion.

In the longitudinal motion and for the value of the moment ratio determined by Margot et al. (2007), we found that there is a resonant forcing between the orbital period of Jupiter (11.86 years) and the free period linked with the libration in longitude (12.06 years). This forced amplitude in this case is around 42 arcsec and is larger than the 88-day contribution (36 arcsec). In addition to this 11.86-year contribution, we were able to determine the most significant planetary perturbations on the libration in longitude. Venus for example should have a 5.66-year contribution with an amplitude about 10% of that of the 88-day libration. The amplitudes of the librations due to Saturn and the Earth are approximately 4% and 2% of the 88-day libration. The results obtained were rigorously checked at each step of the method and we are very confident in the accuracy of our results, as attested by the numerous comparisons performed.

To our knowledge we are the only ones who computed the effect of the planets in the libration in latitude and in the wobble motion with a great accuracy. We were able to show that these librations should be well below the arcsec level and should not be detected by the space missions. However, another resonant forcing might appear in the latitudinal librations (related to the obliquity). The period of the great inequality of Jupiter and Saturn (883 years) and the free period associated with the latitudinal motion (616 years with the same moment ratio as above) are close. Analysing this forcing for different values of the parameters (within their range of uncertainty), we showed that the amplitude of the 883-year libration might rise up to several tens of arcsec when both periods are very close to each other. However, given the long period of this libration and the short period of a space mission, this resonant forcing, should it be detected, would merely be seen as a shift in the obliquity.

With the third degree of freedom, related to the wobble motion of the planet, we computed the motion of the pole of the planet. The planetary perturbations have a very small effect on this degree of freedom and no resonant mechanism was put forward. The motion of the pole should not be larger than a couple of meters on the surface of the planet.

The model used in these studies was that of a planet with an ellipsoidal mantle and a decoupled, spherical liquid core. We also analysed core-mantle interactions, computing various observable variables of the rotation while varying the shape of the core. However, even accurate

measurements of the rotation of the planet should not help determine the shape of the core, but only its size.

Finally we examined two other questions in the rotation. The first one is a more formal study of the secondary resonance between the orbital period of Jupiter and the free period related to the longitudinal motion. We simplified our Hamiltonian to get a second fundamental model of resonance and showed that even in the case of an almost exact resonance, it should not have a great dynamical impact on the rotation. The second study was implemented to get an order of magnitude and a ranking of the direct planetary perturbations of the different planets (torques applied by the planets on the non-spherical Mercury). We showed that these direct perturbations should be at least 10^4 times smaller than the amplitude of the 88-day libration on the longitude.

For all these studies, we compared analytical and numerical approaches. The analytical method used has many advantages. It is very convenient to analyse the origin of each of the different contributions, the free amplitudes are easily put to zero (Mercury is supposed to be at a Cassini equilibrium) and it allows a greater understanding of the dynamical mechanisms ruling the rotation. It is also very convenient whenever one or several parameters of the problem are not well-known. As an example, we could easily get an expression of the longitudinal free period and of the 11.86-year contribution in function of the parameter $(B - A)/C_m$.

However it also has its downsides. To apply our method properly, the Hamiltonian and all the quantities considered must come as Poisson series, that we handle using our series manipulator called the MSNam. Getting these Poisson series often complicates the computations and expansions in the model. A related issue is the size of the Poisson series. We cannot afford to have Poisson series with a number of terms too large, as operations on Poisson series are pretty expensive in terms of CPU time. For instance, when we introduced the indirect planetary perturbations, we had to cut many terms in the expression of the orbital elements. Only a comparison with a numerical study helped us choose the terms to keep and confirmed that this cut was legitimate.

We believe that the analytical and numerical approaches complement each other, and both are necessary for an in-depth understanding of the problem.

Though these different models are quite elaborate, it is still possible to refine them in order to include more effects on the rotation. We mention among others the inclusion of the J_2 of the Sun, a relativistic correction (a direct one, we already have the relativistic corrections on the orbit included in the coefficients of our planetary theory), and of higher-degree spherical harmonics once the data of the MESSENGER will have been processed. A possible difference between the axis of least inertia and the one pointing to Mercury at each perihelion passage implying a non-diagonal matrix of inertia (with a S_{22} coefficient) could also be added to the model.

Another improvement of the method would be to make a few changes to the manipulator to bring it closer to other symbolic manipulators such as Maple. As showed in various chapters, we were often limited by the restriction of the MSNam to use only Poisson series and complicated algebraic operations had to be performed. It sometimes prevented from using the analytical method because of the complicated expressions of some variables and we had to turn to a numerical method only. It would be interesting to allow this series manipulator to be less restrictive and open to a wider class of symbolic operations while keeping its efficiency. This

would require a complete makeover of the MSNam and would certainly not be an easy task.

As for the BepiColombo mission requirements, several improvements in the model are still required. For example the inclusion of the S_{22} in the gravity potential, the choice of another inertial reference frame (Laplace plane) or the creation of a hybrid model taking into account short-period effects for the librations computations (liquid core assumption) and long-period effects for the obliquity equilibrium and the long-term effects (perihelion and node contributions) would be nice additions to this theory.

However the goal of this work was the computation of the short-period effects on the rotation (in 3 and 4 degrees of freedom) and we saw that the accuracy level obtained in our results is large enough for the BepiColombo mission. While the addition of other effects (solar J_2, relativistic correction) would still be very interesting in a theoretical point of view, they would be irrelevant for this mission.

The inclusion of the model developed in this work into some of the subroutines used for the radio-science experiment of BepiColombo (MORE) is already underway and several procedures developed in this work will be included in the software.

A

Expansions of functions in eccentricity and mean longitude

In this appendix, we explain how to expand any function of the normalized radius of the orbit r/a and the true anomaly f in series of the eccentricity e and the mean anomaly l_o.

For this, we use an expansion by Lie transforms (not canonical here):

$$F(r/a, f) \rightarrow G(e, l_o). \tag{A.1}$$

We mention that, in order to have more readable formulas, we simply note r for r/a in the rest of this appendix.

A.1 Methodology

The goal is to express a function of r and f as a function of e and l_o using Lie transforms. The function $F(r, f)$ is decomposed as $F(r, f) = \sum_{i\geq 0} \frac{e^i}{i!} F_i^0$ and the transform of this function is $g(e, l_o) = \sum_{i\geq 0} \frac{e^i}{i!} F_0^i$, where the F_0^i are determined by the following recurrence formula:

$$F_n^i = F_{n+1}^{i-1} + \sum_{j=0}^{n} C_n^j L_{j+1} \left(F_{n-j}^{i-1}\right). \tag{A.2}$$

The operator L_j is defined as

$$L_j(F) = \frac{\partial F}{\partial r} W_{r,j} + \frac{\partial F}{\partial f} W_{f,j} \tag{A.3}$$

and the generators are

$$W_r = \frac{\partial r}{\partial e} = \sum_{i\geq 0} \frac{e^i}{i!} W_{r,i} \tag{A.4}$$

$$W_f = \frac{\partial f}{\partial e} = \sum_{i\geq 0} \frac{e^i}{i!} W_{f,i}. \tag{A.5}$$

A.2 Getting the generators

To find the expression of the generators of this transform, we use Kepler's equation:

$$l_o = E - e\sin E, \tag{A.6}$$

where E is the eccentric anomaly. Derivating this equation with respect to the eccentricity (and bearing in mind that l_o is independent of the eccentricity), we have

$$\frac{\partial l_o}{\partial e} = 0 = \frac{\partial E}{\partial e} - \sin E - e\cos E\frac{\partial E}{\partial e} \tag{A.7}$$

$$\Leftrightarrow \frac{\partial E}{\partial e} = \frac{\sin E}{1 - e\cos E}. \tag{A.8}$$

The true anomaly f and the normalized radius depend on the eccentric anomaly through the following relations:

$$\cos f = \frac{\cos E - e}{1 - e\cos E}, \tag{A.9}$$

$$\sin f = \sqrt{1-e^2}\frac{\sin E}{1 - e\cos E}, \tag{A.10}$$

$$r = 1 - e\cos E. \tag{A.11}$$

These equations will be very useful to determine the generators.

A.2.1 The generator W_r

Let us start by the generator W_r:

$$W_r = \frac{\partial r}{\partial e} = -\cos E + e\sin E\frac{\partial E}{\partial e} \tag{A.12}$$

$$= -\cos E + e\frac{\sin^2 E}{1 - e\cos E} \tag{A.13}$$

$$= \frac{-\cos E + e\cos^2 E + e\sin^2 E}{1 - e\cos E} \tag{A.14}$$

$$= -\frac{\cos E - e}{1 - e\cos E} = -\cos f = W_{r,1} \tag{A.15}$$

and we can note that $W_{r,i} = 0\ \forall i \geq 2$.

A.2.2 The generator W_f

Getting the expression of W_f is more arduous. We use the tangent of f:

$$\tan f = \sqrt{1-e^2}\frac{\sin E}{\cos E - e}, \tag{A.16}$$

and derivating this with respect to the eccentricity, we have:

$$\frac{1}{\cos^2 f}\frac{\partial f}{\partial e} = \frac{1}{(\cos E - e)^2}\left[\frac{-e\sin E}{\sqrt{1-e^2}}(\cos E - e)\right. \tag{A.17}$$

$$\left. + \sqrt{1-e^2}\cos E\frac{\partial E}{\partial e}(\cos E - e) - \sqrt{1-e^2}\sin E\left(-\sin E\frac{\partial E}{\partial e} - 1\right)\right] \tag{A.18}$$

$$\Leftrightarrow r^2\frac{\partial f}{\partial e} = \frac{1}{\sqrt{1-e^2}}\left[- e\sin E(\cos E - e) + (1-e^2)\sin E\right. \tag{A.19}$$

$$\left. + \frac{\partial E}{\partial e}(1-e^2)(\cos^2 E + \sin^2 E - e\cos E)\right] \tag{A.20}$$

$$= \frac{1}{\sqrt{1-e^2}}\left[-e\sin E\cos E + \sin E + (1-e^2)\frac{\sin E}{1-e\cos E}(1-e\cos E)\right] \tag{A.21}$$

$$= \frac{\sin E}{\sqrt{1-e^2}}(2 - e^2 - e\cos E) \tag{A.22}$$

$$= \frac{r\sin f}{1-e^2}(2 - e^2 - e\,(r\cos f + e) \tag{A.23}$$

$$= 2r\sin f - \frac{er^2\sin f\cos f}{1-e^2} \tag{A.24}$$

$$= r^2\sin f\left(\frac{2}{r} - \frac{e\cos f}{1-e^2}\right) \tag{A.25}$$

$$\Leftrightarrow \frac{\partial f}{\partial e} = \sin f\left(\frac{2(1+e\cos f) - e\cos f}{1-e^2}\right) \qquad \left(\text{car } r = \frac{1-e^2}{1+e\cos f}\right) \tag{A.26}$$

$$= \frac{2\sin f + e\sin f\cos f}{1-e^2} \tag{A.27}$$

$$= \frac{4\sin f + e\sin 2f}{2(1-e^2)} \tag{A.28}$$

Expanding the function $(1-e^2)^{-1}$ around $e = 0$, we have

$$W_f = \left(2\sin f + \frac{e\sin 2f}{2}\right)(1 + e^2 + e^4 + e^6 + ...) \tag{A.29}$$

$$= \underbrace{2\sin f}_{W_{f,1}} + e\underbrace{\sin 2f/2}_{W_{f,2}} + \frac{e^2}{2!}\underbrace{4\sin f}_{W_{f,3}} + \frac{e^3}{3!}\underbrace{3\sin 2f}_{W_{f,4}} + \frac{e^4}{4!}\underbrace{48\sin f}_{W_{f,5}} + \frac{e^5}{5!}\underbrace{60\sin 2f}_{W_{f,6}} + ... \tag{A.30}$$

A.3 Example: $F(r, f) = r$

We use the formula described in the methodology section with $f_0^0 = r$ and $f_i^0 = 0\ \forall i \geq 1$. Let us go until the third order.

Order 1 Let us find F_0^1:

$$F_0^1 = F_1^0 + L_1(F_0^0) = 1(-\cos f) = -\cos f \tag{A.31}$$

Order 2

$$F_1^1 = F_2^0 + L_1(F_1^0) + L_2(F_0^0) = 0 + 0 + 0 \tag{A.32}$$

$$F_0^2 = F_1^1 + L_1(F_0^1) = 0 + \frac{\partial \cos f}{\partial f} W_{f,1} \tag{A.33}$$

$$= \sin f.2 \sin f = 1 - \cos 2fn \tag{A.34}$$

Order 3

$$F_2^1 = F_3^0 + L_1(F_2^0) + C_2^1 L_2(F_1^0) + L_3(F_0^0) = 0 \tag{A.35}$$

$$F_1^2 = F_2^1 + L_1(F_1^1) + L_2(F_0^1) = 0 + 0 + \sin f. \sin 2f/2 \tag{A.36}$$

$$F_0^3 = F_1^2 + L_1(F_0^2) \tag{A.37}$$

$$= \sin f. \sin 2f/2 + 2 \sin 2f.2 \sin f \tag{A.38}$$

$$= \frac{9}{2} \sin f \sin 2f \tag{A.39}$$

Finally, we have that

$$r = 1 - e \cos l_o + e^2 \frac{1 - \cos 2l_o}{2} + \frac{e^3}{3!} \frac{9}{4} (\cos l_o - \cos 3l_o). \tag{A.40}$$

This procedure works for any function of f and r. In our case, we apply it to $(r/a)^{-3}$, $\cos f$ and $\sin f$.

B

The changes of variables

In this appendix, we explain our choice of variables.
The change of variables is $(\sigma_1, \Lambda_1, \sigma_2, K) \to (x_1, y_1, x_2, y_2)$, with

$$\begin{cases} \sigma_1 &= x_1 \text{ (Taylor expansion around } \sigma_1 = 0) \\ \Lambda_1 &= \Lambda_1^\star(1+y_1) \\ x_2 &= \sqrt{\frac{2\Lambda_2}{\Lambda_1^\star}}\sin\sigma_2 \\ y_2 &= \sqrt{\frac{2\Lambda_2}{\Lambda_1^\star}}\cos\sigma_2 \end{cases} \tag{B.1}$$

The first reason to perform this change of variables is that the new variables are canonical with multiplier $1/\Lambda_1^\star$.

Another obvious reason is the fact that these variables are non-dimensional and this is always more careful. Should we decide to change our units for example, our expansions would still be valid without any issue.

The last reason for this particular change of variables is that our Hamiltonian is expressed as Poisson series. Before this change, it depends on K through $\sin K$ and $\cos K$. Why bothering to change the variables? Could we not use the variables as they are, since we have no problem with the Hamiltonian yet? The answer is of course no, computing the equilibria, Hamilton's equations would give:

$$\begin{cases} \dot\sigma_1 = \frac{\partial H}{\partial \Lambda_1} + \frac{\partial H}{\partial(\cos K)}\frac{\partial(\cos K)}{\partial \Lambda_1} + \frac{\partial H}{\partial(\sin K)}\frac{\partial(\sin K)}{\partial \Lambda_1} \\ \dot\Lambda_1 = -\frac{\partial H}{\partial \sigma_1} \end{cases} \tag{B.2}$$

$$\begin{cases} \dot\sigma_2 = \frac{\partial H}{\partial(\cos K)}\frac{\partial(\cos K)}{\partial \Lambda_2} + \frac{\partial H}{\partial(\sin K)}\frac{\partial(\sin K)}{\partial \Lambda_2} \\ \dot\Lambda_2 = -\frac{\partial H}{\partial \sigma_2}. \end{cases} \tag{B.3}$$

and the problem is that there is no easy expression for $\frac{\partial(\sin K)}{\partial \Lambda_2}$. Indeed, we have:

$$\cos K = 1 - \frac{\Lambda_2}{\Lambda_1} \text{ et } \sin K = \sqrt{1-\cos^2 K} \tag{B.4}$$

$$\Rightarrow \quad \sin K = \sqrt{2\frac{\Lambda_2}{\Lambda_1} - \left(\frac{\Lambda_2}{\Lambda_1}\right)^2}. \tag{B.5}$$

and this is not (directly) implementable as Poisson series. To solve that, we will perform expansions of $\cos K$ and $\sin K$. Let us consider $a = \sqrt{\frac{2\Lambda_2}{\Lambda_1}}$. We have

$$a = \sqrt{\frac{2\Lambda_2}{\Lambda_1^\star(1+y_1)}} = \sqrt{\frac{2\Lambda_2}{\Lambda_1^\star}}(1+y_1)^{-1/2} \tag{B.6}$$

and

$$\cos K = 1 - \frac{\Lambda_2}{\Lambda_1} = 1 - \frac{a^2}{2} = 1 - \frac{x_2^2+y_2^2}{2}(1+y_1)^{-1}, \tag{B.7}$$

where $(1+y_1)^{-1}$ will be expanded around $y_1 = 0$.
As for $\sin K$, we have

$$\sin K = \sqrt{1-\cos^2 K} = \sqrt{a^2 - \frac{a^2}{4}} = a\sqrt{1-\frac{a^2}{4}} = a\left(1 - \frac{a^2}{8} - \frac{a^4}{128} - \dots\right), \tag{B.8}$$

after expansions around $a = 0$. Is a 5th order expansion enough? Since K is supposed to be close to the inclination ($\approx 7°$), we have $1 - \cos K \approx 0.0075$ and $a \approx 0.122$. As a consequence we have that $a^5/128 \approx 2 \times 10^{-7}$ and the next term would be $a^7/1024 \approx 5 \times 10^{-10}$. We must remember that these terms are inside the perturbation, hence are multiplied by a factor 10^{-5}. Our level of truncation being 10^{-12}, we conclude that a 5th order expansion is well enough.

However we still do not have the expression of $\sin K$ in function of our new variables. To do so, we simply replace a by its expression from equation (B.6) into the equation (B.8). From there, the transition to y_1, x_2, y_2 is easy (using the fact that the Hamiltonian possesses the D'Alembert characteristic).

Bibliography

Anderson J.D., Colombo G., Esposito P.B., Lau E.L. & Trager G.B., 1987, The mass, gravity field, and ephemeris of Mercury, Icarus, 71, 337-349.

Andoyer H., 1926, Mécanique Céleste. Gauthier-Villars, Paris.

Anselmi, A., Scoon, G.E.N., 2001. BepiColombo, ESA's Mercury Cornerstone mission, Planet. Space Sci., 49, 1409.

Beletskii, V.V., 1972, Resonant rotation of celestial bodies and Cassini's laws, Celestial Mechanics, 6, 356-378.

Beletsky, V.V., 2000, Essays on the motion of celestial bodies, Birkhauser Verlag.

Benkhoff J., van Casteren J., Hayakawa H., Fujimoto M., Laakso H., Novara M., Ferri P., Middleton H., Ziethe R., 2010, BepiColombo – Comprehensive exploration of mercury: Mission overview and science goals, Planetary and Space Science, 58, 2-20.

Bois E. & Rambaux N., 2007, On the oscillations in Mercury's obliquity, Icarus, 192, 308-317.

Champenois S., 1998, Dynamique de la résonance entre Mimas et Téthys, premier et troisième satellites de Saturne, Ph.D Thesis, Observatoire de Paris.

Christensen U.R., 2006, Nature, 444, 1056.

Colombo G., 1965, The rotation of the planet Mercury, Nature, 208, 575.

Colombo G., 1966, Cassini's Second and Third Laws, The Astronomical Journal, 71, 891-896.

Comstock R.L. & Bills B.G., 2003, A solar system survey of forced librations in longitude, J. Geophys. Res., 108(E09), 5100.

Correia A., Laskar J., 2004, Mercury's capture into the 3/2 spin-orbit resonance as a result of its chaotic dynamics, Nature, Volume 429, Issue 6994, pp. 848-850.

Correia A., Laskar J., 2009, Mercury's capture into the 3/2 spin-orbit resonance including the effect of core-mantle friction, Icarus, Volume 201, Issue 1, p. 1-11.

Ćuk M. & Burns J., 2004, On the secular behavior of irregular satellites, The Astronomical Journal, 128, 2518-2541.

Deprit A., 1967. Free rotation of a rigid body studied in the phase plane', Am. J. Phs. 35 (5), 424–428.

Deprit A., 1969. Canonical transformations depending on a small parameter, Celest. Mech., 1, 12-30.

De Saedeleer B., 2006, Théorie analytique fermée d'un satellite artificiel lunaire pour l'analyse de mission, University of Namur (FUNDP), Presses Universitaires de Namur.

D'Hoedt S. & Lemaitre A., 2004, The spin-orbit resonant rotation of Mercury: a two degree of freedom Hamiltonian model, Cel. Mech. Dyn. Astr., 89, 267-283.

D'Hoedt S. & Lemaitre A., 2005, The Spin-orbit resonance of Mercury: a Hamiltonian approach, In Transits of Venus: New Views of the Solar System and Galaxy, *Proceedings of IAU Colloquium 196, held 7-11 June, 2004 in Preston, U.K.*, Kurtz, D.W. & Bromage, G.E.(eds.), 263-270.

D'Hoedt S., Lemaitre A., Rambaux R., 2006, Note on Mercury's rotation: The four equilibria of the Hamiltonian model, Cel. Mech. Dyn. Astr., 96, 253-258.

D'Hoedt S., La rotation rigide de Mercure: étude des effets à longues périodes, University of Namur (FUNDP), Presses Universitaires de Namur.

D'Hoedt S. & Lemaitre A., 2008, Planetary long periodic terms in Mercury's rotation: a two dimensional adiabatic approach, Cel. Mech. Dyn. Astr., 101, 127-139.

D'Hoedt S., Noyelles B., Dufey J. & Lemaitre A., 2009, Determination of an instantaneous Laplace plane for Mercury's rotation563, Advances in Space Research, 44, 597-603.

D'Hoedt S., Noyelles B., Dufey J., Lemaitre A., 2010, A secondary resonance in Mercury's rotation, Cel. Mech. Dyn. Astr., in press.

Dufey J., Lemaitre A. & Rambaux N., 2008, Planetary perturbations on Mercury's libration in longitude, Cel. Mech. Dyn. Astr., 101, 141-157.

Dufey J., Noyelles B., Lemaitre A. & Rambaux N., 2009, Latitudinal librations of Mercury with a fluid core, Icarus, 203, 1-12.

Dunne J. A. & Burgess E., The Voyage of Mariner 10: Mission to Venus and Mercury (NASA SP-424) 1978, book found online at http://history.nasa.gov/SP-424/sp424.htm

Ferraz-Mello S., Nesvorný D. & Michtchenko T.A., 1997, On the lack of asteroids in the Hecuba Gap, Cel. Mech. Dyn. Astr., 69, 171-185.

Fienga A. & Simon J.-L., 2004. Analytical and numerical studies of asteroid perturbations on solar system planet dynamics, Astronomy and Astrophysics, 429, 361-367.

Giorgilli A. & Locatelli U., 1997. On classical series expansions for quasi-periodic motions, Mathematical Physics Electronic Journal, 3, Paper 5.

Goldreich P. & Peale S.J., 1966, Spin-orbit coupling in the Solar System, Astronomical Journal, 71, 425.

Henrard J., 1970, On a perturbation theory using Lie transform, Celestial Mechanics, 3, 107-120.

Henrard J., 1973, The algorithm of the inverse for Lie transform, ASSL Vol.39: Recent Advances in Dynamical Astronomy, 250-259.

Henrard J., Lemaitre A., A second fundamental model for resonance, Celestial Mechanics, 30, 197-218.

Henrard J., 1986. Algebraic manipulation on computers for lunar and planetary theories, *Proceedings of the IAU Symposium, 114, Reidel* Kovalevsky, J. and Brumberg, V. (eds.), 59-62.

Henrard J., 1997, The effect of the Great Inequality on the Hecuba Gap, Cel. Mech. Dyn. Astr., 69, 187-198.

Henrard J. & Schwanen G., 2004, Rotation of synchronous satellites: Application to the Galilean satellites, Celestial Mechanics and Dynamical Astronomy, 89, 181-200.

Henrard J., 2005, The rotation of Io, Icarus, 178, 144-153.

Henrard J., 2005, The rotation of Europa, Celestial Mechanics and Dynamical Astronomy, 91, 131-149.

Henrard J., 2005, Additions to the theory of the rotation of Europa, Celestial Mechanics and Dynamical Astronomy, 93, 101-112.

Henrard J. & Lemaitre A., 2005, The Untangling Transformation, The Astronomical Journal, 130, 2415-2417.

Henrard J., 2008, The rotation of Io with a liquid core, Celestial Mechanics and Dynamical Astronomy, 101, 1-12s, Celest. Mech., 3, 107-120.

Hori G., 1966. Theory of general perturbations with unspecified canonical variables, Publications of the Astronomical Society of Japan, Vol 18, No.4, 287-296.

Hough S.S., 1895, Philos. Trans. R. Soc. London A, 186, 469.

Kaula W., 1966. Theory of Satellite Geodesy. Blaisdell Publishing Company.

Laskar J., 1993, Frequency analysis of a dynamical system, Cel. Mech. Dyn. Astr., 56, 191-196.

Laskar J., 2003, Frequency map analysis and quasiperiodic decompositions, in Proceedings of Porquerolles School, arXiv:math/0305364.

Laskar J., Gastineau M., 2009, Existence of collisional trajectories of Mercury, Mars and Venus with the Earth, Nature, Volume 459, Issue 7248, pp. 817-819.

Lemaitre A., D'Hoedt S., Rambaux N., 2006, The 3:2 spin-orbit resonant motion of Mercury, Cel. Mech. Dyn. Astr., 95, 213-224.

Libert A.-S., Dynamique séculaire du problème des trois corps appliqué aux systèmes extrasolaires, University of Namur (FUNDP), Presses Universitaires de Namur.

Margot J.-L., Peale S.J., Jurgens R.F., Slade M.A. & Holin I.V., 2007, Large longitude libration of Mercury reveals a molten core, Science, 316, 710.

Milani A., Knezevic Z., 1990, Secular perturbation theory and computation of asteroid proper elements, Celestial Mechanics & Dynamical Astronomy, 49, 347-411.

Milani, A., Rossi, A., Vokrouhlický, D., Villani, D., Bonanno, C., 2001, Gravity field and rotation state of Mercury from the BepiColombo Radio Science Experiments, Planetary and Space Science, 49, 1579-1596.

Milani, A., Vokrouhlický, D., Villani, D., Bonanno, C., Rossi, A., 2002, Testing general relativity with the BepiColombo radio science experiment, Physical Review D, 66.

Moons, M., 1982, Physical libration of the Moon, Celestial Mechanics, 26, 131-142.

Moons, M., 1993, Averaging approaches, Proceedings of the "Artificial Satellite Theory Worshop", U.S.N.O. Wahsington D.C., p. 201.

NASA website: `http://solarsystem.nasa.gov/planets/profile.cfm?Object=Mercury&Display=Facts`

Noyelles B., Lemaître A. & Vienne A., 2008, Titan's rotation: A 3-dimensional theory, Astronomy and Astrophysics, 478, 959-970.

Noyelles, B., Dufey, J., Lemaître, A., 2010, Core-mantle interactions for Mercury, Monthly Notices of the Royal Astronomical Society, in press.

Peale S.J., 1969, Generalized Cassini's Laws, The Astronomical Journal, 74, 483-489.

Peale S.J., 1974, Possible histories of the obliquity of Mercury, Astronomical Journal, 79, 722.

Peale S.J., 1976, Does Mercury have a molten core, Nature, 262, 765.

Peale S.J., 2005, The free precession and libration of Mercury, Icarus, 178, 4-18.

Peale S.J., 2006, The proximity of Mercury's spin to Cassini state 1 from adiabatic invariance, Icarus, 181, 338-347.

Peale S.J., Yseboodt M. & Margot J.-L., 2007, Long-period forcing of Mercury's libration in longitude, Icarus, 187, 365-373.

Peale S.J., Margot J.-L., & Yseboodt M., 2009, Resonant forcing of Mercury's libration in longitude, Icarus, 199, 1-8.

Pettengill G.H., Dyce R.B., 1965, A radar determination of the rotation of the planet Mercury, Nature, 206, 1240.

Poincaré H., 1910, Sur la précession des corps déformables, Bulletin Astronomique, 27, 321-356.

Rambaux N., Bois E., 2004, Astron. Astrophys., 413, 381.

Rambaux N., Lemaitre A. & D'Hoedt S., 2007, Coupled rotational motion of Mercury, Astronomy and Astrophysics, 470, 741-747.

Rambaux N., van Hoolst T., Dehant V. & Bois E., 2007, Inertial core-mantle coupling and libration of Mercury, Astronomy and Astrophysics, 468, 711-719.

Seidelmann P.K., Archinal B.A., A'hearn M.F., Conrad A., Consolmagno G.J., Hestroffer D., Hilton J.L., Krasinsky G.A., Neumann G., Oberst J., Stooke P., Tedesco E.F., Tholen D.J., Thomas P.C., Williams I.P., 2007, Celes. Mech. Dyn. Astron., 98, 155.

Solomon S., McNutt R., Gold R., and 18 more co-authors, 2001, The MESSENGER mission to Mercury: scientific objectives and implementation, Planetary and Space Science, Volume 49, Issue 14-15, p. 1445-1465.

Touma J., Wisdom, J., 2001, Astron. J., 122, 1030.

Yseboodt M. & Margot J.-L., 2006, Evolution of Mercury's obliquity, Icarus, 181, 327-337.